AERODYNAMICS AND DRYING CHARACTERISTICS OF GRAINS IN TWO-DIMENSIONAL SPOUTED BEDS

By

Muhammad Issa Kalwar

A Thesis submitted to
The Faculty of Graduate Studies and Research
in partial fulfillment of the requirements for
the degree of Doctor of Philosophy

Department of Agricultural Engineering
Macdonald Campus of McGill University
Sainte Anne De Bellevue
Que. Canada. H9X 1C0

ABSTRACT

Ph.D. Muhammad Issa Kalwar Agricultural Engineering

AERODYNAMICS AND DRYING CHARACTERISTICS OF GRAINS IN TWO-DIMENSIONAL SPOUTED BEDS

Two slotted two-dimensional spouted bed units with flexible bed dimensions were designed and fabricated. Static vertical pressure of grains (shelled corn, soybean, and wheat) on the air entry slots in the pilot scale unit indicated that the silo theories are not applicable to predict this pressure accurately without including the bed to air inlet aspect ratio, slant angle, and sphericity of grains. A grain quantitative factor accounting for emptying angle of repose and sphericity of particles was proposed and included with the collected data to develop an empirical regression model.

Aerodynamics of grains (shelled corn, soybean, and wheat) were found to be affected by slant angle, spout width, separation distance, length of bed and the bed geometrical similarity. Mathematical models for the design parameters of the spouted beds were developed following the principles of dimensional analysis and similitude. Model predictions agree closely with the data.

The drying rate of shelled corn in the geometrically similar two-dimensional spouted beds with draft plates was found to depend on the bed geometry and operating parameters. The drying characteristics of corn in the investigated spouted beds was found to be of the thin layer type. The performance of dryers was modeled in the form of the Page's equation. Expressions for the model parameters accounting for bed geometry, grain moisture content, and drying conditions were developed. The developed model predictions agree well with the data from both beds.

RÉSUMÉ

Ph.D. Muhammad Issa Kalwar Génie agricole

CARACTÉRISTIQUES AÉRODYNAMIQUES ET DE SÉCHAGE DES GRAINS DANS LES SÉCHOIRS A DÉGORGEMENT VERTICAL "SPOUTED BED" BI-DIMENSIONNELS

Deux séchoirs à dégorgement vertical "spouted bed" bi-dimensionnels ont été dessinés à l'échelle pilote et construits. Les pressions statiques verticales mesurées à l'embouchure du jet d'air ont démontré que la théorie prédisant la pression statique dans les réservoirs à grain ne peut être utilisée sans tenir compte du rapport de la largeur de la colonne de grain sur celle du jet d'air, de l'angle d'inclinaison de la chute, et de la sphéricité des grains. Un facteur caractérisant l'angle d'écoulement au repos et la sphéricité des particules a été proposé et utilisé pour le développement, par régression, d'un modèle empirique.

Les caractéristiques aérodynamiques des grains (maïs, soya et blé) ont été affectées par l'angle d'inclinaison de la chute, la largeur de l'entrée d'air (spout), la distance de séparation, la longueur du lit, et la similarité géométrique des lits. Des modèles mathématiques basés sur l'analyse dimensionnelle et de similitude ont été développés pour évaluer les paramètres de design. Les valeurs obtenues à partir des modèles étaient en bon accord avec les valeurs mesurées.

Le taux de séchage des grains de maïs dans les deux séchoirs équipés de déflecteurs dépendait de la géométrie du lit et des paramètres d'opération. Sous ces conditions, les caractéristiques de séchage du maïs étaient comparable à celles des séchoirs en couches minces. La performance des séchoirs a été modelée suivant le

modèle proposé par Page et des expressions ont été développées pour tenir compte de la géométrie du lit, de la teneur en eau des grains et des conditions de séchage. Les valeurs prédites à partir du modèle proposé étaient en accord avec les données recueillies.

ACKNOWLEDGMENT

The author wishes to express his sincere appreciations to Dr.G.S.V. Raghavan, the research director, for his advice, encouragement, help, and constructive criticisms and Dr.A.S. Mujumdar, Professor of Chemical Engineering, McGill University, Montreal for his keen interest and encouragement during the course of this study. Special thanks to Dr. T. Kudra, visiting scientist from Poland, for his assistance and encouragement with the experiments and compilation of thesis.

The author also extends appreciations to Dr. E.R. Norris, Dr. M.A. Fanous, Dr. A.K. Watson and Dr. I. Alli for their interest and assistance in this work. The cooperation and assistance of Messrs. Ray Cassidy, Reid Nattress, and Harold Brevoort during the fabrication of scale models and installation of instruments is greatly appreciated.

Thanks are also extended to Dr. K.C. Khatri, Miss Nasreen Bughio, Mr. Karim Chirara, Mr. von H.H. Bernhard, Mr. U.S. Shivhare, Mr. Peter Alvo for reading the manuscript, Mr. Steve Tinker for drafting figures, Mr. Yvan Gariépy for translation of abstract in French, and others friends for their assistance during my studies at the McGill University, Montreal.

The author also gratefully extends thanks to Prof. G.N. Kalwar, Prof. Shaban Kalwar, and late the Prof. Meenhon Khan Abbassi, SAU, Tando Jam, Pakistan. The author wishes to acknowledge the Ministry of Education, Government of Pakistan, Islamabad for the scholarship, to the Sind Agriculture University, Tando Jam, Pakistan for granting study leave, to the Ministry of Education, Government of

Quebec, Quebec, for the "Fonds pour la Formation de Chercheurs et L'Aide à la Recherche" (FCAR) grant and to the Natural Sciences and Engineering Research Council (NSERC) of Canada for an operating grant.

The author is highly indebted to his generous late parents (Mr. and Mrs. Ghulam Rasool Kalwar) for their love, encouragement, and help throughout their lives and to his In-law parents (Mr. and Mrs. Mohammad Hashim Baloch) for love, financial support and patience during my stay along with my family in Canada. I am very grateful to my elder brother Mr. Hamid Khan Kalwar who stimulated my interest in advanced education and who, sadly, passed away during the course of this study and to my uncle Mr. Muhammad Bakhsh Kalwar for support and love after the death of my parents. The author would like to thank his brothers, sisters, brother- and sisters-in-law for their moral support and love. Finally, I am very thankful to my wonderful family for patience, love and being nice to me though I did not share enough time with them during the course of this study.

CONTRIBUTION TO KNOWLEDGE

This study contributes to the knowledge of two-dimensional spouted beds on the aspects of maximum pressure drop, aerodynamics, circulation of particulates, scale-up, and drying of grains. The specific original contributions to knowledge are

1. A new approach is initiated to fraction the maximum pressure drop exhibited in the two-dimensional spouted beds without draft plates. One fraction of the maximum pressure drop (static vertical pressure of grains on air inlet without injecting air through the bed) was investigated in detail. It is pointed out that the pressure of grains on smaller air inlets is higher than on larger ones. The comparison of the bulk storage silo theories with the collected data shows that these theories are not applicable without modification. The major drawbacks of these theories are the exclusion of sphericity of the particles and the inability to account for a slanting base or the bed to air inlet width aspect ratio.

2. To characterize the vertical pressure of grains on the air entry slots of two-dimensional bed units, a new parameter, termed the "grain factor" which accounts for the bulk density, sphericity, and emptying angle of repose of grains is proposed. Considering this concept, an empirical equation was developed for the estimation of static vertical pressure. The predictions of this equation indicate fair repeatability of the experimental data up to a bed height of 1.2 m, but only rough estimates can be done beyond this limit.

3. A new concept of normal distance is proposed in this study to replace the height of entrainment zone or separation distance for the spouted beds having draft tubes. This dimension varies with slant angle, draft tube width, and separation distance.

4. Although the concept of two-dimensional spouted beds is not new, a detailed study of these beds with draft plates was performed with regard to aerodynamics of grains in the fixed bed, and with respect to scale-up by increasing the length of the same bed and by using geometrical similarity at the minimum spouting conditions. The spouted bed design parameters (spouting pressure drop, minimum spouting velocity, solids circulation rate, and average cycle time) are identified and their relationship with the independent dimensionless variables is established following the principles of dimensional analysis and similitude. The agreement of estimations from spouted bed design parameters with the experimental data indicates the significance and reliability of the developed models.

5. For the first time, it has been possible to scale-up the two- dimensional spouted beds with draft plates in two ways: (1) by increasing the length of the same bed and (2) by geometrical similarity. The mathematical models developed for the simulation of air and particle dynamics in the slotted two-dimensional spouted beds with draft plates are also trustworthy for the scale-up of these beds.

6. The application of two-dimensional spouted beds with draft plates to drying of grains (shelled corn) is demonstrated and the factors affecting the batch drying kinetics are identified. It is shown that the drying of grains in this configuration occurs approximately in the form of thin layer drying.

7. The drying characteristics of grains in a two-dimensional spouted bed can now be modelled in the form of a Page equation. Reliable empirical linear relationships for the Page model parameters are developed for simulating the drying of grains in these beds.

8. The design and construction of the pilot scale two-dimensional spouted bed unit with a variety of operational advantages, is considered to be a contribution to the study of spouted bed dynamics.

TABLE OF CONTENTS

LIST OF TABLES

LIST OF FIGURES

NOMENCLATURE

Abbreviation	Description
A	Spouted bed width to air inlet width aspect ratio.
	Empirical constant (function of external drying conditions)
a	Experimental constant (function of external drying variables), dimensionless.
	Longest intercept of grain, mm.
A^*	Area of an orifice after removal of "empty annulus", m^2.
A_b	Cross-sectional area of spouted bed, m^2.
	Internal cross-sectional area of silo, m^2.
A_d	Cross-sectional area of downcomers, m^2.
A_p'	Surface area of single particle, m^2.
Ar	Archimedes number, $[\{g\ d_p^3\ \rho_f(\rho_p - \rho_f)\}/\mu^2]$
A_0	Empirical constant (function of external drying conditions)
A_1	Empirical constant (function of external drying conditions)
B	Empirical constant (function of external drying conditions)
b	Breadth of slot orifice, m.
	Experimental constant (function of external drying variables), /min.
	Longest intercept of grain normal to a, mm.
B_0	Empirical constant (function of external drying conditions)
B_1	Empirical constant (function of external drying conditions)
C	Constant in Beverloo equation, dimensionless.
	Internal circumference of silo or apparatus, m.
C_1	Characteristics abscissa, m.

C.V. Coefficient of variability, percent.

C_n n=0,1, ...4 constants in equations, dimensionless.

c Longest intercept of grain normal to a and b, mm.

D Internal moisture diffusivity of particle, m^2/min.

DB or D.B. Dry basis

D_c Column diameter of a silo or spouted bed, m.

DF Degrees of freedom.

D_i Hydraulic diameter of air entry slot, m.

D_h Hydraulic diameter of an orifice, m.

D^*_h Hydraulic mean diameter of an orifice after removal of "empty annulus", m.

D_o Diameter of an orifice, m.

D_s Hydraulic diameter of spout or draft tube, m.

D_t Diameter of a draft tube, m.

d_i Diameter of air inlet nozzle, m.

d_p Geometric mean diameter of a particle, m.

d_v Diameter of sphere of same volume as particle, m.

F_g Force of gravity per unit volume, N/m^3.

Fr Froude number, $U_f^2/(g\ d_p)$.

G Grain quantitative value, kg/m^3.

g Acceleration due to force of gravity, 9.806 m/s^2.

H_b Height or depth of grains in a silo or spouted bed, m.

H_c Height of the upper cone of grain mass in a silo, m.

H_E Height of entrainment zone or separation distance, m.

H_t Height of draft-tube/plates i.e. height from the bed bottom to the top tip of draft plates, m.

h_c Heat transfer coefficient, $W/m^2.K$

K Boltzmann's constant, erg/mol.K.

K Ratio of lateral to vertical internal pressure.

k Coefficient or constant, dimensionless.

Drying constant (function of external drying variables), /min.

k' Experimental constant (function of external drying variables), /min.

l Length of silo or slot orifice, m.

L_b Length of spouted bed or downcomer or spout (draft tube) or rectangular orifice or air entry slot, m.

M Final moisture content, dry basis (decimal).

Molecular weight of gas (air), g/mol.

Volume-average or average moisture content, dry basis (decimal).

MAE Mean absolute error.

MR Moisture ratio = $(M - M_e)/(M_o - M_e)$.

MSE Mean square error.

M_b Mass of grains in the spouted bed, kg.

M_d Grain moisture content, dry basis (percent).

M_e Equilibrium moisture content (EMC) of solids, dry basis (decimal).

M_o Initial moisture content of solids, dry basis (decimal).

M_p Mass down flow rate of solids in downcomers, kg/s.

M_{pu} Solids circulation rate in bed, kg/((m bed length).s).

M_s Surface moisture content of solids, dry basis (decimal).

Nu	Nusselt number = $\{(h_c\ d_p)/\lambda\}$, dimensionless.
n	Experimental constant (function of external drying variables), dimensionless.
	Number
P_{BP}	Absolute barometric pressure, Pa.
P_f	Force due to friction between walls and grains, N.
P_s	Spouting pressure drop, Pa.
P_u	Lateral or horizontal force on one side of silo, N.
P_v	Vertical pressure of grains on silo bottom (active case), N/m^2.
Q_f	Volumetric flow of fluid (air) through the spouted bed, m^3/s.
Q_p	Volumetric flow rate of grains in downcomers, m^3/s.
R	The universal molar gas constant, 8.314 J/(g-mole) K.
RH	Relative humidity at the air inlet of spouted bed, percent.
Re	Reynolds number = $\{(U_j\ d_p\ \rho_f)/\mu\}$, dimensionless.
R_h	Hydraulic radius of a silo or spouted bed, m.
R^2	R-SQUARE (the square of the multiple correlation coefficient).
r	Radius of particle or radial distance from axis, m.
	Reference dimensions
r_v	Radius of particle estimated from d_v, m.
SE	Standard error of estimate.
SVP	Static vertical (bottom) pressure, Pa.
s	Side of square or rectangular silo, m.
T	Absolute dry bulb temperature, K.
T_b	Bed temperature (downcomers), °C
T_i	Inlet air temperature, °C

T_m Average bed temperature (downcomers), °C.

T_p Particles or material temperature, °C.

T_w Total weight of grains, N.

T_x Exit or exhaust air temperature, °C.

t Time, min.

t_c Average cycle time, sec.

t_p Thickness of draft plate or tube, m.

U_f Minimum superficial velocity of air through the bed for spouting, m/s.

U_j Air velocity through inlet slot, m/s.

U_{ms} Minimum superficial fluid velocity for spouting, m/s.

V_b Volume of spouted bed, m^3.

V_p Average downward particle velocity in downcomers, m/s.

V_p' Volume of single particle, m^3.

w width or breadth of square or rectangular silo, m.

WB or W.B. Moisture content on wet basis.

W_b Width of spouted bed, m.

W_d Width of a downcomer of spouted bed, m.

W_i Width of air entry slot, m.

W_o Normal distance of orifice, m.

W_s Width of draft tube or channel or spout, m.

X Square root of the reduced weight-average residence time of grains in batch drying.

z Correction factor in Beverloo et al. (1961) equation, dimensionless.

α Significance level in STEPWISE Regression.

λ Thermal conductivity, W/m.K

ρ_b Bulk density of grains, kg/m^3.

ρ_f Dry air density, kg/m^3.

ρ_p Particle density of grains, kg/m^3.

ε Characteristic energy of interaction between the molecules (maximum energy of attraction between a pair of molecules), erg/mol.

ε/K Absolute temperature, K.

ε_v Voidage in the spouted bed downcomer = $\{1-(\rho_b/\rho_p)\}$, dimensionless.

θ_s Slant angle, degree.

θ_f Angle of friction between grains and wall, degree.

θ_i Angle of internal friction, degree.

θ_r Emptying angle of repose, degree.

θ_x Angle of rupture, degree.

μ Coefficient of internal friction, dimensionless.

Absolute viscosity, kg/m.s = (0.1 x Equation 9.1).

μ' Coefficient of external friction, dimensionless.

Ω_u A function of the dimensionless temperature, KT/ε.

σ Characteristic diameter of molecule (the "collision diameter"), Å.

ϕ Sphericity of grains, dimensionless.

π PI = 3.141593

I INTRODUCTION

1.1 General.

The availability of high quality cereal grains is essential to the survival of mankind on this planet. Almost all of the world's annual production is dried prior to use and storage and the importance of drying to moisture contents at safe storage levels with respect to storage life, nutritive value, and flavour is well documented (Brooker et al. 1974; Hall 1980). In many producing regions, climatic conditions are such that natural drying is not possible, hence the development of various types of commercial dryers. While there is no question that the dryers presently in use work, the magnitude of time and energy costs for grain drying world-wide is such that improvements are welcome.

Research has indicated that spouted bed dryers, which are specialized units for contacting granular solids with fluids, can improve upon the performance of conventional units in terms of energy use, drying rate and uniformity of drying (Becker and Sallans, 1961; Peterson, 1962). Unlike conventional dryers, spouted beds can provide regular recirculation and mixing of grains in the bed. This permits the use of higher inlet temperatures without damaging grains and ultimately leads to faster drying. Spouted beds may also be used for heating, roasting, cooling, mixing, dehusking and blending, thus representing a multi-purpose investment to the farm community.

Although spouted beds are recognized to have the potential to improve existing grain drying technology, the design problems to be described in the next section must be overcome before spouted bed dryers find their place at the commercial level.

1.2 Nature of the Problem.

The spouted bed is a general term for any apparatus designed to contact solid particles with a spouting fluid. This type of apparatus was introduced in the early 1950's and termed conical-cylindrical spouted beds (CSB's) because of the cross-sectional geometry. The process of spouting is achieved by supplying air as a jet at the centre of the bed bottom. In principle, the grains are spouted from the bed bottom by the jet (dilute phase) and fall to the top of the bed to join the downcomer (dense phase). The downcomer moves uniformly towards the bed bottom where grains are again entrained by the spouting air. A schematic diagram of the circulation in a CSB is shown in Figure 1.1.

Although cereal grains have been dried on laboratory, pilot, and industrial scales in such dryers (Mathur and Gishler, 1955b; Becker and Sallans, 1961; Peterson, 1962; Malek and Lu, 1964; Brunello et al., 1974b; Zuritz and Singh 1980), CSB's never appeared commercially. The main problems were: 1) high blower capacity requirements related to pressure drop before and after spouting, unequal grain residence times due to entrainment along the height of the spout well-above the bed bottom, compromise of air flow parameters for drying due to requirements for stable spouting, and limited drying capacity related to scale-up problems (Mathur and Epstein, 1974b; Mujumdar and Raghavan, 1984; Pallai et al., 1984).

One approach to overcoming these problems was to install a draft tube above the air inlet. This development resulted in better grain circulation, reduced pressure

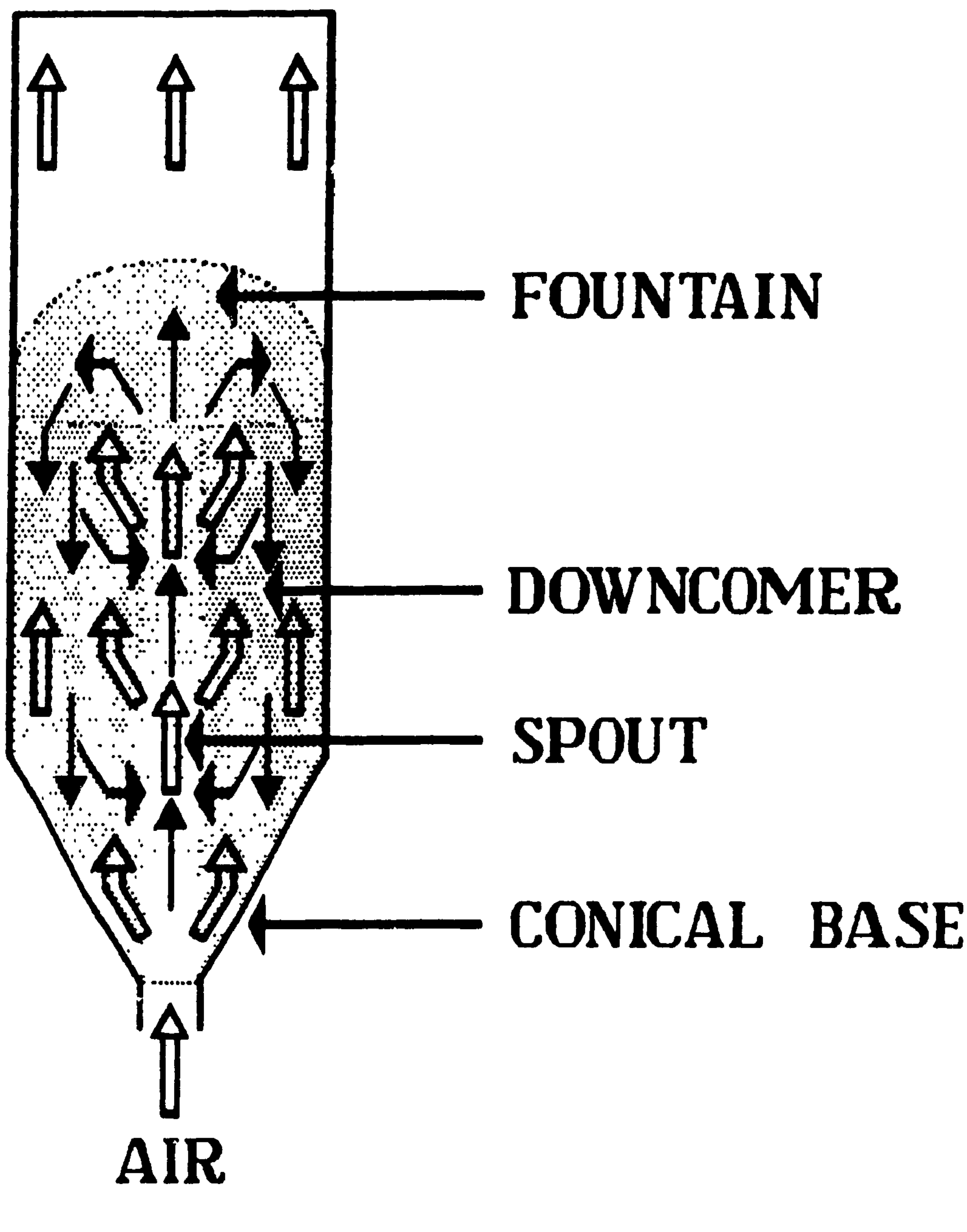

Figure 1.1 Schematic diagram of a conventional cylindrical spouted bed.

drop, lower air velocity requirements and increased maximum spoutable bed height, albeit at the penalty of retarded mixing (Buchanan and Wilson, 1965; Khoe and Brakel, 1980; Claflin, 1982). However, this led to more complex designs while leaving the problems of drying capacity and scale-up unresolved (Mujumdar, 1984). Spouted beds were also studied by the Russians (Mathur and Epstein, 1974b). They used units with rectangular cross-sections of small aspect ratio and sloped sides. Although they managed to achieve stable spouting using bed width to air entry slot width ratios of 10 to 20, wall effects, or "three-dimensionality", prevented them also from overcoming the drying capacity and scale-up problems of CSB's. The idea of a "fully two-dimensional" spouted bed (2DSB) was then proposed by Mujumdar (1982), principally as an approach to resolving scale-up problems.

A 2DSB has plane walls with slanting bases on both narrow sides and has an air entry slot at the centre of the bed width running parallel to the bed length as shown schematically in Figure 1.2. The rectangular geometry makes the 2DSB easier to fabricate than the cylindrical bed and is readily adapted to scale-up studies. A laboratory scale unit can be considered to be a thin vertical slice of the proposed large scale industrial unit (ie. just shorter along the length axis). The behaviour observed in the laboratory scale model should then be applicable to the large scale model if the wall effects are quantified.

A 2DSB exhibits peak pressure drop before the onset of spouting and spouting pressure drop after spout formation as is the case in CSBs (Anderson et al., 1984). Minimization of these pressure drops is important in design since they relate to required blower capacity. The peak pressure drop exhibited during spout formation is thought to be influenced partially by the vertical pressure of grains.

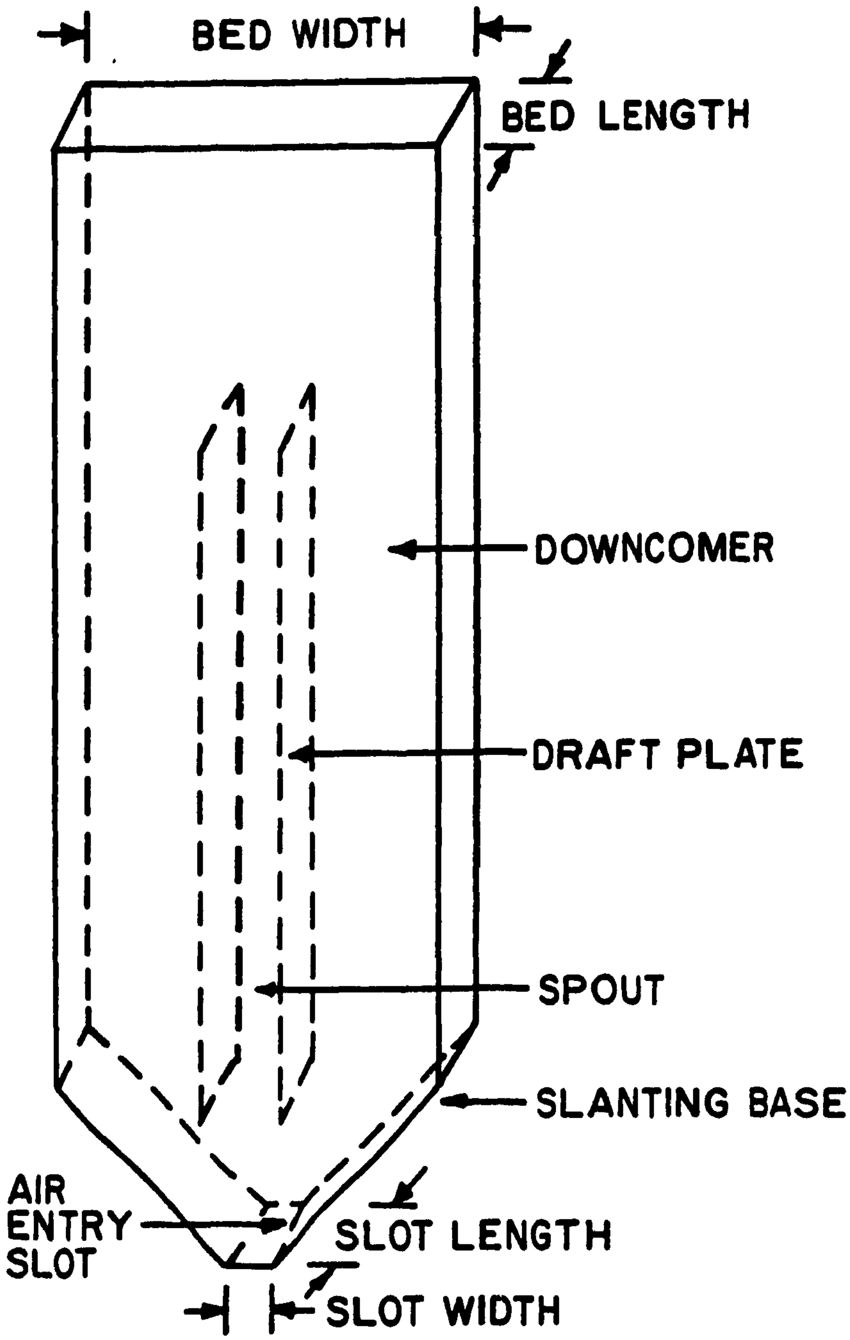

Figure 1.2 Schematic diagram of a slotted two-dimensional spouted bed with two draft plates.

The vertical pressure of grains during spout formation is difficult to measure, but can be if the bed is static and nonaerated; in this situation, the bulk storage theories can be used for prediction.

Draft plates installed on both sides of the air entry slot in a 2DSB act in a similar manner a draft tube in the CSB (Law et al., 1984, ibid., 1986; Kalwar et al., 1988). This configuration favours plug flow of grains which helps to ensure uniform drying, this in contrast to beds without draft tubes, where significant variation in moisture content of the drying particles has been reported (Viswanathan and Lyall, 1984). When the draft plates are present in a bed of given dimensions, spouting pressure drop, air flow through the bed, and solids circulation rate vary when either slant angle, spout width, or separation distance is changed. This is illustrated in Figure 1.3. In scaling-up a 2DSB by increasing the aspect ratio between the sides of bed (i.e. increasing bed length), it is assumed that spouting pressure drop, air inlet flux and particle velocity vary linearly from the laboratory scale models if the width and height of the bed are held constant.

The particles in the dilute phase are fully exposed to the spouting air. In the dense phase, grains are exposed to lower air flow rates, but for a much longer time. This results in the tempering of grains, moisture migration towards the surface of grains, and some evaporation due to the sensible heat gained while passing through the dilute phase. Slotted 2DSB's with draft plates are therefore seen to operate in an alternating two-stage mode with respect to heat transfer.

After studying drying rate curves and temperatures in the annulus of a CSB with draft tube, Khoe and Brakel (1980) concluded that drying only takes place in the draft tube and the recirculation zone, and that there is virtually no moisture

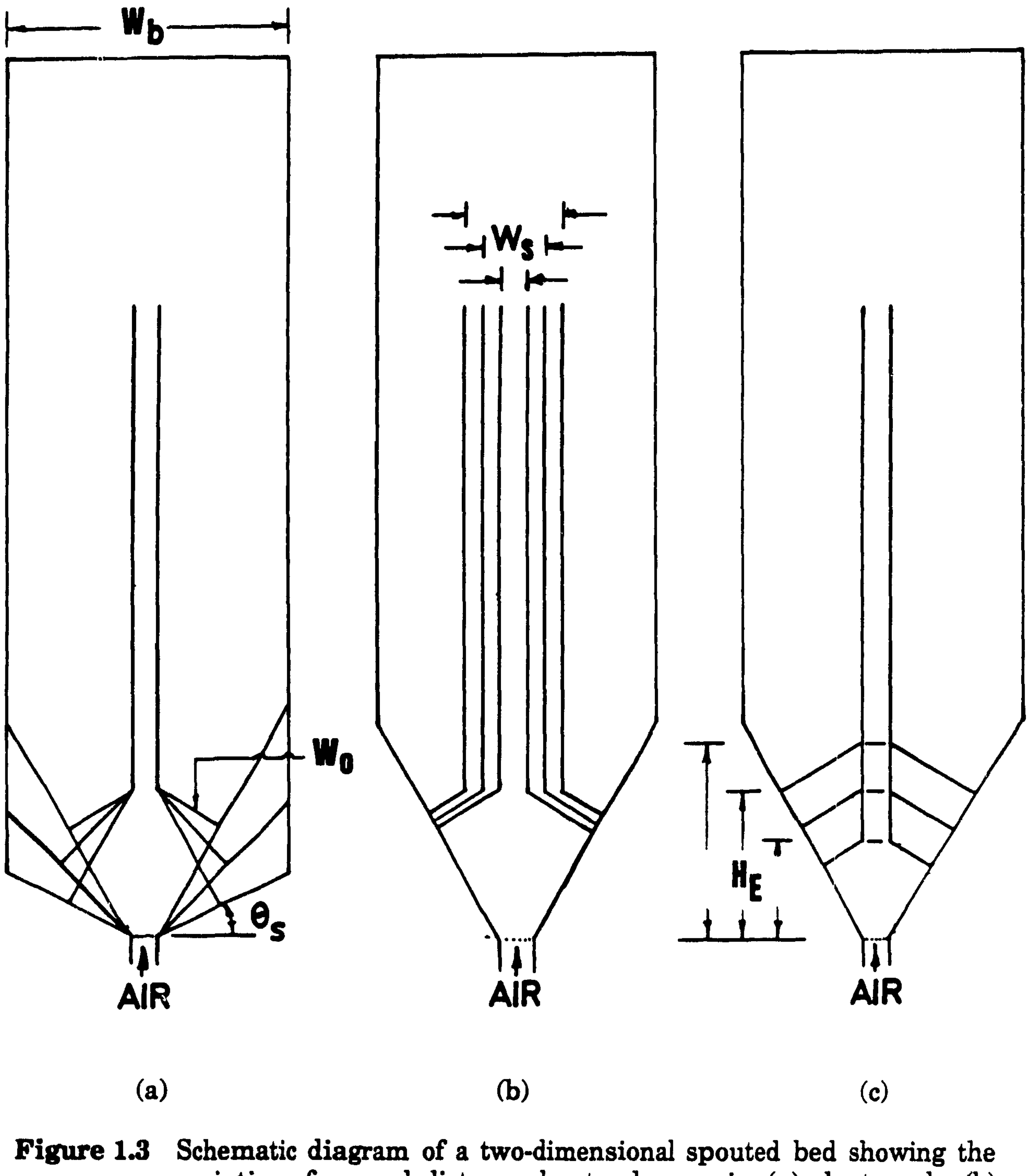

Figure 1.3 Schematic diagram of a two-dimensional spouted bed showing the variation of normal distance due to changes in: (a) slant angle, (b) draft tube width, and (c) separation distance.

transfer to the air in the annulus. The investigations of Khoe and Brakel (1980) and Claflin and Fane (1983, 1984b) show that about three quarters of the total air flow passes through the draft tube. This observation led to the hypothesis of thin layer drying in the dilute phase of a spouted bed with draft tube. Thin layer drying refers to the process in which all grains are fully exposed to the drying air under constant drying conditions, i.e. at constant air temperature and humidity. Generally, drying in a fixed bed with bed heights up to 20 cm (with a sufficient air-to-grain ratio) can be considered to be thin layer drying (Chakraverty and De, 1981). However, the conditions for thin layer drying are fulfilled only in the draft tube of a 2DSB after the initial drying stage. The drying of grains in the dense phase (downcomers) cannot be treated as thin layer drying. Our hypothesis on two-stage drying therefore boils down to thin layer drying in the draft channel and some tempering in the downcomer. We may therefore expect the general validity of a thin layer equation with some modifications due to the influence of dense phase conditions.

1.3 Statement of Problem.

Since the discovery of spouted beds, several kinds of cereal grain have been dried successfully in CSB dryers on laboratory and pilot scales. When the CSB's were scaled-up to increase the drying capacity, the scaled-up versions did not perform similarly with respect to spouting behaviour and drying (Pallai et al., 1984). The modification of bed geometry was therefore the focus of attempts to minimize the existing spouted bed limitations. Of the various modifications of spouted beds found in the literature, 2DSB's equipped with draft plates exhibited the best potential for design simplification and flexibility (Mujumdar, 1984).

The intent of this research was therefore to fully investigate the factors influencing the spouting and drying characteristics of slotted 2DSBs with draft plates while taking into account grain particle parameters in order to provide a sound basis for the design of commercially viable units. Shelled corn, soybean and wheat were chosen as the test materials because of their importance in Canadian and global agriculture.

1.4 Objectives.

The objectives for this research work were:

1. To design and construct a slotted two-dimensional spouted bed unit which could accommodate variable bed sizes and slant angles.
2. To determine the static vertical pressure of grains on slots (air-entry) in nonaerated 2-dimensional beds with different slant angles and bed heights at a fixed bed width and compare results with bulk storage theory predictions.
3. To determine the air and particulate flow characteristics in a slotted 2DSB while varying slant angle, draft tube width and separation distance.
4. To study the dynamics of air and cereal grains in relation to scale-up by increasing the length of bed.
5. To study the drying characteristics of grains with heated air in the two-dimensional spouted beds.
6. To develop mathematical models for static vertical pressure, aerodynamics and drying of grains.

1.5 Scope of the Research.

The static vertical pressure of grains on the air inlet of pilot scale two-dimensional spouted bed apparatus without injecting air through the bed was limited to laboratory investigations and experimental data were compared with predictions from bulk storage theories.

A greater proportion of the research was devoted to the mathematical modelling and laboratory data collection on the spouting pressure drop, the minimum spouting velocity, solids circulation rate, and the average cycle time in the two slotted 2DSBs equipped with solid wall draft plates. The mode of investigation in these beds was three fold: (1) Dynamics in the pilot scale spouted bed, (2) Scale-up of the pilot scale spouted bed by increasing the length of bed, and (3) Scale-up by geometrical similarity at a fixed bed height (135 cm) and fixed bed width to air entry slot width aspect ratio of 15. The application of 2DSBs to grain was limited to shelled corn, soybean, and wheat.

Emphasis was also given to the drying characteristics and dryer performance modelling of shelled corn in the geometrically similar slotted 2DSBs with draft plates at standard bed settings. The spouted beds were operated in batch mode under limited operating and drying conditions.

II REVIEW OF LITERATURE

2.1 Geometry of Spouted Beds.

2.1.1 Effect of bed dimensions on spouting.

It has been found that spouting is stable only under certain conditions of bed geometry. The description of these conditions in terms of relative bed and particle dimensions has been the subject of many investigations. Relevant findings in this area are discussed below.

Becker (1961) observed spouting grains in cylindrical columns. He noted that the maximum spoutable bed height decreases as the inlet diameter (d_i) increases. For a given bed height and column diameter (D_c), he observed a limit to inlet diameter beyond which spouting was no longer possible. The critical point, defined in terms of the ratio D_c/d_i is about 3. The upper limit of this ratio is said to be 22.5 (Pallai et al.1984) and the optimum value is in the range of 6 to 10.

It has also been noted that for a given bed diameter, spouting also depends on the size of solids to be spouted. Pallai et al., (1984) tested various materials in cylindrical vessels having diameters ranging from 0.06 to 0.58 m and indicated that the optimum ratio of column to particle diameter, D_c/d_p, is between 25 and 200. According to Becker (1961) and Nemeth et al. (1983), the air inlet to particle diameter ratio, d_i/d_p, for good spouting is in the range of 3 to 30. Epstein and Chandnani (1987) have also supported this criterion for both coarse and fine particles.

For conical spouted beds, the limiting ratios of bed-surface to inlet diameter has been established by the Russians (Mathur and Epstein, 1974b). This ratio is said to be dependent on the Archimedes number for materials of 0.36 to 9 mm diameter. The Russians have also studied slotted two-dimensional spouted beds with sloped walls (Mujumdar, 1984) and found that bed to air inlet width ratios of 10 to 20 yielded stable spouting (Anderson et al., 1984).

The practical range of ratios between bed height and diameter of CSB's is from 2 to 6 and the spouting technique is applicable to coarse granular materials usually greater than 1 mm in diameter (Mathur and Epstein, 1974b). It is concluded that similar practical limits should be applicable to a 2DSB for stable spouting.

2.1.2 Slant angle.

Early work on grain circulation in spouted beds showed that there were dead or motionless zones in the bed. The idea of slanting the conical base to overcome such dead zones was implemented by Mathur and Gishler (1955a). They used a slant angle of 47.5° in a drying experiment on wheat. Thorley et al. (1959), also using wheat as a test material, tried angles of 45°, 60° and 85°. They reported that the effects of slant angle were mainly on the rate of cross flow of solids into the spout but were negligible in relation to minimum spouting velocity. They also indicated some effects of slant angle on air flow through the annulus. An angle of 60° was thereafter generally accepted and used. However, little attention was paid to slant angle effects on the dynamics of CSB's once draft tubes were introduced to minimize problems of spouting pressure drop, minimum spouting velocity, air-flow through the downcomer, particle re-entrance in the spout and particle circulation rate.

Slant angle has also been largely ignored in more recent work on 2DSB's with or without draft plates. Anderson et al. (1984) studied the pressure drop and the minimum spouting velocity in an asymmetric 2DSB without draft tube and a fixed slant angle of 60°. Verlaan (1984) used a slant angle of 45° in a 2DSB with and without draft plates. It would appear that the conclusions of Thorley et al. (1959) have obviated slant angle as a useful parameter other than for preventing dead zones; however, that and most other work was based on spouted bed operation using only one type of cereal grain. Since both the static and aerodynamic properties of grain vary, the slant angle may yet prove to be a non-trivial design parameter.

2.2 Static Pressure of Particulates on Air Inlets.

The earliest silo designers assumed that the grain static vertical and lateral pressures are similar to those of liquids and estimated them as functions of height and bulk density. However, it later became clear that the above assumption of hydrostatics was incorrect because part of the weight was balanced by friction along the walls. The theories which improve on the hydrostatic approach are discussed in the following section.

2.2.1 Silo theories.

A. Janssen theory

The major change in computation of pressures was brought by Janssen (1895) who assumed that the stresses built up by the stored grains in a silo are independent of the horizontal coordinates and that the ratio of lateral to vertical pressure is constant relative to depth of fill for all points on the horizontal plane. Janssen considered a thin horizontal layer of stored grain in a silo and analyzed the vertical forces in order to predict the static vertical pressure at a depth H_b:

$$P_v = \left(\frac{F_g R_h}{\mu' K}\right)[1 - \exp(-\mu' K(H_b/R_h))] \tag{2.1}$$

Where $R_h = D_c/4$ for circular silo, $R_h = s/4$ for square silo, and $R_h = A_b/C$ for silos with other cross-sections. Based on the Rankine theory, which states that a plastic equilibrium exists in a grain mass when every part of it is just on the point of falling in shear or the particles are on the point of moving relative to one another, Koenen (1896) proposed the following formula to calculate the K-ratio for the active case of static pressure for the cohesionless granules:

$$K = \left(\frac{1 - \sin\theta_r}{1 + \sin\theta_r}\right) = \tan^2(45 - \frac{\theta_r}{2}) \tag{2.2}$$

B. Airy theory.

Airy (1897) put forward a more explicit theory than Janssen's. He included the wall friction and the internal friction coefficients. Airy assumed that the ultimate load carried by the silo is equal to the weight of a cone formed by a granular mass whose sides are at the angle of repose. He treated the grain mass as a semi-fluid and assumed that the pressure on the wall is due to a wedge of grain between the wall and the plane of rupture. Based on these assumptions, he developed two cases; the first being that the plane of rupture cuts the surface of grains within the bin, and the second being that the plane cf rupture intersects the side of the bin wall. For the first case (shallow bins or bunkers), he considered the forces for a grain mass of one meter thickness and calculated the lateral force:

$$P_u = 0.5\ F_g H_b^2 \left[\frac{\tan\theta_x - \mu}{(1-\mu\mu')\tan\theta_x + (\mu+\mu')\tan^2\theta_x}\right] \tag{2.3}$$

where,

$$\tan\theta_x = \sqrt{\mu\frac{1+\mu^2}{\mu+\mu'}}$$

The force due to wall and grain friction is then:

$$P_f = \mu' P_u C$$

and the static vertical pressure is:

$$P_v = \left[\frac{(T_w - P_f)}{A_b}\right] \tag{2.4}$$

In the second case, where the depth of grain in the bin is greater than:

$$H_b = w\ \tan\theta_x$$

the maximum horizontal force on one side of the bin holding a one meter thick grain mass is:

$$P_u = 0.5\ F_g w(2H_b - w\tan\theta_x)\left[\frac{\tan\theta_x - \mu}{1-\mu\mu' + (\mu+\mu')\tan\theta_x}\right] \tag{2.5}$$

where,

$$\tan\theta_x = \sqrt{\left(\frac{1+\mu^2}{1+\mu'}\right)\left(2\frac{H_b}{w} + \frac{1-\mu\mu'}{\mu+\mu'}\right)} - \left(\frac{1-\mu\mu'}{\mu+\mu'}\right)$$

The static pressure of grains on the bottom of a bin may be estimated by using equation (2.4). However, for other sizes of silos, the pressure determination is more complex and lengthy.

C. Reimbert and Reimbert theory.

Reimbert and Reimbert (1976) considered a horizontal unit thickness dH_b in the interior of silo that exerts a lateral pressure on the whole perimeter of silo walls. As the depth of material increases, the lateral pressure reaches a limit where the actual weight of assumed unit thickness is balanced by the wall friction. The load on the bottom is then equal to the total weight of grains minus the load balanced by the walls due to friction. Accordingly, the mean vertical pressure is:

$$P_v = F_g\left[H_b\left(1 + \frac{H_b}{C_1}\right)^{-1} + \frac{H_c}{3}\right] \tag{2.6}$$

The C_1 for four sides of the rectangular silo is:

$$C_1 = \frac{s}{\pi\mu' K} - \frac{H_c}{3} \qquad (2.7)$$

where,

$$H_c = \left(\frac{w}{2}\right)\tan\theta_r$$

and,

$$s = \frac{2wl - w^2}{l}$$

2.2.2 **Critical analysis of the silo theories.**

While carrying experiments on wheat in a wooden bin, Janssen (1895) found that $\mu' = 0.3$ and $K = 0.67$. However, Jamieson (1903) found $K = 0.6$ for wheat; Ketchum (1907) reported K for wheat to vary between 0.3 and 0.6; Mohsenin (1970) reported that Lorenzen found K between 0.33 and 0.44 when the moisture content of wheat varied 7.3 % to 17.1 % (wet basis); and Reimbert and Reimbert (1976) mentioned that K varies with granular mass depth and with the shape of silo. Pieper and Wenzel (1962) reported from their experiments that $K = 1 - \sin\theta_r$; Homes (1973) reported $K = 0.45$; and Jenike et al. (1973) published $K = 0.4$ stating that it gave better estimates with the Janssen method. Gaylord and Gaylord (1984) and Safarian and Harris (1985) have reported that the German Silo Code, the Soviet Silo Code, and the U.S. Silo Code Standards recommend estimation of static filling pressures by the Janssen method, but all codes suggest some modifications.

According to Ketchum (1907) and Safarian and Harris (1985) the pressures estimated with the Airy method are somewhat higher than those estimated with the Janssen method. However, Ketchum (1907) compared the Airy estimates with the actual data and found that it under-estimates the floor pressures in most of the cases he tested. The literature reviewed indicated that the Airy method is not in practice because it is more complex and is no more accurate than the Janssen or Reimbert and Reimbert methods.

Reimbert and Reimbert (1976) showed that their method is valid and more accurate in estimating the static pressures. According to Britton (1977), Manbeck et al. (1977), Gaylord and Gaylord (1977), Curtis and Stanek (1979), Smith and Lohnes (1980), Gaylord and Gaylord (1984), and Safarian and Harris (1985) the Reimbert and Reimbert (1976) method has not yet been accepted as widely as the Janssen method. However, these authors reported that the Reimbert and Reimbert method is gaining popularity among the silo design engineers and the silo manufacturers. Moreover, Safarian and Harris (1985) reported that the static lateral pressure measurements generally support application of the Janssen method, whereas the static vertical pressures are generally better predicted by the Reimbert and Reimbert method. Safarian and Harris (1985) have reported that the Reimbert and Reimbert method have been approved by the present French Silo Design Code and the U.S. Silo Standards (ACI 313-77), and these authors do apply the Reimbert and Reimbert method in their silo design approach.

The critical review of silo theories indicates that the Janssen theory of 1895 and the Reimbert and Reimbert theory of 1976 are more accurate in the prediction of silo static pressures compared to the other silo theories. Moreover, they are very simple and easy to use in calculations. Since the rectangular silo configuration is similar to the 2DSBs, both theories were considered for the interpretation of static vertical pressure of grains for the nonaerated packed beds.

2.2.3 Angles of repose and internal friction and K-ratio in silo theory.

The literature referred to in Table 2.1 indicates that the emptying angle of repose of cereal grains is not necessarily constant for a given type of grain. Mohsenin (1970) reported that Lorenzen showed that the angle of repose varies with the moisture content of grains. Qazi (1975) wrote that the angle of repose varies with the bulk density, the stickiness of material, the moisture content, and the particle shape.

Ketchum (1907) stated that the angle of internal friction is generally greater than the angle of repose. However, Mohsenin (1970) explained that, according to Lorenzen, the angle of internal friction of grains is always less than the angle of repose and varies with the moisture content of grains. Reimbert and Reimbert (1976) state that the angle of internal friction of a particular type of grain varies from a lower value to a higher value than the angle of repose, and suggested that in cases where no information is available, that the angle of repose be used as the minimum angle of internal friction. Safarian and Harris (1985) reported that the American Silo Code (ACI 77-313), the French Silo Code, the German Silo Code, the Soviet Silo Code, and the United Kingdom Silo Code all suggest using the angle of repose as the minimum angle of internal friction.

It is concluded, after investigating Ketchum (1907), Mohsenin (1970), Reimbert and Reimbert (1976), and Staley (1981) that the K-ratio varies with type of grain, moisture content of grain, depth of grain in silo, and silo shape.

Table 2.1 Angle of repose, angle of internal friction and K-ratio of grains.

Type of grains	Angle of repose	Angle of internal friction	K-ratio	Reference
	Degree	Degree		
Shelled corn	27.50	----	----	Airy (1897)
	----	----	0.39-0.53	Mohsenin (1970)
	36.00	----	----	Qazi (1975)
	27.00	----	----	Anonymous (1977)
	16 - 27	----	0.650	Staley (1981)
	27.00	-----	0.376	Gaylord and Gaylord (1984)
	25.00	21.50-31.0	0.32-0.46	Reimbert & Reimbert (1976)
Soybean	28.81	----	----	Mohsenin (1970)
	29.00	----	----	Anonymous (1977)
	29.00	----	----	Staley (1981)
Wheat	----	----	0.670	Janssen (1895)
	25.00	----	----	Airy (1897)
	28.00	----	0.596	Jamieson (1903)
	----	----	0.30-0.60	Ketchum (1907)
	29.6-41	23.5-32.5	0.33-0.44	Mohsenin (1970)
	----	55.00	----	Mathur and Epstein (1974a)
	26-28	----	----	Anonymous (1977)
	28.00	53.80	----	Epstein et al. (178)
	25-28	32.00	0.30-0.50	Staley (1981)
	29.00	----	0.347	Gaylord and Gaylord (1984)
Grain seeds	23-37	----	0.600	Safarian and Harris (1985)
	28-31	----	----	Qazi (1975)

2.3 Flow of Particulates Through Orifices.

Granular materials like cereal grains, fertilizers, and other food and industrial products are generally stored in bins, bunkers and hoppers. They are removed from the containers by gravity flow through circular, square, or rectangular orifices. A survey of literature (Ketchum, 1907; Stahl, 1950; Franklin and Johanson, 1955; Beverloo et al., 1961; Ewalt and Buelow, 1963; Chang et al., 1984; Gregory and Fedler, 1987; Fedler and Gregory, 1989) show that the granular flow through orifices is different from liquid flow. Nedderman (1985) reported that the discharge rate of a coarse granular material through a circular orifice in the base of a cylindrical bunker is unaffected by the diameter of the bunker or the depth of the material. This is due to the fact that the dimensions of bins are much larger than those of the orifices. Also, over a range of intermediate particle sizes, the flow rate varies little with particle diameter. Nedderman (1985) suggested that under these circumstances the only mathematically permissible form of the flow rate dependence is:

$$M_p - g^{0.5} \rho_b D_o^{2.5} \tag{2.8}$$

In practice, however, the value of the exponent of D_o varies in the range of 2.9 to 3.0. But, Beverloo et al. (1961) had found a correction factor $z = \kappa d_p$ where κ is approximately 1.5 for spheres and is much larger for angular particles. This modification gave rise to the Beverloo equation:

$$M_p = C\, \rho_b\, g^{0.5}\, (D_o - \kappa d_p)^{2.5} \tag{2.9}$$

where C is about 0.58 and is said to be independent of the angle of internal friction θ_i. Moreover, Beverloo et al. (1961) suggested that for noncircular orifices, the hydraulic mean diameter D_h should be used instead of D_o. Nedderman (1985) therefore modified the Beverloo model in the light of $A^*D^*_h$, where A^* and D^*_h are the area and hydraulic mean diameter of the orifice after removal of an "empty annulus" of width $0.5\kappa d_p$. Thus the Beverloo equation may be best written in the form:

$$M_p = \left(\frac{4}{\pi}\right) C\, \rho_b\, A^*(g\, D^*_h)^{0.5} \tag{2.10}$$

For a l x b slot orifice where l >> b, $D^*_h = 2(l - \kappa d_p)$, so that,

$$M_p = \left(4\frac{\sqrt{2}}{\pi}\right) C\, \rho_b\, g^{0.5}(1 - \kappa d_p)(b - \kappa d_p)^{1.5} \tag{2.11}$$

The Beverloo model also ignores the effect of cone angle in the case of conical hoppers which can be included as $\tan\theta_s$. Moreover, the literature indicates that the moisture content of the product also slightly influences the gravity flow of grains through the orifices. Chang et al. (1984) proposed that C and the power of D_o are functions of moisture content. A curvilinear empirical equation for each C and power of D_o was developed for shelled corn for the moisture content range 12.3 to 22.3 % (WB). However, their equations were developed from data on circular and square orifices located in the bottom of test silos.

Stahl (1950) reported that the flow of grains from a vertical orifice was one-third that from a horizontal opening. Ewalt & Buelow (1963) studied the flow of shelled corn from bins with various orifice sizes and placement. They concluded that there was no direct relationship between the flows through vertical and horizontal openings. They developed an empirical model for the estimation of gravity flow of shelled corn (MC 12.4 % DB) through a rectangular vertical orifice:

$$Q = 0.0573\, L^{1.75}\, W^{1.5} \tag{2.12}$$

where, Q is the volume flow rate (bushels/min), L is the orifice length (inches), and W is the orifice width (inches). Although the above empirical equation is dimensionally inconsistent and cannot be directly applied, it provides sound information about the effect of orifice dimensions.

The review of granular flow through orifices indicates that the flow is affected by: the orifice shape and dimensions; orifice location in the silo; the size, shape, surface characteristics and moisture content of particles; angle of repose or internal friction; hopper angles and filling method. Theoretical and empirical models do not account for most of these factors due to difficulty in measuring or assuming numerical values and are thus limited in design applications.

2.4 Aerodynamics of Spouted Beds.

Most of the literature reviewed in the following sections deals with CSB geometry. While the material may not be directly applicable to slotted 2DSBs with draft plates/tubes, the reviewed material should provide some basis for the development of models for the slotted 2DSBs with draft plates.

2.4.1 **Spouting pressure drop.**

When grains in a slotted 2DSB with draft plates are spouting, a pressure drop occurs due to grain transport in the spout and entrainment zone and due to the separation distance into the downcomer which is termed as spouting pressure drop. Buchanan and Wilson (1965) introduced the concept of draft tubes in CSBs in the name of Fluid-lift Solids Recirculator. This concept was later applied to the drying of grains in CSB's by Khoe and Brakel (1980), Claflin and Fane (1983, 1984a, 1984b) and Viswanathan (1986). It is noted that the pressure drop is always lower when draft tubes are used. Claflin and Fane (1983 and 1984b) reported that the spouting pressure drop in cylindrical beds with solid draft tubes was 80 % to 40 % of that in beds without solid draft tubes when the separation distances were 10 cm to 20 cm, respectively. Claflin and Fane (1983) viewed the draft tube CSB as a pneumatic conveyer (the spout) operating in parallel with a packed bed (the annulus). Their experimental data deviated from pneumatic theory predictions by 20 % when the separation distances were in the range of 5 cm to 17 cm. From this review it is concluded that pneumatic theory can not be applied to spouted beds with different geometries with great precision, but that it is adequate for rough estimates. Other disadvantages of this theory are complexity and the iterative nature of solutions which make its application to spouted beds less attractive.

Barroso and Massarani (1984) stated that the spouting pressure drop decreases as draft tube diameter increases but increases with increasing separation distance. They developed spouting pressure drop equations for soybeans and rice as a function of separation distance. Since their models do not fully account for the particle and spouting fluid properties and bed geometry, they cannot be applied with confidence to other bed geometries.

Some spouting pressure drop data for full and half 2DSBs with draft plates were presented by Law et al. (1986). Different grains and their mixtures were used to study the spouting pressure drop at superficial velocities greater than the minimum spouting velocity. The spouting pressure drop was higher at the minimum superficial velocity than at superficial velocities greater than the minimum spouting velocity. These data may be useful in the current investigation for comparison at the minimum spouting conditions if the particle and air properties are available.

2.4.2 Minimum spouting velocity.

The minimum spouting velocity is considered to be an air velocity through the bed at which a stable spouted bed can be obtained. This air velocity varies with solid and air properties and with bed geometry. Following the dimensional analysis, Mathur and Gishler (1955a), developed an empirical equation for estimating the minimum spouting velocity for CSBs:

$$U_{ms} = \frac{d_p}{D_c}\left(\frac{d_i}{D_c}\right)^{\frac{1}{3}}\left[2gH_b\left(\frac{\rho_p - \rho_f}{\rho_f}\right)\right]^{\frac{1}{2}} \tag{2.13}$$

Since then, many empirical, semi-empirical, and theoretical models were developed for the CSBs geometry (Becker, 1961; Smith and Reddy, 1964; Charlton et al., 1965; Kugo et al., 1965; Gay et al., 1970; Brunello et al., 1974a; Kmiec, 1980; Littman and Morgan III, 1983). The majority of the models reviewed (Mathur and

Epstein, 1974a; Asenjo et al., 1977; Epstein and Grace, 1984; Bridgewater, 1985; Lim and Grace, 1987; Passos et al., 1987; Littman and Morgan III, 1989) indicate that the empirical equation of Mathur and Gishler (1955a), although simple, yields reasonable values of the minimum spouting velocity if the bed diameter is not greater than 0.50 m.

Buchanan and Wilson (1965) studied the air flow rate required for minimum spouting at different draft tube separation distances from the nozzle located at the base. When the separation distance of the draft tube was decreased from 18.8 cm to 3.3 cm, the minimum air flow required for spouting was reduced by 50 percent. Khoe and Brakel (1980), Claflin (1982), and Claflin and Fane (1983, 1984b) studied the mass flow and volumetric flow rates of air passing through the draft tube and downcomer, rather than the minimum spouting velocity, as a function of the separation distance. Claflin and Fane (1984b) applied pneumatic theory to CSBs with draft tubes and showed that this theory overestimated their annulus air flow data by 20 % to 30 % depending on the draft tube diameter. Barroso and Massarani (1984) developed models for estimating the minimum spouting velocities of soybeans and rice using the Mathur and Gishler (1955a) model and separation distance as a parameter. The empirical models of Barroso and Massarani (1984) may only be applied to similar beds and particles since their models do not fully consider the bed geometry, spouting fluid and particle properties. Use of their models is also restricted to bed diameter less than or equal to 0.50 m.

Anderson et al. (1984), Verlaan (1984) and Law et al. (1984) measured the spouting velocity in 2DSBs while varying the bed height. Law et al. (1986) placed draft plates in the 2DSBs and studied the superficial air velocity while varying the slot width, the separation distance and the spacing between the two draft plates. The above review indicates that the superficial spouting velocity through the slotted 2DSBs varies with those parameters. This means that the air flow through the bed with draft tube is not the same as that in CSBs or 2DSBs without draft tubes.

2.4.3 **Solids circulation rate.**

The solids circulation rate in a CSB can be estimated if the particle velocity above the cone and the particle voidage are known either in the spout or in the downcomer. Many investigators have followed the latter procedure to estimate the solids circulation rate because the particle velocity at the wall and the voidage are easily estimated for the downcomer (Mathur and Epstein 1974a, 1974b). The particle velocity in the downcomer is measured by tracking the particles in the cylindrical portion of the bed. The solids circulation rate may be expressed as:

$$M_p = V_p A_d \rho_b \tag{2.14}$$

However, the particle velocity (V_p) at the wall in a downcomer is greatly influenced by the inlet air velocity, the inlet nozzle width, spout width, and the draft tube separation distance. Such analysis was performed by Claflin and Fane (1984b) for the estimation of total mass through-put into the spout for a draft tube CSB with the assumption that solids enter the spout evenly over the whole separation distance. Their empirical equation for the estimation of solids circulation is:

$$M_p = 224.2\ (H_E\ Q_f)^{0.7}\ M_b^{0.3} D_t^{1.22} \tag{2.15}$$

The empirical model of Claflin and Fane (1984b) for solids throughput in the spout cannot be applied to other bed geometries with confidence. Its application to similar geometries may even be hazardous because comparison with other data has not been reported and their data accounts for only one experimental bed. Hence, equation (2.15) can not be used for 2DSBs with draft plates, but the information about the significant factors may be helpful in mathematical modelling. Law et al. (1986) studied the slotted 2DSBs with draft plates and found that the solids circulation rate varies with the slot width, spout width, air flow, separation distance, and bed height. They suggested an empirical relationship of the form:

$$M_{pu} = k\ (U_j)^{0.5} \tag{2.16}$$

where k is a function of the particle properties and the bed geometry. The suggestion of Law et al. (1986) seems to be very informative for developing the mathematical model for solids circulation rate, but it does not provide a detailed parametric relationship for the 2DSBs with draft plates. Therefore, further experimental studies and mathematical modelling of the solids circulation rate are strongly required.

The studies in cylindrical spouted beds have shown that there are significant effects of particle shape and surface characteristics on the solids circulation. A regular pattern of solid flow may not be possible if the spouting material is rough or sticky or includes impurities that may cause channelling of solids and dead zones above the slanting base. Even the size distribution of particles can affect the spouting of a bed. However, these effects are difficult to evaluate and quantify.

2.4.4 **Average cycle time.**

The main feature of spouted beds is the continuous movement of particles between the spout and the downcomer of the bed which can be quantitatively described by the cycle time. This continuous movement of particles has a significant effect on the performance of spouted beds in applications such as drying, granulation, and coating (Mathur and Epstein, 1974b). The investigations of Thorley, et al. (1959) and Becker (1961) in CSBs without draft tubes indicate that the cycle time can be quantitatively estimated, with or without solids circulation rate in conjunction to bed geometry, particle properties, and volumetric gas flow. Thorley, et al. (1959) simply estimated the mean cycle time by dividing the total mass of particles in the bed by the solids circulation rate. Becker (1961) described cycle time of several grains without using the solids circulation rate and said his equation is roughly compatible. The comparison of Becker's relationship with the data of Thorley, et al. (1959) indicated serious underestimation. The approach of Thorley, et al. (1959) agreed very well with the measured values (Mathur and Epstein, 1974b).

2.5 Heat and Mass Transfer.

2.5.1 **Heat Transfer.**

There have been a number of studies of heat transfer in CSB's. Mathur and Epstein (1974b) reported gas-to-particle heat transfer coefficients in the spout and downcomer regions of 400 W/m^2-K and 50 W/m^2-K, respectively. While drying rough rice in batches in a draft tube CSB, Khoe and Brakel (1983) found heat transfer coefficients in the range of 439 W/m^2-K to 608 W/m^2-K when the inlet air temperature was maintained at 66° C and the moisture content of rice was reduced from 30 % to 18 % wet basis. Claflin and Fane (1984a) dried wheat in batches of 15 kg to 18 kg from 11.50 % to 4.76 % wet basis with inlet air temperatures in the range of 80° C to 120° C in a draft tube CSB. They found heat transfer coefficients of 100 W/m^2-K in the spout region. The only study providing the convective heat transfer coefficients in a 2DSB is that of Kudra et al. (1989). Using Linde Molecular Sieves (type 13X) as the test material, the gas-particle heat transfer coefficients were in the range of 16.8 to 49.1 W/m^2-K for beds with draft plates and 29.0 to 74.8 W/m^2-K for beds without draft plates under the same operating conditions. The particle Nusselt numbers found in this research were 0.866 to 6.21 and 2.22 to 9.44 respectively. Kudra et al. (1989) developed the following empirical relationship between Nu, the fluid-particle transport mechanism and bed geometry:

$$Nu = 1.975 R_e^{0.64} \left(\frac{H_b}{d_p}\right)^{-1.2} \left(\frac{H_b}{W_d}\right)^{0.45} \left(\frac{W_o}{d_p}\right)^{0.26} \tag{2.17}$$

in the range of $1670 \leq R_e \leq 7400$, $56 \leq H_b/d_p \leq 247$, $1.15 \leq H_b/W_d \leq 2.69$, and $4.20 \leq W_o/d_p \leq 17.6$. It is pointed out that the equation (2.17) seems to be applicable in this study because the geometric and operating parameters may fall in the specified ranges.

2.5.2 Drying.

When moisture content is above hygroscopic levels, grains may exhibit constant heat transfer rates. In practice, however, drying of grains takes place only during the falling rate period. This can be interpreted in terms of moisture diffusion which decreases as the water content of grain decreases. Many theories have been proposed to explain the movement of moisture from the interior of grains (Brooker et al., 1974; Fortes and Okos, 1980; Bakker-Arkema, 1986) but it is generally agreed that the process is governed by liquid diffusion, vapour diffusion or both.

It is believed that once the drying process of a single particle is analyzed and the drying rate obtained, the solution can be used for a multi-particle system if the drying conditions are similar to those for a single particle. Aside from the mechanism of moisture migration, the moisture content of the drying particle is monitored and plotted versus time as an average moisture content or moisture ratio. These drying plots are referred as the drying curve and the characteristic (or normalized) curve, respectively.

Experimental studies (Henderson and Pabis, 1961; Spencer, 1972) have shown that some volume contraction (shrinkage). However, the shrinkage phenomenon cannot be incorporated into the analysis of the drying process due to lack of data on the phenomenological and coupling coefficients for agricultural materials.

A. Theoretical equations.

Newmen (1931) and Sherwood (1931) have proposed Fick's second law for thin layer drying of solids during the falling rate period. The exact form of the diffusion equation depends upon the assumptions made regarding the shape of the kernel and the nature of the mass-transfer resistance. Assuming that the moisture movement takes place by liquid diffusion and that the diffusion coefficient is constant, the drying of particles in spherical coordinates may be written as:

$$\frac{\delta M}{\delta t} = D\left[\frac{\delta^2 M}{\delta r^2} + \frac{2}{r}\frac{\delta M}{\delta r}\right] \tag{2.18}$$

The solution of equation (2.18) for spheres, bricks, and cylindrically- shaped objects is an infinite series (Bird et al., 1960; Carslaw and Jaeger, 1959; Crank, 1975). Assuming a uniform initial moisture content and constant boundary conditions for a drying particle,

$M(r, 0) = M_o$, $M(r_v, t) = M_e$, and $M(0, t) =$ finite,

one may write the series solution of the diffusion equation after integrating over the initial value of the radius of an equivalent sphere of a particle:

$$\frac{M - M_e}{M_o - M_e} = \frac{6}{\pi^2}\sum_{n=1}^{\infty}\frac{1}{n^2}\exp\left(-\frac{n^2\pi^2 D}{r_v^2}\right)t \tag{2.19}$$

Using Fick's law of diffusion and the concept of surface moisture content (dynamic equilibrium moisture content) Becker and Sallans (1961) obtained the following expression for batch drying:

$$\frac{M - M_s}{M_o - M_s} = \frac{6}{\pi^2} \sum_{n=1}^{\infty} \frac{1}{n^2} \exp\left(- \frac{n^2 \pi^2 X^2}{9} \right) \tag{2.20}$$

where,

$$X = \left(\frac{A_p'}{V_p'} \right) (D \times t)^{0.5} = \left(\frac{3}{\phi} r_v \right) (D \times t)^{0.5}$$

for nonspherical shapes and the diffusion coefficient (D) is a function of particle temperature according to Arrhenius' law (Becker, 1959; Singh et al., 1972; Zaremba, 1977; Sharaf-Eldeen et al., 1979). Equation (2.20) would yield the drying time for a whole batch because all the grains are subject to the same drying conditions and residence time. Assuming that the internal grain temperature gradients are negligible, the grain is homogeneous, and the moisture content is in the range of 12 to 26 % wet basis, Becker and Sallans (1961) obtained the following equation for the diffusion coefficient for wheat grains:

$$D = 0.4596 \exp\left[- \left(\frac{51050}{RT} \right) \right] \tag{2.21}$$

Chu and Hustrulid (1968) considered coupled heat and mass transfer for corn kernels in the temperature range of 49° C to 71° C and moisture content in the range of 25 to 36 per cent (wet basis). They proposed the following equation for the diffusion coefficient:

$$D = 1.5134 \exp\left((4.5\times10^{-4}T - 5.485\times10^{-2})\, M_d - \left(\frac{2513}{T}\right)\right) \tag{2.22}$$

B. Semitheoretical equations.

Aside from the theoretical formulations of the thin layer phenomenon, semitheoretical thin layer equations have gained wide acceptance. If the drying time is long enough, or the moisture ratio is less than 0.6, the analytical solution of the drying rate can be expressed in few terms of the infinite series. A single term approximation was used by Simmonds et al. (1953), Hustrulid and Flikke (1959), Allen (1960), Henderson and Pabis (1961) and Boyce (1965):

$$\frac{M - M_e}{M_o - M_e} = a \exp(-bt) \tag{2.23}$$

If the constant "a" in the above equation is equal to unity, the equation is reduced to the same form as Newton's law of cooling for highly conductive materials.

A moisture relationship analogous to temperature in heat transfer analysis is often used in grain drying. It is based on the assumption that the rate of moisture loss of a grain kernel is proportional to the difference between the kernel moisture and its equilibrium moisture content (as governed by the conditions of the surrounding medium). Lewis (1921) expressed this analogy in the form:

$$\frac{dM}{dt} = -k(M_o - M_e) \qquad (2.24)$$

where k is known as the drying constant. The solution of equation (2.24) for a constant temperature and humidity is obtained by integrating drying rate with respect to time for appropriate initial and boundary conditions:

$$MR = \exp\,(-kt) \qquad (2.25)$$

Page (1949) introduced an exponent n to time t to better fit his thin layer drying data of shelled corn collected over more than 100 hours. His equation was:

$$MR = \exp\,(-k' t^{n}) \qquad (2.26)$$

Page (1949) noted that the value of n depended on the relative humidity of the drying air. van Rest and Isaacs (1966), Flood, et al. (1972), and Agrawal and Singh (1977) used this equation in analyzing thin-layer drying.

C. Empirical equations.

Though the theoretical and semitheoretical solutions to thin layer drying are well known, empirical thin layer equations are also acceptable in the drying of grains. Thompson, et al. (1968) developed a quadratic equation to describe the thin layer drying of shelled corn at temperatures in the range of 60° C to 150° C:

$$t = A \ln MR + B\,(\ln MR)^2 \qquad (2.27)$$

where, A and B are temperature dependent empirical coefficients. Henderson and Henderson (1968), Nellist and O'Callaghan (1971), Rowe and Gunkel (1972), Henderson (1974) and Nellist (1976) have fitted a two term series of negative exponential to thin layer drying experimental data for rice, shelled corn, and rye grass seeds:

$$MR = A_0 \, e^{-B0\, t} + A_1 \, e^{-B1\, t} \tag{2.28}$$

Henderson and Henderson (1968) and Rowe and Gunkel (1972) suggested the differentiation of the above equation for use as the drying rate equation in deep bed drying analyses.

The thin layer drying equations reviewed here represent the drying of grains with internally controlled moisture transfer with various levels of accuracy. The Page equation seems to be the best because it is simple and fits exponential data well. This equation was selected as the principal one in this study.

D. Equilibrium moisture content.

The equilibrium moisture content of grains in a given environment may be defined as the moisture content that would be approached if the grains were exposed to that environment for a long time or when the free energy change between grains and the surrounding environment is zero at a particular temperature. The corresponding relative humidity is called the equilibrium relative humidity (ERH) or the equilibrium relative pressure. The equilibrium moisture content may be static when the static methods of saturated salt and acid solutions are used to achieve the equilibrium, and dynamic when the surface moisture concentration of a hygroscopic material is in equilibrium with the drying conditions. Becker and Sallans (1955) used the dynamic equilibrium moisture content to evaluate the surface moisture content of wheat kernels during drying. However, Bakker-Arkema and Hall (1965) did not accept the concept of dynamic equilibrium moisture content. Angladette (1963) postulated that because of the difficulty in obtaining static equilibrium moisture content data, some investigators use dynamic equilibrium moisture content, since it could be obtained from a drying curve.

In this century, many attempts to determine _e EMC of cereal grains have been made and some of the well known research may be found in (Becker and Sallans, 1956; Hall and Rodriguez-Arias, 1958; Chung and Pfost, 1966). A number of theoretical, semitheoretical, and empirical models have been proposed to model the experimental data of the EMC. ASAE has accepted the Handerson-Thompson and Chung-Pfost equations as the standard EMC models for cereal grains. However, these models are recommended for the range of 20 to 90 % equilibrium relative humidity within the temperature range of 10 to 50 °C.

In reality, the relative gas humidity during high temperature drying of grains is often very low, below 20 %. Any extrapolation in these data or applications of EMC models for drying at temperatures higher than 50 °C should be exercised with caution.

III THEORY AND MODEL DEVELOPMENT

3.1 Aerodynamic of Spouted Beds.

The two-dimensional spouted bed is a modified form of the conical-cylindrical spouted bed. It has a rectangular bed cross- section and vertical plane walls. The process of spouting in a 2DSB is the same as that in a conical-cylindrical spouted bed. The spouting air enters the bed through a slot located at the centre of the bottom of bed and runs parallel to the length of the bed. The insertion of draft plates above the air entry slot in the bed, parallel to the length, provides two independent downcomers (silo models), one on each side of the spout. As the draft plates are fixed in the bed for a required separation distance, a rectangular orifice (as discussed in Chapter I) is formed on the side of spout in each downcomer.

The flow of grains through these orifices should be governed partially by bulk solids flow laws. The air flowing through the air entry slot has to pick up the grains coming from the orifices, accelerate and convey them over the separation distance to the top of the bed, and overcome air loss through grain voids via the rectangular orifices to the downcomers for smooth operation of the bed. When the spouting fluid can overcome the forces of inertia, gravity, friction and fluid viscosity, which lead to a spouting pressure drop during operation, a systematic cyclic pattern of solids movement can be established.

Basically, spouting pressure drop, minimum spouting velocity, solids circulation rate, and average cycle time are the major parameters which shape-up the systematic operation of a slotted 2DSB with two draft plates and are very important from the design and scaling point of view. These parameters are being considered for the development of mathematical models based on dimensional analysis and similitude principles for a batch type slotted 2DSB with two draft plates.

In a two-dimensional spouted bed with draft tube or plates, the air passing through the bed has to accelerate as well as convey the grains coming from the rectangular orifices in the vertical direction for the stable operation of bed. In this situation, the total spouting pressure drop at the bottom of the bed varies with the size of rectangular orifice, size of spout, size of air inlet, height of draft tube or plates, the ratio of solids to air, type of solids to be spouted, fluid properties, and other bed geometry.

Spouting pressure drop theory indicates that the air flow through the bed and the solids circulation rate are not the fixed constants but are functions of other variables. For a given bed geometry, the spouting air flow through the bed varies with slant angle, spout width, normal distance, width of bed, length of bed, height of bed, height of draft plates, particle properties, and fluid properties. The solids circulation rate is partially governed by the coarse granular solids flow through an orifice and the superficial air velocity through the bed. According to the theory of coarse granular flow, the solids flow through an orifice varies with orifice location in bin, inclination of the stagnant zone boundary, dimensions of the orifice, certain physical properties of grains, and to some extent with the moisture content of grains.

The time taken by particles to make the journey from the top of the downcomer back to their starting points is of considerable interest in solids mixing, heat treatment, cooling, and drying applications. Previous studies have shown that the proportion of time spent by a particle in the spout or draft tube is insignificant compared to time spent in the downcomer (Thorley et al., 1959; Becker, 1961; Gay et al., 1970). Hence, the average cycle time should be dependent on the total mass of solids in the bed, the solids circulation rate, width of the downcomer, slanting angle, and normal distance. Other factors which may effect the average cycle time may be air flow and some material properties.

The variables that were important for the analysis of air and solids dynamics were selected according to the information given in the literature on bulk solids flow through orifices and 2DSBs. A list of pertinent variables for the mathematical modelling of 2DSBs with draft plates is given in Table 3.1. It should be noted that not all of these variables are necessarily important for each operational phase of spouted beds.

The normal distance (W_o) of the rectangular orifice was calculated from the geometrical relationship (see section 9.2) of H_E, W_s, and θ_s:

$$W_o = \left[H_E - \left[\left[\frac{(W_s - W_i)}{2}\right] + t_p\right]\tan\theta_s\right]\cos\theta_s \qquad (3.1)$$

Table 3.1 The pertinent variables for the mathematical modelling of fluid and particle dynamics in the 2DSBs with draft plates.

No	Variable	Symbol	Units
	Fluid		
1	Spouting pressure drop	P_s	$ML^{-1}T^{-2}$
2	Superficial velocity	U_f	LT^{-1}
3	Density	ρ_f	ML^{-3}
4	Viscosity	μ	$ML^{-1}T^{-1}$
	Gravitational force		
5	Acceleration due to gravity	g	LT^{-2}
	Particle		
6	Particle velocity	V_p	LT^{-1}
7	Volumetric flow rate	Q_p	L^3T^{-1}
8	Solids circulation rate	M_p	MT^{-1}
9	Mass of wet solids	M_b	M
10	Average cycle time	t_c	T
11	Diameter	d_p	L
12	Sphericity	ϕ	--
13	Bulk density	ρ_b	ML^{-3}
14	Particle density	ρ_p	ML^{-3}
15	Voids	ε_v	--
	Bed		
16	Width	W_b	L
17	Width of a downcomer	W_d	L
18	Length or depth	L_b	L
19	Height of bed	H_b	L
20	Height of draft plates	H_t	L
21	Air-entry slot width	W_i	L
22	Hydraulic diameter of air inlet	D_i	L
23	Slant angle	θ_s	--
24	Spout or draft tube width	W_s	L
25	Hydraulic diameter of spout	D_s	L
26	Normal distance	W_o	L
27	Hydraulic diameter of orifice	D_h	L

Since the system of spouting in this configuration is very complex in comparison to conventional CSBs, a dimensional analysis scheme was employed. The relevant variables for 2DSB dynamics (i.e. spouting pressure drop, minimum spouting velocity, solids circulation rate, and average cycle time) are listed in Table 3.2 with the following assumptions:-

1) Bulk solids consist of particles so small in comparison to the bed dimensions that they can be considered to be a continuous mass.
2) Bulk solids have the same mechanical properties in any direction in bed.
3) The rate of flow of grains through the orifice is independent of bed height because normal distance is always less than bed height.
4) Frictional forces between particles in downcomers and the column walls are negligible compared to other forces.
5) Grains are uniform in shape and free flowing.
6) The void fraction in the downcomer is uniform and is approximately equal to that of a loose packed bed.
7) The particles move through the downcomers in a plug flow manner.
8) Grains are linearly distributed over the entrainment zone and are picked up by air uniformly.
9) Solids velocity in the downcomer is much lower than the fluid velocity and may therefore be neglected.
10) Air compressibility is neglected due to the relatively low pressures involved.
11) Resistance to air flow through the downcomers is higher than in the spout.

12) The error induced by grain moisture content on the rate of grain flow through the orifice is within experimental error.

13) The effects produced by broken seeds, straw, foreign materials, and bed shrinkage are not incorporated in the mathematical model.

It should not be assumed that all the variables in Table 3.2 constitute a unique set. They were chosen because they appeared convenient for the experimental and analytical phases of the study.

Buckingham (1914) states that if there is a dimensionally homogeneous equation relating n quantities defined in terms of r reference dimensions, then the equation may be reduced to a relationship between (n-r) independent dimensionless products (DPs or PI) provided that the members of the reference set be themselves chosen so as to be independent of one an other. Exceptions to this rule sometimes occur (Nelson 1960, Isaacson and Isaacson 1975). Hence, the fundamental basis for Buckingham's PI theorem is that a valid physical equation must be dimensionless, or reduce to like dimensions on both sides of the equality sign. Table 3.1 reveals that there can be three reference dimensions of MLT for mathematical modelling. The reference dimensions for MLT were selected on the bases of ease of use, influence, independence from one an other, and review of literature on spouted beds and granular flow through orifices. In view of this, the selected repeating variables for spouting pressure drop, minimum spouting velocity, solids circulation rate, and average cycle time are given in Table 3.3 along with the variables representing the MLT reference dimensions.

Table 3.2 The relevant variables for the mathematical models for air and particulate dynamics in the 2DSBs with draft plates.

No	Symbol	Mathematical models			
		P_s	U_f	M_p	t_c
1	P_s	+	-	-	-
2	U_f	+	+	+	-
3	ρ_f	+	+	+	-
4	μ	+	+	+	-
5	g	+	+	+	-
6	V_p	-	-	+	-
7	Q_p	+	-	-	-
8	M_p	-	-	-	+
9	M_b	-	-	-	+
10	t_c	-	-	-	+
11	d_p	+	+	+	+
12	ϕ	+	+	+	+
13	ρ_b	-	-	+	-
14	ρ_p	+	+	+	-
15	ε_v	+	+	+	-
16	W_b	+	+	-	-
17	W_d	-	-	-	+
18	L_b	+	+	+	-
19	H_b	+	+	-	+
20	H_t	+	+	+	-
21	W_i	+	+	+	-
22	D_i	+	-	+	-
23	θ_s	+	+	+	+
24	W_s	+	+	+	-
25	D_s	+	+	+	-
26	W_o	+	+	+	+
27	D_h	+	-	+	+
	Total	21	17	19	12

Note:- + Variable in the theoretical model

- Variable not in the theoretical model

Table 3.3 Repeating variables for the mathematical models for air and particle dynamics in the 2DSBs with draft plates and variables representing mass, length, and time.

No	Symbol	Mathematical models			
		P_s	U_f	M_p	t_c
1	ρ_f	-	+	+	-
2	g	+	+	+	-
3	M_p	-	-	-	+
4	M_b	-	-	-	+
5	d_p	-	+	-	+
6	ρ_p	+	-	-	-
7	H_t	+	-	-	-
8	W_o	-	-	+	+
	L	H_t	d_p	W_o	d_p
	M	$\rho_p H_t^3$	$\rho_f d_p^3$	$\rho_f W_o^3$	M_b
	T	$(H_t/g)^{1/2}$	$(d_p/g)^{1/2}$	$(W_o/g)^{1/2}$	M_b/M_p

3.1.1 Spouting Pressure Drop

According to Issacson and Issacson (1975), in the dimensional matrix, let the first variable be the dependent variable, let the second variable be that which is easiest to regulate experimentally. Let the third variable be that which is next easiest to regulate experimentally and so on. In this way, the pertinent variables proposed in Table 3.2 for the modelling of spouting pressure drop were arranged and then reproduced:

$$f\,(P_s,U_f,\rho_f,\mu,g,Q_p,d_p,\rho_p,\phi,\varepsilon_v,W_o,D_h,\\ W_s,D_s,\theta_s,L_b,H_b,W_i,D_i,W_b,H_t) = 0 \tag{3.2}$$

Taking the independent variables from equation (3.2) and using the repeating variables for the MLT reference dimensions given in Table 3.3, the following dimensionless PI numbers were generated for the P_s:

$$f\left(\begin{array}{c}\frac{P_s}{g\rho_p H_t},\frac{U_f^2}{gH_t},\frac{\mu^2}{g\rho_f^2 d_p^3},\frac{Q_p}{Q_f},\frac{d_p}{H_t},\frac{\rho_p-\rho_f}{\rho_f},\ \phi,\ \varepsilon_v,\frac{W_o}{H_t},\\ \frac{D_h}{H_t},\frac{W_s}{H_t},\frac{D_s}{H_t},\ \theta_s,\frac{L_b}{H_t},\frac{H_b}{H_t},\frac{W_i}{H_t},\frac{W_b}{H_t},\frac{D_s}{D_i}\end{array}\right)=0 \qquad (3.3)$$

The dimensionless numbers can be transformed in to some well known dimensionless numbers in order to simplify the relationship for spouting pressure drop. The number of dimensionless terms should however remain the same after transformation, otherwise, the new products do not form a complete set. The transformed numbers which were used in the analysis of data for establishing the following relation for spouting pressure drop are shown:

$$F\left(\begin{array}{c}\frac{P_s}{g\rho_p H_t},F_r,A_r,\frac{Q_p}{Q_f},\frac{d_p}{H_t},\frac{\rho_p-\rho_f}{\rho_f},\ \phi,\ \varepsilon_v,\\ \frac{W_o}{H_t},\frac{D_h}{D_s},\frac{W_s}{W_i},\frac{D_s}{d_p},\ \theta_s,\frac{L_b}{W_o},\frac{H_b}{H_t},\frac{W_i}{d_p},\frac{D_s}{D_i},\frac{W_b}{W_o}\end{array}\right)=0 \qquad (3.4)$$

However, this is not a unique set, since other groups of eighteen independent dimensionless products could be formed from the PI numbers given in equation (3.3) by multiplication or division. It should be noted that this procedure of theoretical development of spouting pressure drop was applied to the minimum spouting velocity, the solids circulation rate, and the average cycle time regardless of number of pertinent variables.

3.1.2 Minimum Spouting Velocity.

The relevant variables from Table 3.2 for the development of the model for superficial spouting velocity through the spouted bed were arranged:

$$f\,(U_f,\ \rho_f,\ \mu, d_p,\ \rho_p,\ \phi,\ \varepsilon_v,\ g, W_o,\ W_s, D_s, \theta_s, H_b, L_b, W_i, W_b, H_t) = 0 \qquad (3.5)$$

Considering the constituting variables given in equation (3.5) and applying the repeating variables for MLT from Table 3.3, the following dimensionless numbers were obtained:

$$f\left(\begin{matrix}\dfrac{U_f^2}{gd_p}, \dfrac{\mu^2}{g\rho_f^2 d_p^3}, \dfrac{\rho_p-\rho_f}{\rho_f}, \phi, \varepsilon_v, \dfrac{W_o}{d_p}, \dfrac{W_s}{d_p}, \\ \dfrac{D_s}{d_p}, \theta_s, \dfrac{H_b}{d_p}, \dfrac{L_b}{d_p}, \dfrac{W_i}{d_p}, \dfrac{W_b}{d_p}, \dfrac{H_t}{d_p}\end{matrix}\right) = 0 \qquad (3.6)$$

The DP's of equation (3.6) were transformed into the following DP's for establishing the relation for superficial spouting velocity through the spouted bed at the minimum spouting conditions:

$$F_r = f\left(A_r, \frac{\rho_p-\rho_f}{\rho_f}, \phi, \varepsilon_v, \frac{W_o}{L_b}, \frac{W_s}{W_i}, \frac{D_s}{W_o}, \theta_s, \frac{W_s}{H_b}, \frac{W_b}{H_t}, \frac{d_p}{W_i}, \frac{W_b}{W_o}, \frac{H_t}{H_b}\right) = 0 \quad (3.7)$$

3.1.3 Solids Circulation Rate

The relevant variables given in Table 3.2 for the development of the model for the solids circulation of rate (average particle velocity) were arranged:

$$f\,(V_p, d_p, \rho_p, \phi, \varepsilon_v, g, U_f, \rho_f, \mu, W_o, D_h, W_s, D_s, \theta_s, L_b, W_i, D_i, H_t) = 0 \quad (3.8)$$

Taking the considered variables in equation (3.8) and using the repeating variables from Table 3.3, the following dimensionless numbers were developed:

$$f\left(\begin{array}{c}\dfrac{V_p}{(gW_o)^{0.5}}, \dfrac{d_p}{W_o}, \phi, \varepsilon_v, \dfrac{U_f^2}{gW_o}, \dfrac{\mu^2}{g\rho_f^2 W_o^3}, \dfrac{\rho_p-\rho_f}{\rho_f}, \\ \dfrac{D_s}{D_h}, \dfrac{W_o}{W_i}, \dfrac{L_s}{W_o}, \dfrac{W_s}{W_i}, \theta_s, \dfrac{W_b}{W_o}, \dfrac{D_s}{D_i}, \dfrac{H_t}{W_o}\end{array}\right) = 0 \quad (3.9)$$

The PI numbers given in equation (3.9) were transformed in to the following dimensionless numbers:

$$\frac{V_p}{(gW_o)^{0.5}} = f\left(\begin{array}{c}\frac{d_p}{W_o},\phi,\varepsilon_v,F_r,A_r,\frac{\rho_p-\rho_f}{\rho_f},\frac{D_s}{D_h},\frac{W_o}{W_i},\\ \frac{W_s}{W_o},\frac{W_s}{W_i},\theta_s,\frac{L_b}{W_o},\frac{D_s}{D_i},\frac{H_t}{W_o}\end{array}\right) = 0 \qquad (3.10)$$

The theoretical solids circulation rate would then be:

$$M_p = \rho_b A_d V_p \qquad (3.11)$$

or,

$$\frac{M_p}{\rho_b A_d (gW_o)^{0.5}} = f\left(\begin{array}{c}\frac{d_p}{W_o},\phi,\varepsilon_v,F_r,A_r,\frac{\rho_p-\rho_f}{\rho_f},\frac{D_s}{D_h},\frac{W_o}{W_i},\\ \frac{W_s}{W_o},\frac{W_s}{W_i},\theta_s,\frac{L_b}{W_o},\frac{D_s}{D_i},\frac{H_t}{W_o}\end{array}\right) = 0 \qquad (3.12)$$

3.1.4 Average Cycle Time.

The relevant variables from Table 3.2 which may constitute the mathematical model of average cycle time were arranged:

$$f\,(t_c,M_p,M_b,d_p,\phi,W_o,\theta_s,D_h,H_b,W_d) = 0 \qquad (3.13)$$

Taking the pertinent variables from equation (2.13) and using the repeating variables given in Table 3.3, the following dimensionless PI numbers were generated:

$$f\left(\frac{t_c M_p}{M_b},\phi,\theta_s,\frac{W_o}{d_p},\frac{D_h}{d_p},\frac{H_b}{d_p},\frac{W_d}{d_p}\right) = 0 \tag{3.14}$$

The dimensionless numbers in equation (3.14) were transformed in to the following DPs to simplify the relationship for average cycle time:

$$\frac{t_c M_p}{M_b} = f\left(\phi,\frac{W_o}{d_p},\theta_s,\frac{d_p}{D_h},\frac{H_b}{W_o},\frac{W_d}{D_h}\right) \tag{3.15}$$

3.2 Drying of grains.

A spouted bed with draft tube or plates operates under two distinct regions as does the conventional spouted beds: (1) Dilute phase in draft tube/channel (spout) and fountain, and (2) Dense phase in the downcomer (annulus). In the dilute phase, the circulating particles are fully exposed to the turbulent flow of the spouting medium. The average mass flow of gas in the spout region is often two to three orders of magnitude higher than in the downcomer, whereas the volume concentration of particles is at most one-fifth of that in the dense phase (Mathur and Epstein, 1974b; Khoe and Brakel, 1980; Claflin and Fane 1984b). Under these conditions, the drying gas would attain thermal equilibrium with bed particles within a few cm of its entry into the downcomer, while the distance necessary for the spout gas to achieve equilibrium would be greater by one or two orders of magnitude (Epstein and Mathur, 1971). However, the temperature inside the particles will not be the same as the surface temperature because of the short residence time (less than 1 second) of particles in the spout region. The interparticle and intraparticle gradients developed in the dilute phase are effectively relaxed in the dense phase. The time required to reach a uniform temperature in the particles under typical conditions would be in the range of 5 to 10 seconds. These conditions are fulfilled only in the downcomers where the time spent by the particles is usually higher than 10 seconds. After tempering, the particles in the lower parts of a falling bed will be a few degrees cooler than they were at the top of the dense phase. When the particles reach the entrainment zone and contact much hotter gas, a temperature gradient inside the grain redevelops. During batch drying, the bed attains an approximately uniform temperature after a certain time interval, and this temperature rises to a near constant value after long time. That temperature is, however, lower than the inlet air temperature due to heat losses from the dryer unit.

As soon as the batch of grains is placed in the spouted bed, the warming-up of grains begins and the moisture starts to evaporate from the surface of particles. As the drying continues, the surface moisture content of grains diminishes and moisture has to come from the interior of particles by liquid and/or vapour diffusion. However, as the surface layer of grains dries, the interior moisture must cross many layers to reach the surface. This results in a decreasing of the drying rate. Hence, the drying rates of grains increase with temperature and fall with time.

The thin layer model of removal of moisture from the surface of grains in spouted beds with draft tube is fully justified in the dilute phase where air flow is about three times that in the downcomers. In the dense phase, the residence time of particles is of the order of a minute or two at air flow rates about one-fourth of the total air flow through the bed. This does not satisfy the conditions for thin layer drying, but minimum drying is nevertheless expected. Since the majority of heating and moisture removal takes place in the dilute phase with relaxing effects in the dense phase, the drying process in a spouted bed with or without draft tube may be considered to be thin layer drying if the relaxation effects in the downcomer are taken into account. Furthermore, it can be represented by non-steady-state heat and mass equations, mass and energy balances on grain and air, and necessary boundary conditions (Becker and Isaacson, 1970). The equations (2.18) through (2.28) can be used for this purpose.

A similar non-steady-state approach can be applied to account for temperature variations in a grain kernel over time using necessary boundary conditions. Drying in the falling rate period per cycle of a particle can then be determined using the full temperature-moisture history and the intraparticle gradients by numerical solutions along with the knowledge of longitudinal profiles of gas and particle velocities, gas temperature, voidage in the spout, average cycle time, and mass of grains in the bed. The conditions attained at the end of one cycle will be the initial conditions for the next cycle. This approach leads to rigorous and tedious calculations for finding the required moisture content in the grains. Hence, batch drying of grains in the spouted bed is very complex and theoretical models based on diffusion may not account for all aspects of biological materials.

The drying behaviour of individual grains can be described by the differential diffusion equation (2.18) quite accurately if the relationships of diffusion coefficient to moisture content and temperature are known. However, the possible errors in measuring the dimensions of a grain kernel and in estimating the value of the diffusion coefficient from the moisture content and temperature data limits the applicability of this equation. Therefore, the use of semi-empirical models is often preferred (Misra and Brooker, 1980; White et al., 1981; Hutchinson and Otten, 1983; Syarief et al., 1984; Li and Morey, 1984; Bruce, 1985; Byler et al., 1987; Li et al., 1987; Jayas and Sokhansanj, 1989). The best one appears to be the Page model (Equation 2.26) which overcomes the shortcomings of the exponential model by providing a tempering effect with time and adjusts for error resulting from the neglection of internal resistance to moisture transfer. Accounting for tempering effects makes the Page model particularly suitable for modelling the conditions of draft tube spouted beds where the moisture relaxation is pronounced. To verify the other models, the diffusion type equation (2.23) and the lump parameter equation (2.25) were also considered for modelling the drying of shelled corn in the two similar slotted two- dimensional spouted beds with draft plates.

The modified Henderson and Chung-Pfost models can be used to estimate the equilibrium moisture content (M_e) for shelled corn. However, they can not be applied with confidence if the air relative humidity at the inlet conditions is below 20 % (ASAE). The literature searched indicated that the data collected by Hall and Rodriguez-Arias (1958) on shelled corn covers the range of relative humidity in experiments; thus they were used for the empirical models.

To develop the relevant relationships the following assumptions have been made:-

1) Shrinkage of grains during drying has a negligible effect on moisture diffusivity and hydrodynamics conditions. However, some reduction in the height of bed

and the average cycle time occurs due to shrinkage in bed volume as drying proceeds.

2) The grain is homogeneous and isotropic.

3) The major fraction of heat and mass transfer takes place in the dilute phase relative to that in the downcomer, the fraction of total residence time spent by the kernel in the spout is insignificant.

4) In most cases, the inlet temperature of a spouted bed can be so high that equilibrium relative humidity may be considered to be zero. Similarly, the equilibrium moisture content can be assumed equal to zero.

IV EXPERIMENTAL MATERIALS AND PROCEDURES

4.1 Design and Fabrication of Spouted Beds.

The mechanical design of the pilot scale slotted 2DSB was primarily aimed to permit variation of bed length, bed width, slant angles, air entry slots, separation distance, and spout width. A rectangular frame with four support legs was made from angle iron. Four iron bars were bolted on the legs at some distance below the top rectangular frame. On the length side bars two screw bolts were installed for achieving vertical motion or levelling of the bed. Two angle-irons of about two meters in length were fixed onto the two screw bolts parallel to the width side of the rectangular frame. On each angle-iron, two screw rods of one meter length, starting from the centre line of the rectangular frame were installed with proper bushings, controls, and long nuts for obtaining different bed lengths, airtight conditions in the bed, and horizontal to and fro motion of width sides of the bed. Two wooden planks were fixed with proper attachments on the long nuts, starting from centre line of the rectangular frame parallel to the length side of the rectangular frame. The sides of the bed were constructed using plexiglas and reinforced with angle-irons. The width sides of bed were rigidly fixed at the inner edge of each wooden plank. The length sides of the unit can be clamped on the width sides of the bed. The fabricated unit can accommodate different slantings on the length sides. This pilot scale unit was built with 0.75 m width, 0.0 to 0.47 m length, and 2.0 m height. The designed unit can handle a maximum volume of 0.705 m^3 of grain excluding the fountain portion. The pilot scale two-dimensional spouted bed unit with draft plates is shown in Figure 4.1.

Figure 4.1 A view of the pilot scale two-dimensional spouted bed unit.

A steel structure with bottom dimensions of 2.5 m x 4.5 m and top dimensions of 1.3 m x 2.5 m was designed and fabricated. A hopper with discharge gate was made of sheet metal and was fixed on four legs with holes for vertical movement. Hopper legs were then fixed to the top of the steel structure on the two steel bars for horizontal movement at a fixed vertical height.

The spout pressure measuring taps were positioned starting at 0.01 m and at intervals of 0.10 m from the bottom of the bed through out the height. The spout pressure drop taps were fixed on one width side of the bed. The downcomer pressure measuring taps were installed on a length side of the bed above the slanting base at an interval of 0.10 m.

A laboratory scale two-dimensional unit was also built for geometrical similarity purposes. This unit was fabricated with fixed dimensions of 0.50 m x 0.04 m x 1.50 m. A separate rigid base structure was built from the angle irons with a wooden plank on it, on which this unit was fixed. The laboratory scale model can have different slantings and air-entry slot widths. The spout pressure drop taps were installed at 0.01 m and others at intervals of 0.05 m from the bottom to top of the unit on one side of the spout. The downcomer pressure taps were positioned on a length side of the unit at an interval of 0.05 m above the slanting base.

A complete air supply pipe system was fabricated from the sheet metal for both units. The system was fitted with pressure and air regulating valves/gates, thermal anemometer, pitot tubes, electric heaters, thermocouples and interchangeable air inlet pipes. Parts such as load cell assembly, static vertical pressure plates, air entry slot nozzles, screens, slanting angles, draft plates, thermocouples, grain samplers, and deflectors for the two units were made from different materials as the research work progressed.

A number of test runs to determine optimum deflector placement were performed with the pilot-scale unit and various grain types. It was found that they should be placed above the draft plates at a height equal to 30% of the draft plate height.

4.2 Static Vertical Pressure.

4.2.1 Apparatus and materials.

The proposed experiments on the static vertical pressure of grains on the air-entry slots were performed in the pilot scale unit without injecting air through the bed. For this purpose, a bed length of 0.05 m and bed to air-entry aspect ratios of 5, 10, and 15 were chosen. The bed to air-entry width aspect ratios of 5, 10, and 15 resulted in air-entry areas of 0.05 x 0.15 m^2, 0.05 x 0.075 m^2, and 0.05 x 0.05 m^2, respectively. For these areas, three plexiglas plates, 0.047 x 0.147 m^2, 0.047 x 0.072 m^2, and 0.047 x 0.047 m^2 were cut. A load cell mounting jack was fabricated from angle irons with a vertical screw rod at the top. The Daytronic model 152A-100 transducer (load cell) was mounted on top of the screw rod (Figure 4.2) firmly and the selected plexiglas plate was fixed on it.

The reviewed literature on silo pressures and spouted beds showed that wheat grain has been investigated widely while only a few studies were done on barley, beans, corn, oats, peas, and flax seed. Since corn grain is grown and artificially dried on a large scale in the North America, it was chosen for this study. Wheat was also chosen because of its importance worldwide and for data evaluation

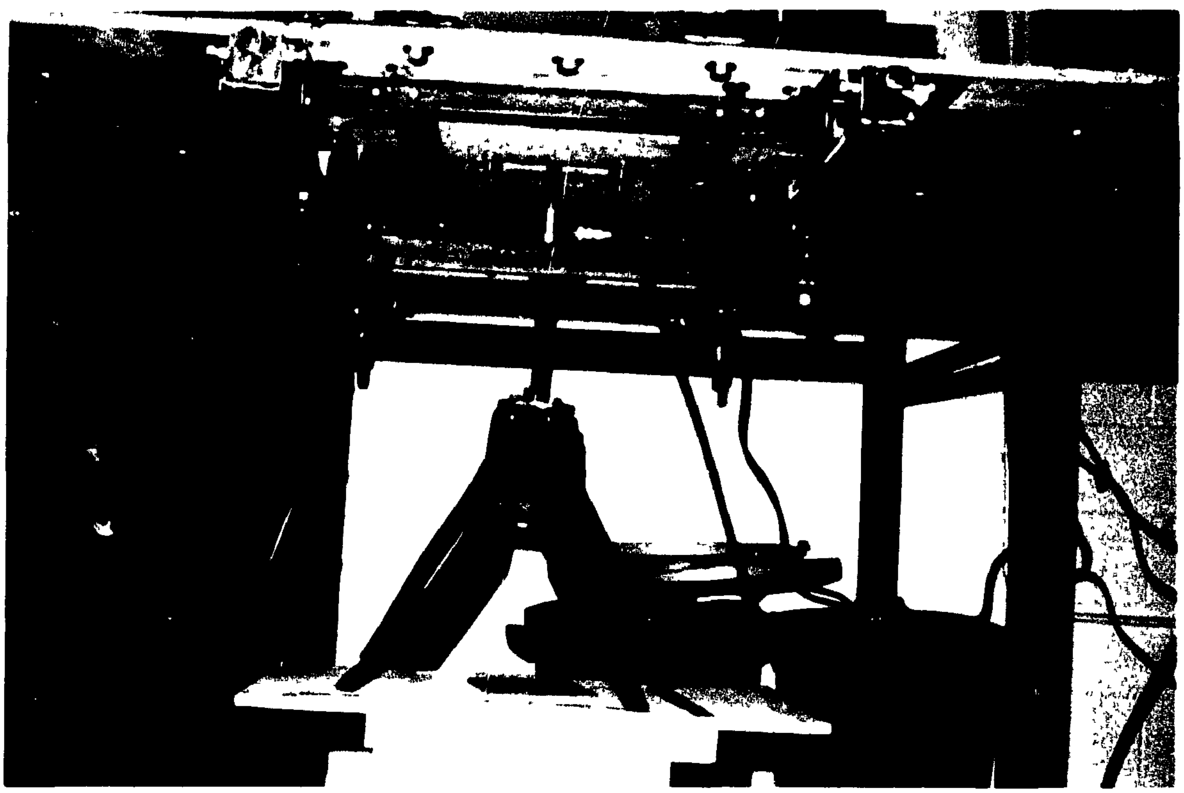

Figure 4.2 Load cell along with mounting jack in use.

purposes. In addition, soybean was chosen because it has approximately the same bulk density as wheat but has more sphericity or roundness.

The experiment to determine the static vertical load of grain mass on the air-entry slot of a two-dimensional nonaerated spouted bed was performed with combinations of the following variable settings: (a) bed to air-entry area aspect ratios of 5, 10, and 15; (b) slantings of 0°, 30°, and 60°; (c) bed heights of 0.4 m, 0.8 m, 1.2 m, and 1.6 m; (d) grain varieties - shelled corn (yellow dent), soybean (maple arrow), and wheat (laval-19).

4.2.3 Design of experiment and procedures.

A split-split-split plot experiment in randomized complete block design with three replications was adopted for these experiments because of the unit assembling and dismantling difficulties. The bed to air-entry slot area aspect ratios were randomized to main plots, the slant angles randomized to subplots, the grain varieties were randomized to the sub-subplots, and the packed bed heights were randomized to the sub-sub-subplots.

The unit was clamped, then the load cell was fixed to the appropriate plexiglas plate, calibrated, placed at the air- entry slot and adjusted to the required level (Figure 4.2). The grain hopper gate was fixed about 0.2 m above the top of the unit for all experimental runs. The hopper gate was closed and approximately 0.125 m^3 volume of grain was placed in the hopper. The X-Y Recorder output was brought to zero and the data recording button was turned on. The hopper gate was opened quickly to the fixed position. The grain discharge rate was about 2.4 m^3/hr. When the required packed bed height of grains was approached, the gate was closed quickly. When the X-Y Recorder pen achieved a linear horizontal state, data recording was stopped. The unit was completely emptied and the grains were weighed to an accuracy of ± 10 g. In this way, a total of 324 data points were collected to represen 'he behaviour of grain static vertical pressure.

4.3 Dynamics of Spouted Bed.

4.3.1 Apparatus and materials.

The dynamics experiments were carried out in the pilot scale unit. The width and height of the bed were held constant at 75 cm and 135 cm, respectively. The bed width to length aspect ratio was also kept constant at 15, giving a bed length of 5 cm. The air entry slot was kept constant at a bed width to air entry slot width aspect ratio of 15, giving an air entry slot width of 5 cm. The length of the air entry slot was the same as that of the bed i.e. 5 cm. A large-mesh screen was placed over the air entry slot to prevent grains from falling into the air inlet duct. The separation distances considered were 2, 3, and 4 times the air entry slot width i.e. 10 cm, 15 cm, and 20 cm. The spout widths selected were 1, 1.5, and 2 times the air entry slot width i.e. 5 cm, 7.5 cm, and 10 cm. These choices were based on previous findings (Buchanan and Wilson, 1965; Khoe and Brakel, 1980; Claflin and Fane, 1983; Law et al., 1984; Law et al., 1986). Three pairs of draft plates were made from steel channel. The length of each pair was 125 cm, 120 cm, and 115 cm. The width of all draft plates were equal to the bed length i.e. 5 cm. A curved deflector was also made from sheet metal.

The literature on spouted beds indicates that slant angles of 45° and 60° are equally adapted to CSB's and 2DSB geometries. Hence, both slant angles were used in these experiments. The same grain varieties - shelled corn (Yellow dent), soybean (Maple arrow), and wheat (Laval-19) - as used in the vertical static pressure study were used in the current experiments. The beds were spouted in a batch mode at air-inlet temperatures ranging from 14.7° to 33.6° C under steady state conditions.

4.3.2 Design of experiments and procedures.

A split-split-plot experiment in randomized complete block design with three replicates was selected for these experiments. Slant angles were randomized to the main plots, draft tube widths were randomized to the subplots and separation distances were randomized to the sub-subplots. A screen was placed on the air entry slot and the unit was clamped tightly. The curved deflector was fixed to the proper height as explained in the section 4.1.

A variety of grains was placed in the hopper and the blower was turned on. A bleed valve between the blower and the bed was adjusted to get the minimum air flow through the empty bed. The grain was then discharged from the hopper into the bed at a minimum fixed rate. As the bed height gradually increased, the spouting pressure and air flow through the bed were continuously adjusted by closing the bleed valve until stable spouting was achieved. When the required bed height (i.e. 135 cm) was attained, the hopper valve was closed and the bleed valve was tuned to the minimum spouting conditions. The bed was spouted until steady state conditions were reached. The data on spouting pressure drop, air velocity through the air entry slot, particle velocity, particle cycle time (limited to third replicate only) for each type of grain, inlet air temperature, and atmospheric pressure were recorded. Grains from the bed were removed and weighed to an accuracy of ± 10 g.

The spouting pressure drop was measured using a calibrated transducer equipped with a digital voltmeter with accuracy ± 0.5 % (Figure 4.3). The velocity of air through the conveying pipe was measured with dwyer pitot tubes (accurate to ± 3 %) using a calibrated transducer with accuracy ± 0.4 % or a Dwyer Thermal Anemometer (series 470) accurate to ± 3 %. Particle velocities in the downcomers were measured by noting the time of passage of individual coloured grains at 0.075 m, 0.175 m, 0.275 m, and 0.375 m from the centre of spout between the top of the bed and above the slanting base. The particle cycle times were measured in the downcomers at the same distance from the centre of the spout as for particle velocities. Inlet air temperatures were measured with J-type thermocouples via a digital thermometer accurate to ± 0.5° C. 162 data points were obtained for each variable. Moisture content was determined on grain samples before and after each run.

4.4 Standardization of Spouted Beds.

In a spouted bed, there are two crucial factors with respect to drying of grains and operation of the bed. For drying of grains, solids to air mass ratio is very important and from the operational point of view, spouting pressure drop is very important. It was therefore decided that further experiments on scale-up and drying of shelled corn should be carried out with standard settings of slant angle, spout width, and separation distance in order to find an optimum solids to air mass ratio at the lower spouting pressure drop. To achieve this objective, the minimum spouting velocity, solids circulation rate, and spouting pressure drop data were analyzed using the STATGRAPHICS (1989) package. The analysis showed that the magnitude of solids-to-air mass and solids-to- air volumetric flow rate ratios for a slant angle 60° were about 4.0 and 4.9 times higher than for a slant angle 45°. However, there was almost no difference in spouting pressure drop due to slant angle. A slant angle of 60° was therefore chosen for further work.

The analyzed data indicated that there were also significant differences due to spout width and separation distance (significance level of 0.01). The means of solids-to-air mass ratio and spouting pressure drop were plotted (Figures 4.3, 4.4, respectively). The plots indicate that the spout width 0.075 m and the separation distance 0.15 m are very promising for drying of cereal grains. Therefore, a slant angle of 60°, a spout width of 0.075 m (1.5 times the air-entry slot width), and a separation distance of 0.15 m (3 times the air-entry slot width) were adopted as the standard settings for the slotted two-dimensional spouted beds with two draft plates.

4.5 Scale-up.

4.5.1 Apparatus and materials.

This study was performed in two geometrically similar slotted 2DSB units with two draft plates. The laboratory scale had dimensions of 0.50 m x 0.04 m x 0.90 m. The air entry slot width was 0.033 m and a slant angle of 60°, (see section 4.4). An air entry duct system, a pair of slant angles, a pair of draft plates of 0.80 m length, and a deflector were fabricated from sheet metal with width equal to the

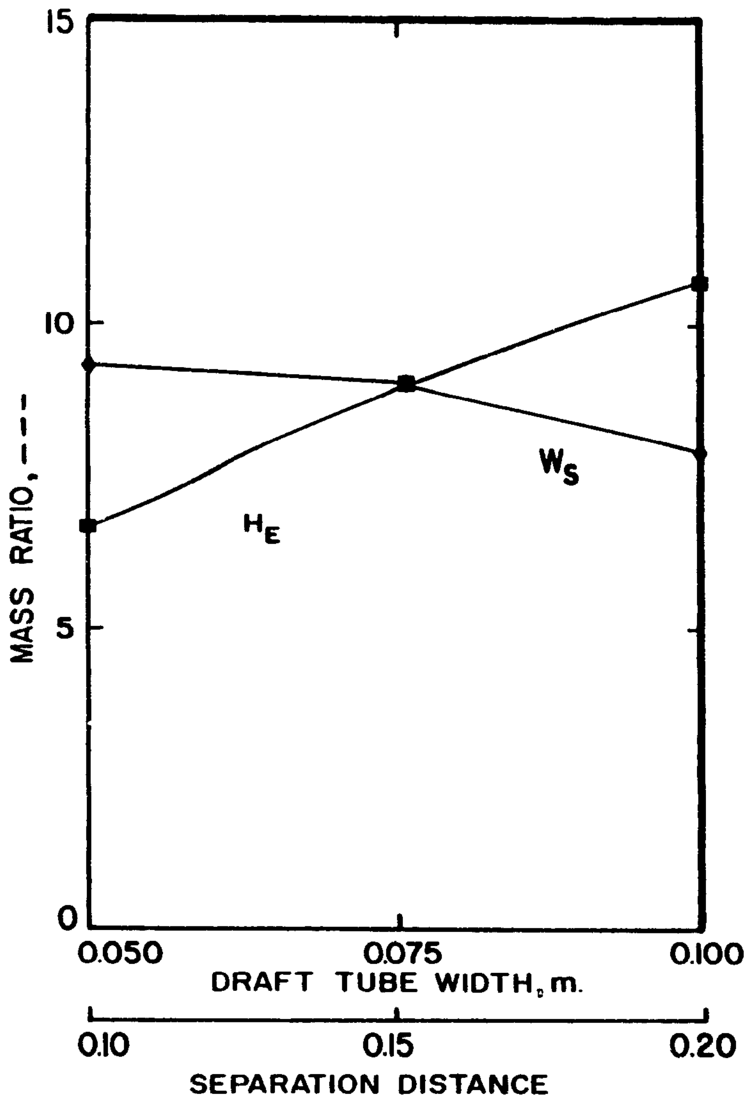

Figure 4.3 Solids to air mass ratio as the function of draft tube width and separation distance for pilot scale.

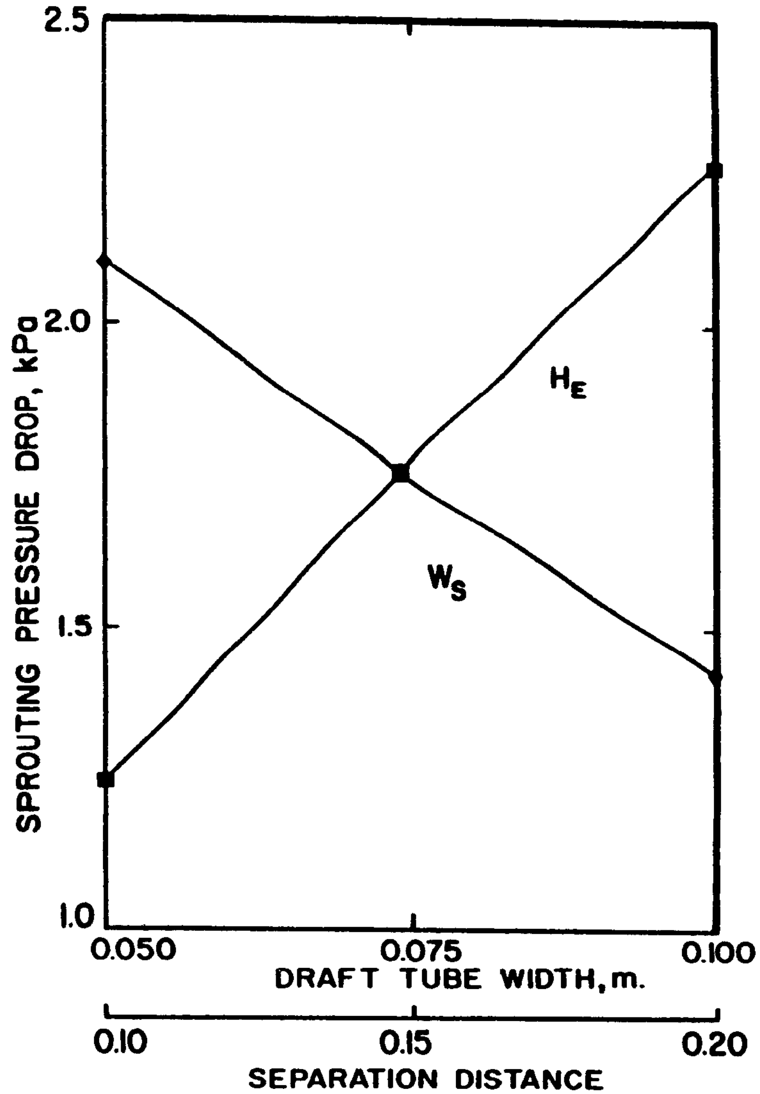

Figure 4.4 Spouting pressure drop as the function of draft tube width and separation distance for pilot scale.

bed length (0.04 m). The spout width was 0.05 m (1.5 times the air entry slot width) and the separation distance was 0.10 m (3 times the air entry slot width).

The dimensions of the pilot scale unit were 0.75 m x 0.06 m x 1.35 m. The air entry slot width was 0.05 m and the slant angle was also 60°. An air entry duct system, a pair of slant angles, a pair of draft plates of 1.20 m length, and a deflector were fabricated from sheet metal with width equal to the bed length (0.06 m). The separation distance was 0.15 m (3 times the air entry slot width) and the spout width was 0.075 m (1.5 times the air entry slot width).

The scale-up achieved by increasing the bed length was performed in the pilot scale unit. The bed lengths of interest were 0.05 m, 0.075 m, 0.10 m, 0.125 m, and 0.15 m. Five air-entry slot ducts, five pairs of draft plates of length 1.2 m, and five deflectors were manufactured from sheet metal with widths equal to the various bed lengths. Five pairs of slant angles were also built to suit the bed lengths.

The same grain varieties used in the previous experiments were purchased during the harvesting season. Sufficient quantities of undried shelled corn and dried soybean and wheat grains were stored in a refrigeration unit at 4° C until used. The grains were spouted in batch mode at air-inlet temperatures ranging from 20° to 44.5° C under steady state conditions.

4.5.2 Design of experiment and procedure.

A split-plot experiment in randomized complete block design with three replicates was planned for studying the laboratory and pilot scale units. Bed sizes (laboratory or pilot) were randomized to the main plots and the grain varieties were randomized to subplots.

A split-plot experiment in randomized complete block design with three replicates was selected for the scale-up achieved by increasing the length of pilot scale bed. The bed lengths were randomized to the main plots and the grain varieties were randomized to the subplots. The procedure followed in Section 4.3.2 was followed.

4.6 Drying of Shelled Corn.

4.6.1 **Apparatus and materials.**

The drying of shelled corn was performed in the geometrically similar two slotted 2DSBs with draft plates and slant angle of 60°. The dimensions of the laboratory scale bed unit were 0.50 m x 0.04 m x 1.50 m, air entry slot width 0.033 m, spout width 0.05 m, separation distance 0.10 m, and the length of draft plates 0.80 m. The dimensions of pilot scale bed unit were 0.75 m x 0.06 m x 2.00 m, air entry slot width 0.05 m, spout width 0.075 m, separation distance 0.15 m, and length of draft plates were 1.20 m. Two samplers per bed were installed for collecting grain samples during drying runs. Adequate thermocouples were positioned in the both beds for recording air and material temperatures as shown for laboratory scale in Figure 4.5 and for pilot scale models in Figure 4.6. Four electric 6000 Watt heaters were also installed in the air conveying duct with proper controls and regulators.

Shelled corn (yellow dent) was used in this investigation based on its importance in this part of the world. The beds of shelled corn were spouted in

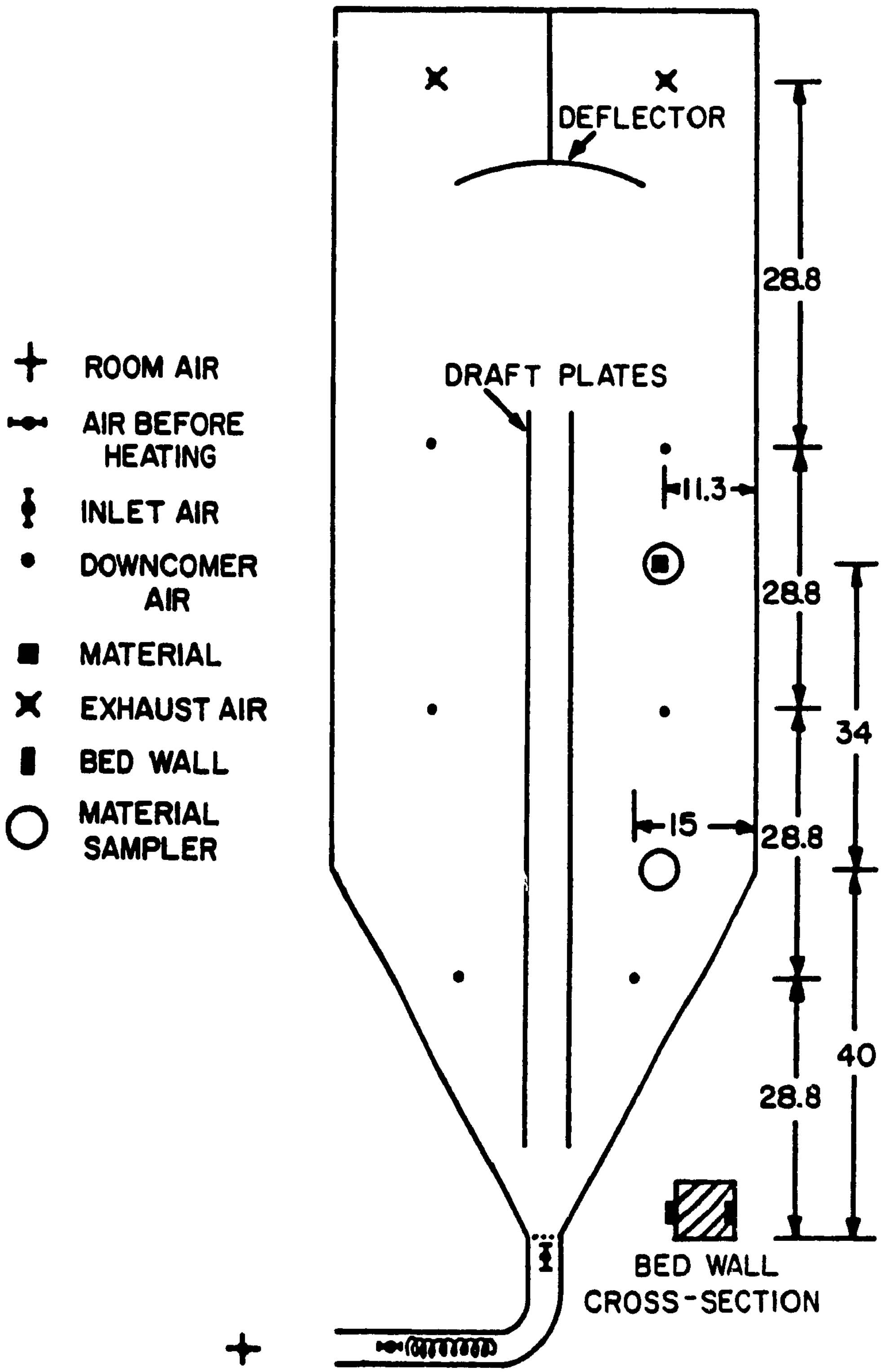

Figure 4.5 Location of thermocouples in the laboratory scale bed.

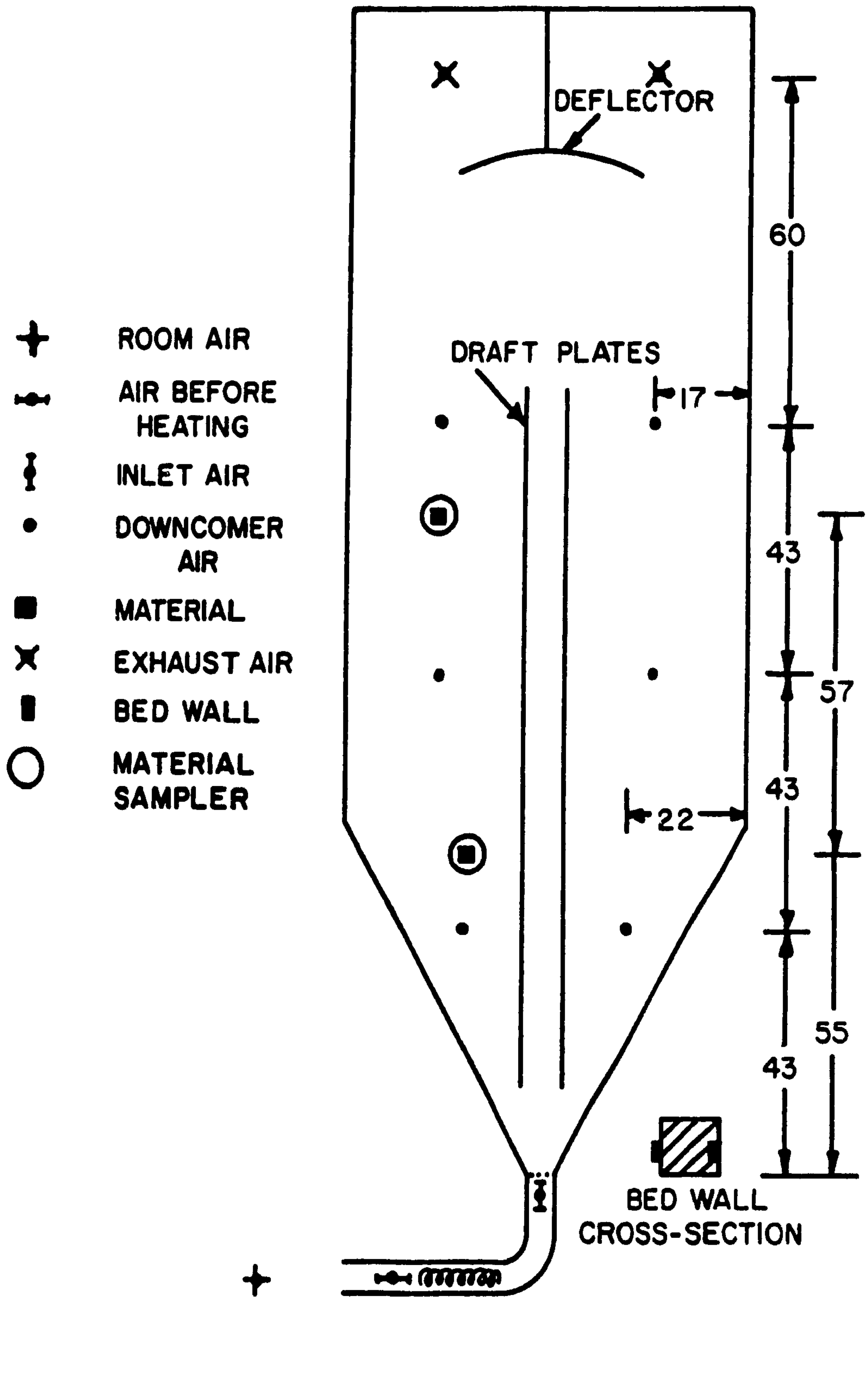

Figure 4.6 Location of thermocouples in the pilot scale bed.

batch mode at air-inlet temperatures of 50°, 70° under steady state conditions. Additional runs at 90° C were performed in the laboratory scale bed.

4.6.2 Design of experiment and procedure.

A split-split-plot experiment in randomized complete block design with one replicate was adopted for the drying runs in the two similar spouted beds with draft plates. The bed sizes (laboratory or pilot) were randomized to the main plots, the air inlet temperatures were randomized to the subplots, and the bed heights were randomized to the sub-subplots.

The air supply blower was turned on and the bleed valve between the blower and the bed was adjusted using previous working experience to a minimum air flow through the empty bed. The electric heaters were then turned on and the temperature regulator was adjusted to the selected inlet temperature. The empty bed was left for warm-up from two to four hours in order to achieve steady state conditions. Wet grain was then put in the hoppers and discharged quickly into the bed. Temperature readings and grain samples were collected at intervals of five minutes. The data on spouting pressure drop, air velocity through air supply duct, particle velocities, cycle times, atmospheric pressure, and mass of grains were noted as explained in section 4.3.2. The drying of shelled corn was terminated after one to two and half hours depending upon inlet temperature and bed height.

Inlet air temperature was maintained to within ± 1° C by an electric heater fitted with autotransformers and temperature controller. Dry and wet bulb temperatures at the blower inlets were measured with a sling psychrometer at the beginning and end of each experimental run. Relative humidity was thus obtained.

The inlet and outlet air temperatures as well as the air temperature in the downcomers along the height of bed were monitored with K-type open junction thermocouples (Omega Engineering Corp.). The bed material temperature was measured by thermocouples mounted inside the two samplers. The wall temperature, needed for heat loss calculations, was measured by two thermocouples embedded 0.5 mm in the downcomer wall and attached to it by silver epoxy. The temperature at all measuring points was recorded by an OM-302 Temperature Logger (Omega Engineering Corp.) having an accuracy of $\pm$ 0.5 °C.

Grain samples of 40 g to 100 g were also collected before the drying of each batch to determine initial moisture content. The initial temperature of each drying batch was also noted, using a mercury thermometer.

4.7 Physical Properties of Materials.

4.7.1 **Grain.**

The grain samples collected during the static vertical pressure, aerodynamics, scale-up, and drying of shelled corn were weighed with an accuracy of $\pm$ 0.001 g. The samples were dried in a convection oven using the ASAE (1982) standard procedure of moisture measurement for grain and seeds. The oven dried samples were placed in the desiccator and were reweighed after cooling. The grain moisture data was used to calculate wet and dry basis moisture contents.

The three major axes of the grain varieties used in these experiments were measured with a metric vernier calliper having a least count of 0.01 mm. Grain samples of 32 kernels per variety were taken at random and their triaxial dimensions were measured (see Tables A.1 and A.2) according to the standard method reported by Mohsenin (1970). The geometric mean diameter and the sphericity of grains were calculated from the triaxial dimensions by the following equations:

$$d_p = (abc)^{\frac{1}{3}} \quad (4.1)$$

and,

$$\phi = \frac{geometric\ mean\ diameter}{major\ diameter} = \frac{(abc)^{\frac{1}{3}}}{a} \quad (4.2)$$

The bulk densities of the grains were determined before and after the experiments using a one litre pyrex graduated cylinder. The grains were freel poured in the graduated cylinder and their mass was determined using an electronic balance accurate to ± 0.01 g (sec Tables A.1 and A.2).

Particle densities were determined using distilled water and toluene ($C_6H_5CH_3$) in specific gravity bottles or pycnometers. The pycnometer method described by Mohsenin (1970) was followed and grain samples having kernels in the range of 200 to 300 were used for calculating the specific gravity of each grain variety (see Tables A.1 and A.2).

The emptying angles of repose for grains used in the static vertical pressure studies were determined in the pilot scale unit using flat bottoms and leaving a 0.05 m x 0.05 m air-entry slot area. The air-entry slot was closed at the bottom the bed was charged to about 0.45 m depth The air-entry slot was slowly brought to the fully-open position and when the flow of grains through the slot completely stopped, the angles formed on both sides were measured (see Table A.1).

4.7.2 Fluid.

The viscosity of air passing through the spouted beds was estimated using the empirical equation (9.1) and the air inlet temperatures. Air density was calculated using the following formula:

$$\rho_f = \frac{P_{BP}}{RT} \tag{4.3}$$

V RESULTS AND DISCUSSION

The basic pillars of this research were the two-dimensional spouted bed units described in CHAPTER IV: "EXPERIMENTAL MATERIALS AND PROCEDURES". The major aspects studied were: (1) Static vertical pressure, (2) Aerodynamics, (3) Scale-up, and (4) Drying of grains. Shelled corn, soybean, and wheat were used as test materials in the first three parts in order to incorporate grain particle characteristics to the applicability of 2DSB's. Only one grain type, shelled corn, which is very important to the agricultural sector in this part of the world, was used as a test material in the drying studies due to time limitations.

Evaluation of the potential of 2DSB's with draft plates was based on the aerodynamics, scale-up, and drying aspects of this study. The mathematical models for spouting pressure drop, minimum spouting velocity, solids circulation rate, average cycle time, and drying of grains were developed using the concepts of dimensional analysis and similitude. The comparisons of model predictions with the collected data exhibit generally very good agreement.

5.1 Static Vertical Pressure of Grains.

5.1.1. Static vertical pressure on air-entry slots.

The static load of grains on the slots for each data point was estimated using the transducer calibration curve and the recorded analogue output. The static load of grains was divided by their respective areas to obtain the static vertical (bottom) pressure. The initial moisture contents of shelled corn, soybean, and wheat were 14.8 %, 14.8 %, and 13.8 % respectively. The variations in initial moisture contents during the experiment were 1.17 %, 1.40 %, and 0.81 % and were therefore not considered large enough to be included as covariables in the analysis. Analysis of variance was performed on the entire static vertical pressure data set in order to determine which factors most influenced this parameter. The analysis procedure described in Gomez and Gomez (1984) was implemented using the SAS (1985) package. Results from this analysis (Table 5.1) showed that the bed width to slot width aspect ratio, the slant angle, the type of grain, and the bed height, as well as their interactions affect the static vertical pressure. It was therefore concluded that there are differences due to all of the factors investigated. The variation of static vertical pressure with bed heights, grains, slant angles, and aspect ratios are shown in Figure 5.1.

The static vertical pressure at an aspect ratio of 5 was compared with those at aspect ratios of 10 and 15. The aspect ratios 10 and 15 resulted in 6.6 % lower and 14.8 % higher static vertical pressures than the aspect ratio 5. This is of interest since it points to an optimum aspect ratio in the range of 10.

Slant angles of 30° and 60° resulted in 7.4 % lower and 5.4 % higher static vertical pressures, respectively, than a slant angle 0° (flat bottom). Thus, the least static vertical pressure was seen to occur at a slant angle almost equal to the mean emptying angle of repose (30° 12' 48") of grains as calculated from Table A.1. These results indicate that there is a range of slant angles that produce minimum bed static vertical pressure and which are related to grain particle and static properties.

The reaction of factor G also supports this conclusion. The soybean beds with bulk density 746.4 kg/m^3 and wheat beds with bulk density 774.3 kg/m^3 produced 26.2 % higher and 31.4 % lower static vertical pressures compared to shelled corn

Table 5.1 Analysis of variance of static vertical pressure for grains on air inlet of pilot scale unit.

Source	DF	Sum of squares	Mean square	F value	Pr > F	C.V.
Total correct	323	344,617,402.9				
Block	2	126,849.8	63,424.9	2.76	0.1769	
A	2	18,476,903.4	9,238,451.7	401.35	0.0001	
Error (a)	4	92,074.6	23,018.7			5.54
θ_s	2	6,804,406.7	3,402,203.3	27.69	0.0001	
$A*\theta_s$	4	8,017,946.4	2,004,486.6	16.31	0.0001	
Error (b)	12	1,474,344.4	122,862.0			12.81
G	2	139,556,103.7	69,778,051.9	446.39	0.0001	
A*G	4	8,662,103.2	2,165,525.8	13.85	0.0001	
θ_s*G	4	12,449,789.9	3,112,447.5	19.91	0.0001	
$A*\theta_s*G$	8	7,437,475.0	929,684.4	5.95	0.0001	
Error (c)	36	5,627,395.5	156,315.5			14.44
H_b	3	64,964,375.3	21,654,791.8	285.15	0.0001	
$A*H_b$	6	14,412,722.6	2,402,120.4	28.64	0.0001	
θ_s*H_b	6	5,873,469.9	978,911.6	11.67	0.0001	
$A*\theta_s*H_b$	12	9,960,081.8	830,006.8	9.89	0.0001	
$G*H_b$	6	6,454,653.7	1,075,775.6	12.82	0.0001	
$A*G*H_b$	12	12,233,074.0	1,019,422.8	12.15	0.0001	
θ_s*G*H_b	12	4,782,581.8	398,548.5	4.75	0.0001	
$A*\theta_s*G*H_b$	24	3,621,551.7	150,898.0	1.80	0.0176	
Error (d)	162	13,589,499.4	83,885.8			10.58

SVP mean = 2737.22 Pa

with bulk density 731.8 kg/m^3 (Table A.1). Hence, soybean beds showed the highest static vertical pressure in spite of a lower bulk density than wheat (3.7 %). When the sphericities and the emptying angles of repose from Table A.1 for shelled corn, soybean, and wheat along with their static vertical pressures are compared, it may be concluded that the static pressure of grains on the air-entry slot varies with the sphericity and emptying angle of repose. Moreover, the bed heights 0.8 m, 1.2 m, and 1.6 m produced static vertical pressures 44.6 %, 57.8 %, and 51.0 % higher than a bed height of 0.4 m. The bed height 1.2 m produced the highest static vertical

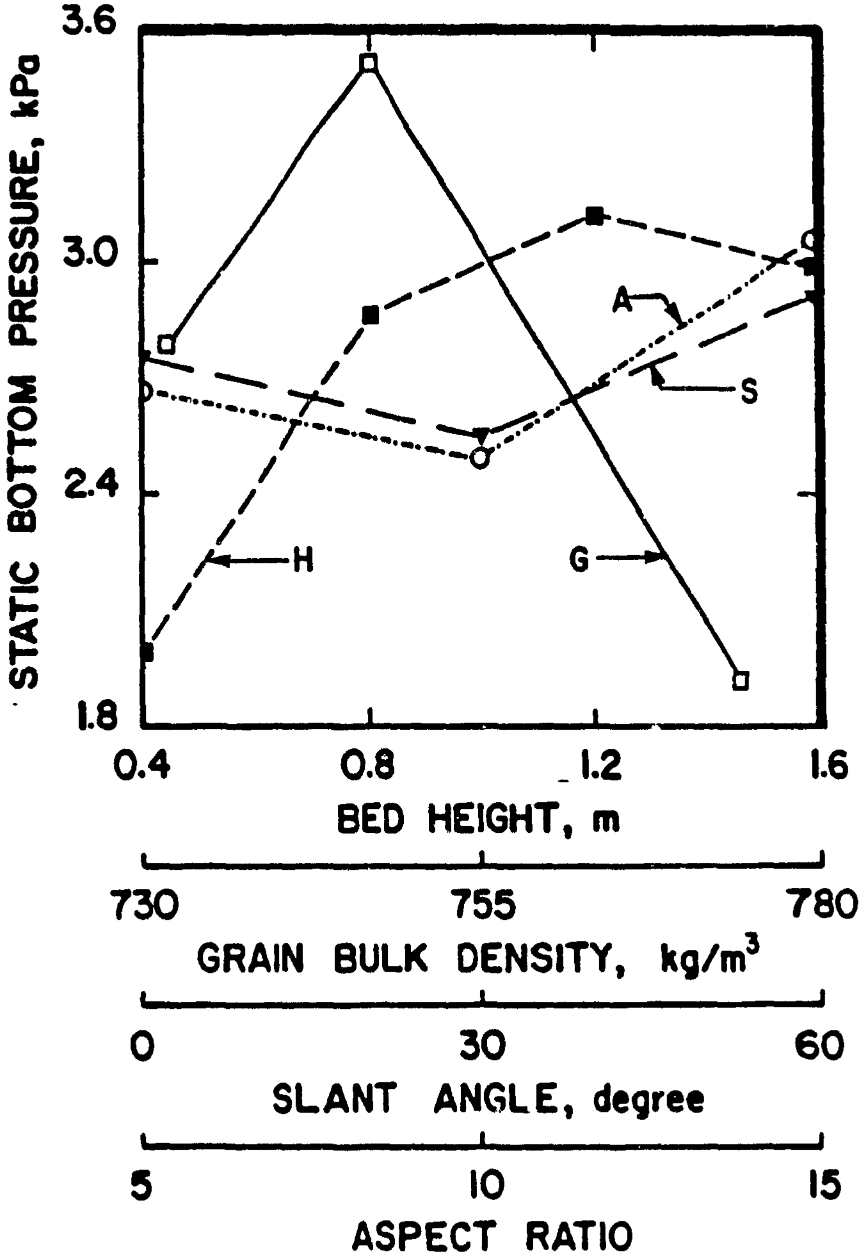

Figure 5.1 Static vertical pressure vs. bed height, bulk density, slant angle, and aspect ratio.

pressure. That the height 1.6 m resulted in lower static vertical than that of 1.2 m is due to the packing effect of grains in the beds. This effect was physically observed when the height of grain in the two-dimensional vessel surpassed 0.85 m and was frequently observed while charging the unit with wheat grains.

5.1.2. Silo theory comparison with static vertical pressure data.

The Janssen and Reimbert and Reimbert theories were used for comparison with the present results due to simplicity and better predictability of static vertical pressures. The K- ratios for shelled corn and wheat from the literature exhibited wide discrepancies and no values for soybean were found. K-ratios were therefore estimated using the emptying angles of repose from Table A.1 in equation (2.2). The estimates were: 0.345, 0.292, and 0.358 for shelled corn, soybean, and wheat respectively. Since the coefficients of external friction of grains on plexiglas were not available, values of 0.12, 0.17, and 0.17 , respectively, for Teflon (Anonymous, 1977) were used.

The static vertical pressure of grains on the slots with flat bottom were estimated by the Janssen method as well as the Reimbert and Reimbert method. The observed and estimated values of static vertical pressure vs. bed height of shelled corn, soybean, and wheat are shown in Figures 5.2 through 5.10 for various aspect ratios as indicated.

The static vertical pressures of shelled corn on the slot of aspect ratio 5 with flat bottom at 0.4 m, 0.8 m, 1.2 m, and 1.6 m bed heights were compared with the predicted values. The Janssen estimates were within +1.7 % to -6.9 % error and the Reimbert and Reimbert method underestimated observed values by -1.3 % to -

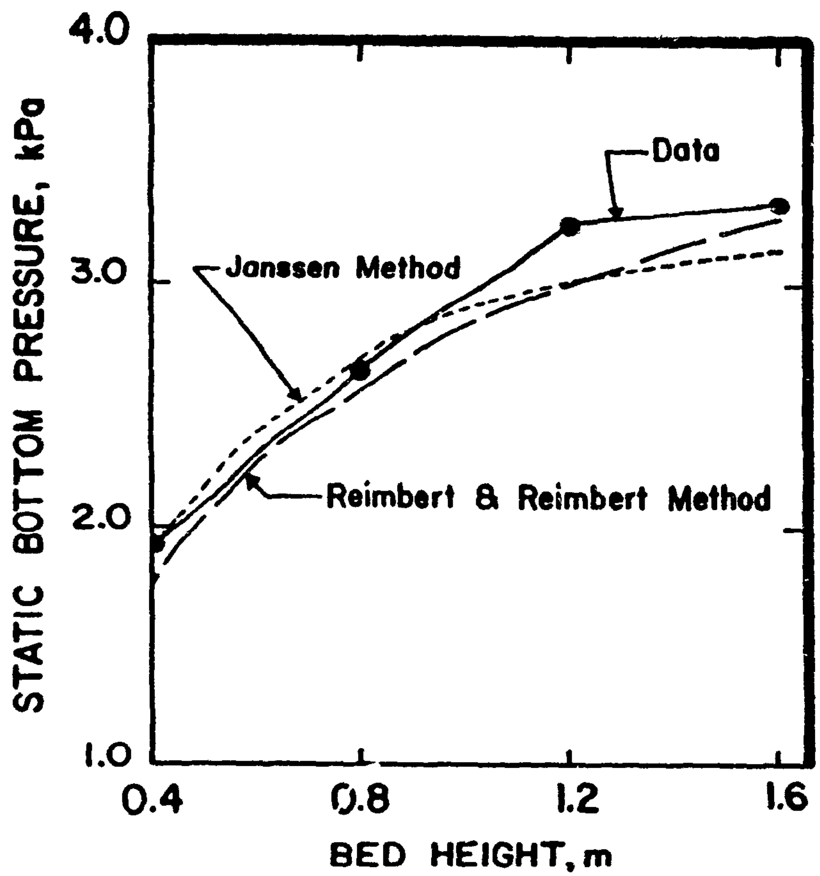

Figure 5.2 Flat bottom bed - Comparison with silo theories for shelled corn. A = 5.

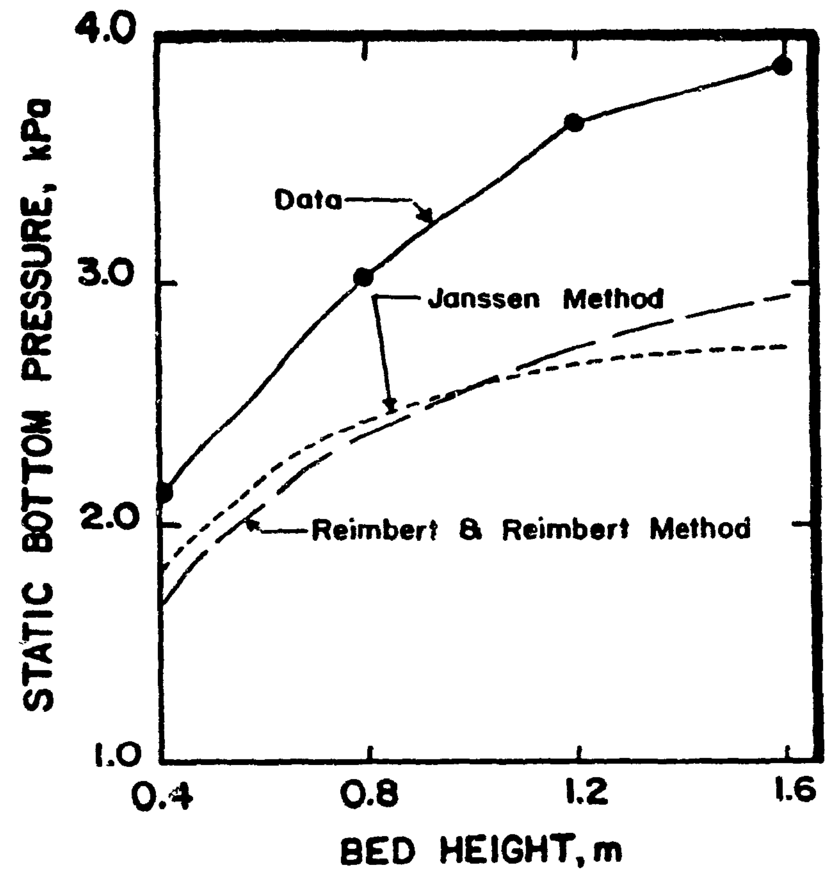

Figure 5.3 Flat bottom bed - Comparison with silo theories for soybean. A = 5.

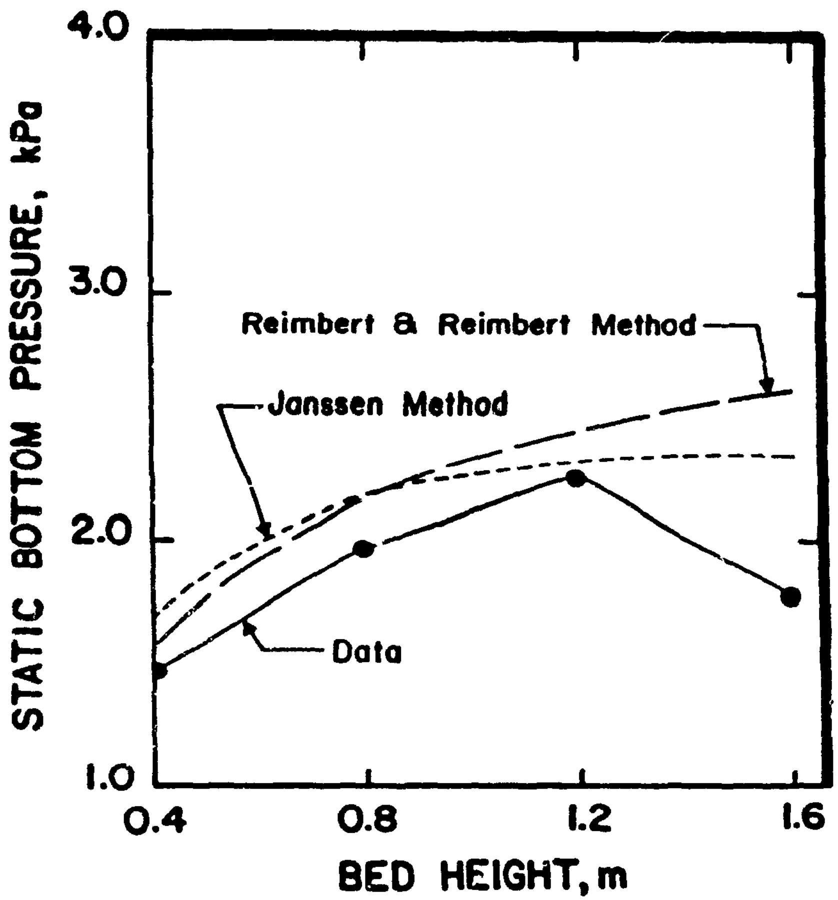

Figure 5.4 Flat bottom bed - Comparison with silo theories for wheat. A = 5.

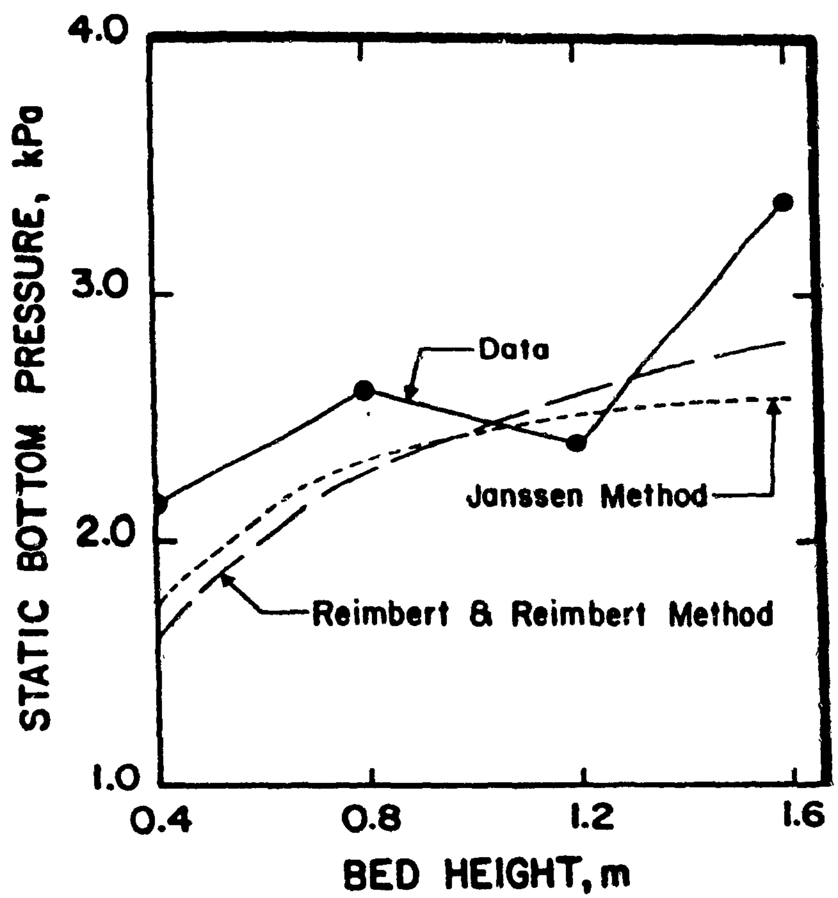

Figure 5.5 Flat bottom bed - Comparison with silo theories for shelled corn. A = 10.

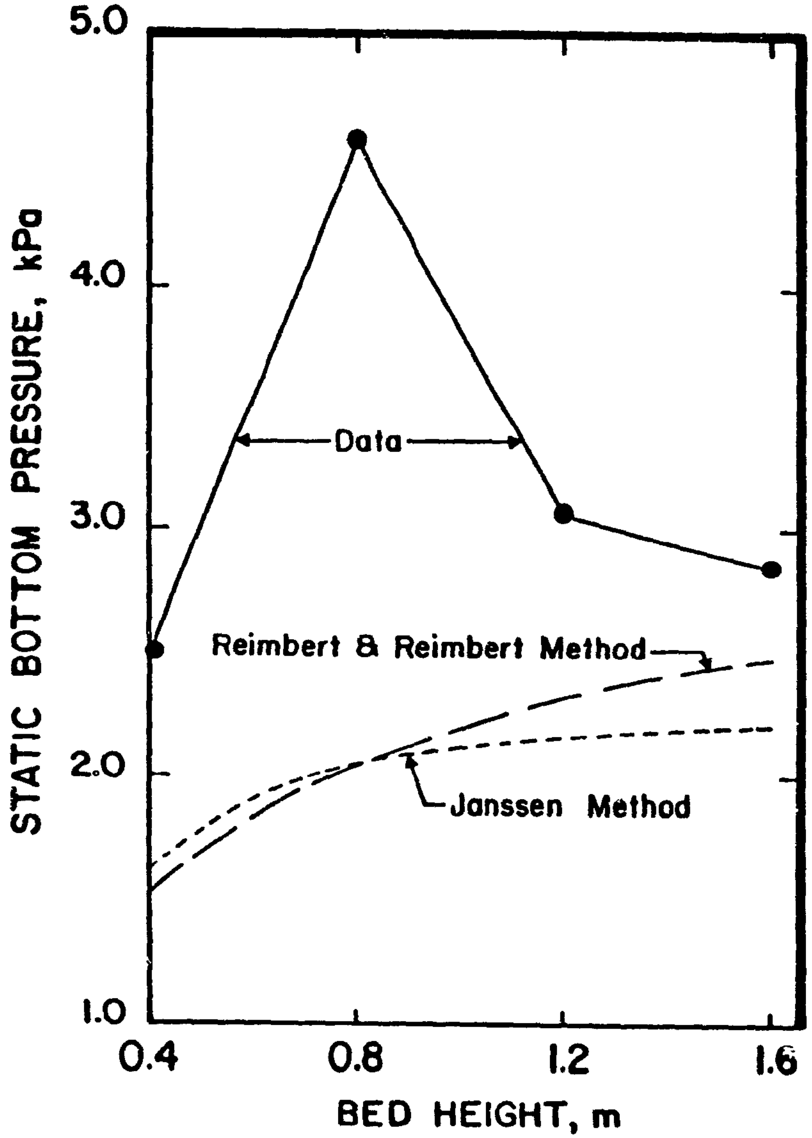

Figure 5.6 Flat bottom bed - Comparison with silo theories for soybean. A = 10.

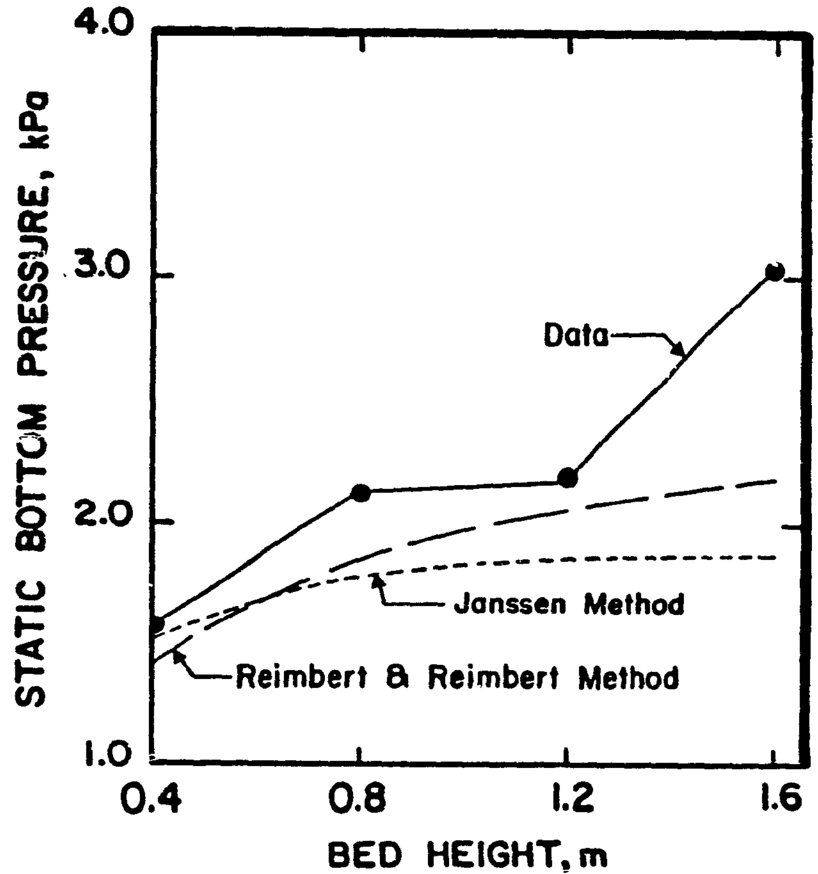

Figure 5.7 Flat bottom bed - Comparison with silo theories for wheat. A = 10.

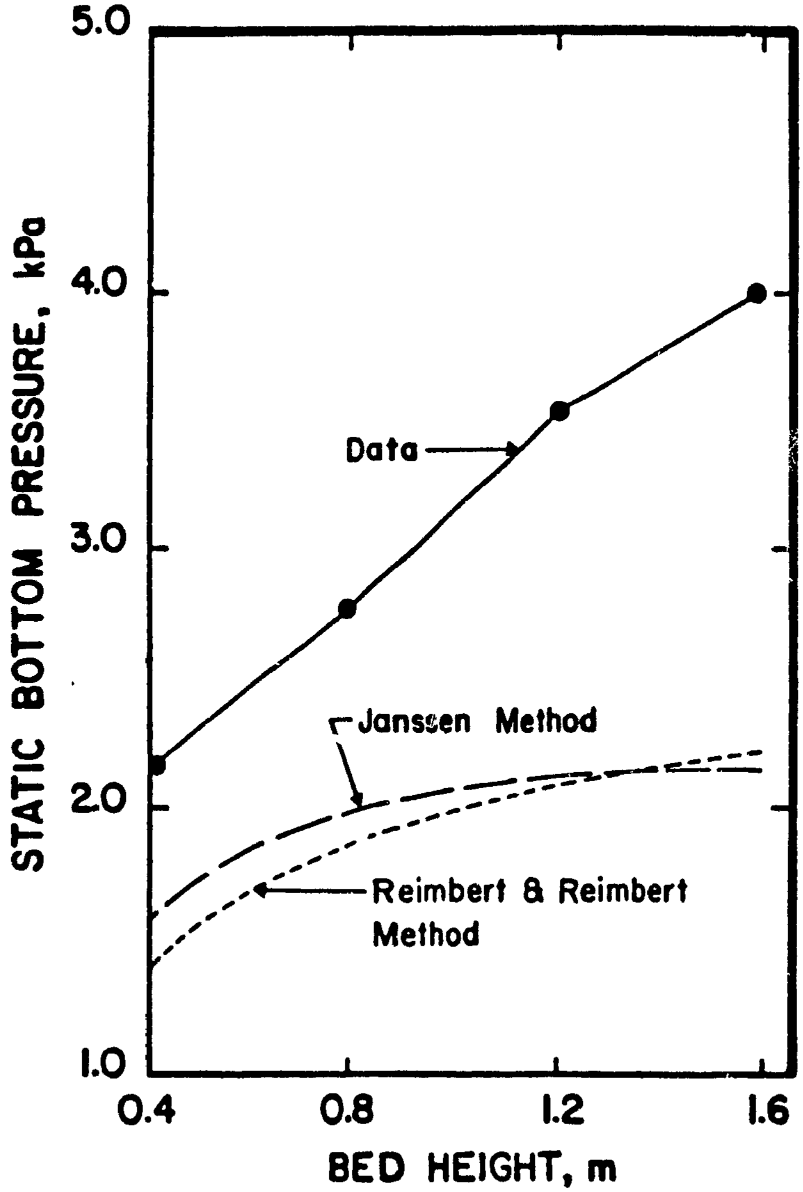

Figure 5.8 Flat bottom bed - Comparison with silo theories for shelled corn. A = 15.

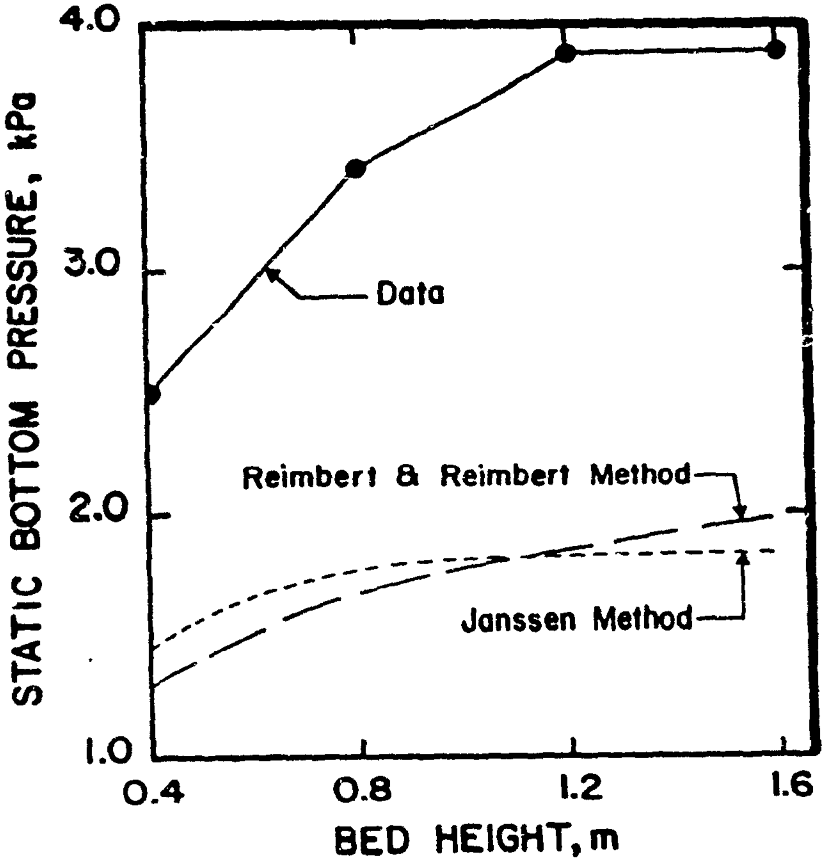

Figure 5.9 Flat bottom bed - Comparison with silo theories for soybean. A = 15.

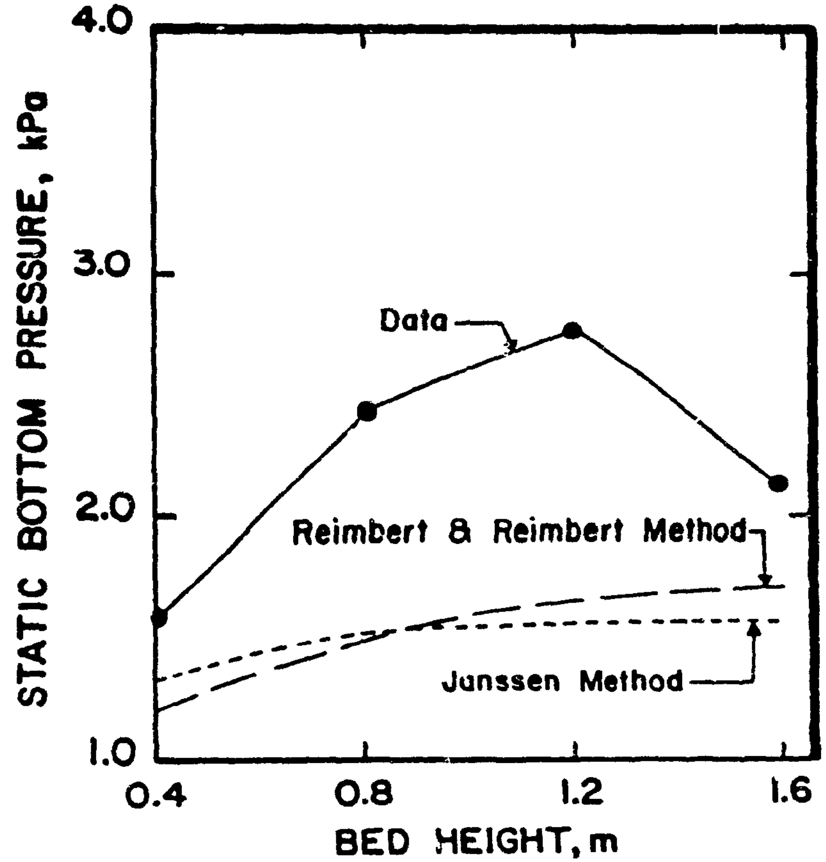

Figure 5.10 Flat bottom bed - Comparison with silo theories for wheat. A = 15.

7.7 % (Figure 5.2). This figure also indicates that the Janssen method under-estimates with errors of increasing magnitude but that the Reimbert and Reimbert method under-estimates with errors of decreasing magnitude as the bed height increases. The Janssen and the Reimbert and Reimbert predictions as well as the observed flat bottom data with aspect ratio 5 for soybean are plotted in Figure 5.3 which demonstrates that both theories underestimate with errors of increasing magnitude as the bed height increases. This comparison indicates that both methods grossly underestimated the static vertical pressure. The Janssen method underestimated by 14.3 % to 30.3 % while the Reimbert and Reimbert method underestimated by 20.6 % to 26.4 %. However, both methods overestimate the static vertical pressure for wheat; the error is 1.8 % to 30.5 % by the Janssen method and 7.9 % to 45.9 % by the Reimbert and Reimbert method (Figure 5.4)

When the flat bottom data and the silo theories for the slot with aspect ratio 10 are compared for shelled corn, soybean, and wheat; the Janssen and Reimbert and Reimbert methods are seen to estimate within +5.2 % to -24.1 % and +8.2 % to +23.9 % for shelled corn, -22.5 % to -55.2 % and -13.0 % to -55.5 % for soybean and -4.9 % to -38.4 % and -6.2 % to -28.4 % for wheat, respectively. This shows that as the bed heights of shelled corn and soybean increase, the deviation between the observed and the predicted values of static vertical pressure decreases (Figures 5.5, 5.6), but that the deviation increases in the case of wheat (Figure 5.7). Wide disagreement between observed and predicted values is also exhibited in the case of an aspect ratio of 15 (Figures 5.8, 5.9, 5.10). The deviation between the observed and estimated values for all grains diverged as the height of bed increased.

In general, it was noted that as bed height increased, the deviation between observed and estimated values increased in the negative direction when considering the same aspect ratio for flat bottomed vessels. Similarly, as the aspect ratio increased, the deviation between observed data and estimated values increased in the negative direction in the case of a 0^{o} slant angle. Hence, neither method of estimation was generally applicable to static beds in the form of a two-dimensional nonaerated spouted bed because neither was sensitive to bed length to slot width aspect ratio or to slant angle.

These comparisons of experimental results with predictions from silo theories indicated that the silo theories are not applicable without modification to static vertical pressure at the air entry slots of nonaerated beds. Accordingly, empirical model was developed.

5.1.3 Statistical model.

The effect of factor G in Figure 5.1 indicates that the type of grain could not be represented solely as a function of bulk density. It may be assumed that aside from bulk density, the angle of repose or the K-ratio, the grain sphericity, the moisture content, and the angle of external friction are also important grain characteristics. To account for these, the "quantitative factor" has been proposed in this work. This factor can be derived as follows: take the classical theory of Janssen (1895) and assume all other factors to be constant. The grain quantitative value is then bulk density divided by K-ratio. If K = 0.49 for corn and K = 0.42 for wheat as reported by Mohsenin (1970), the quantitative value of corn is 1493.5 kg/m^3 and of wheat is 843.5 kg/m^3. However, these quantitative values have no proper magnitude.

Now, assuming as did Koenen (1896) that the K-ratio is a function of the emptying angle of repose, and that there exists the Rankine active state in the grain mass, the K-ratio for shelled corn, soybean, and wheat estimated previously was 0.345, 0.292, and 0.358, respectively. When the emptying angle of repose and the K-ratio were plotted in Figure 5.11 against the factor G static bottom pressures, both parameters produce exactly the same curve, but with positive and negative slopes. Hence, both curves should have the same R-Square values with positive and negative correlations. It was more convenient to consider the curve with positive correlation with the data, and at the same time as the emptying angle of repose increases the bottom pressure also increases. It is also already known that the K-ratio is not constant even for the same type of grain. Hence, this term was not considered for further calculations. Moreover, it was assumed that the $\tan\theta_r$ has a direct effect to reduce the bulk density weight action towards the bottom of apparatus. When the $\tan\theta_r$ of corn, soybean, and wheat was multiplied with the respective grain bulk densities, values of 408.5 kg/m^3, 489.4 kg/m^3, and 415.5 kg/m^3 were obtained respectively. These grain actions indicated that the order of grain quantitative values were not correct according to the static vertical pressure of respective grain.

Covariable sphericity of grain values from Table A.1 were plotted in Figure 5.11. It is clear that the sphericity has direct effect on the bottom action of each type of grain, and was assumed as a straight line between zero and one. When respective type of grain sphericity value was multiplied with ρ_b x $\tan\theta_r$ the

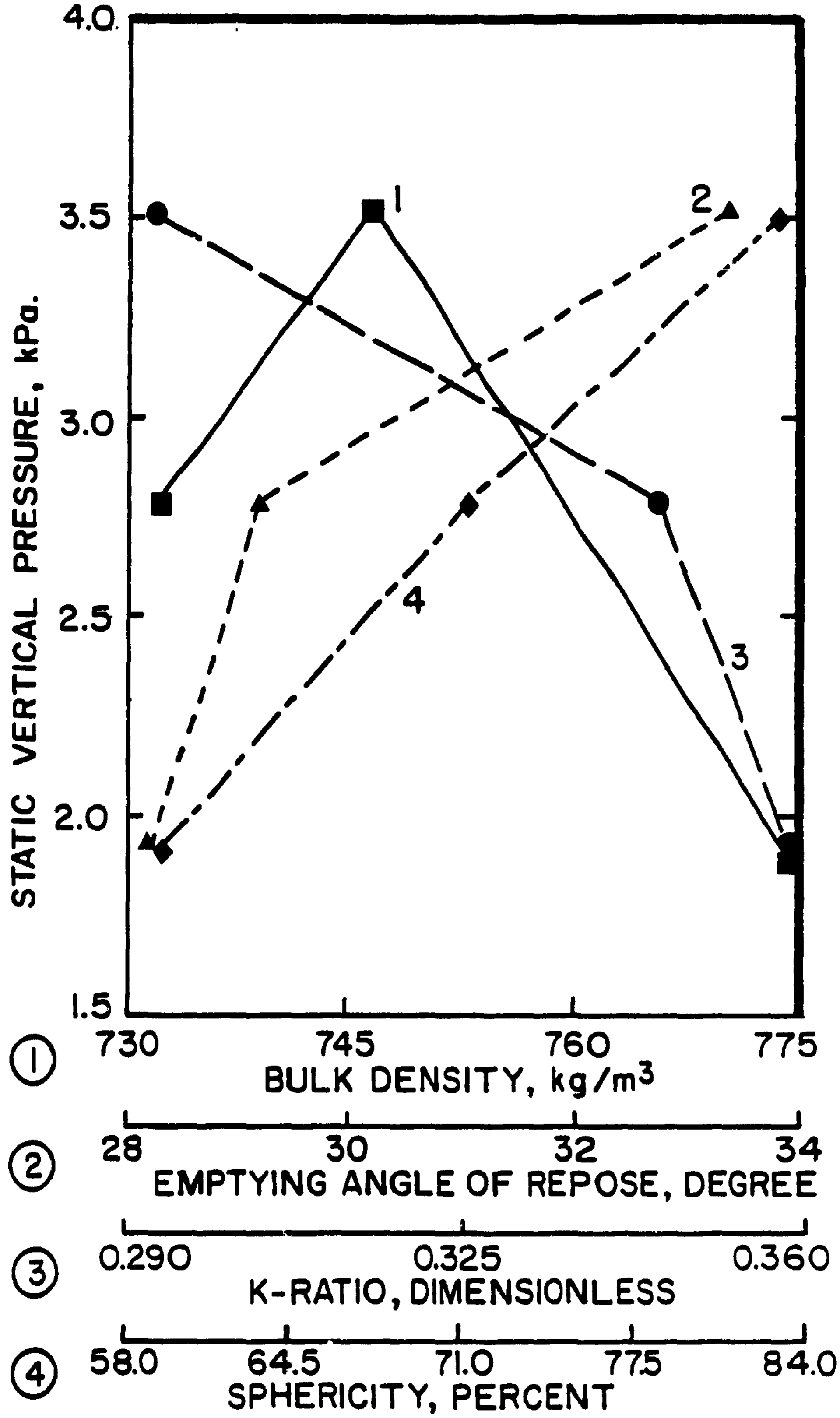

Figure 5.11 Static vertical pressure vs. bulk density, emptying angle of repose, K-ratio, and sphericity.

quantitative value of corn = 289.5 kg/m^3, of soybean = 405.9 kg/m^3, and of wheat = 246.7 kg/m^3 was obtained. When these quantitative values were plotted in Figure 5.12, a better curve with reasonable trend was obtained. It was not possible however to include the effect of moisture content because it was approximately constant at 13.9+_0.9 % wet basis in all grains. The above quantitative values were used in the SAS STEPWISE program with the Backward Elimination option (SAS 1985) at 0.0001 significant level, and the following linear model with R-square = 84.9 % was obtained:

$$SVP = \left(\begin{array}{r} -5679.38 + 39.99G + 2.56AGH_b - 0.0132A\theta_s GH_b \\ -0.125A^2GH_b - 0.0585G^2 + 2.97\times10^{-6}A^2\theta_s G^2H_b + 7.05GH_b^2 \\ - 2.71AGH_b^2 - 27.43A^2H_b^2 + 0.3207A^2GH_b^2 \\ + 2.437\times10^{-4}A\theta_s^2GH_b^2 - 1.313\times10^{-5}A^2\theta_s^2GH_b^2 \\ - 2.941\times10^{-4}A^2G^2H_b^2 - 0.002465A\theta_s GH_b^3 \end{array} \right) \quad (5.1)$$

where,

$$G = \rho_b * \phi * \tan\theta_r$$

Estimated values were generated using equation 5.1 and compared with the experimental data (Table 5.2). The agreement is good for a flat bottom ($\theta_s = 0^o$) for all the bed to slot width aspect ratios and all slant angles when the aspect ratio is 5. The estimates tend to deteriorate as the aspect ratio and slant angle increase. This could be the result of the orientation and sphericity of the particles. Corn and

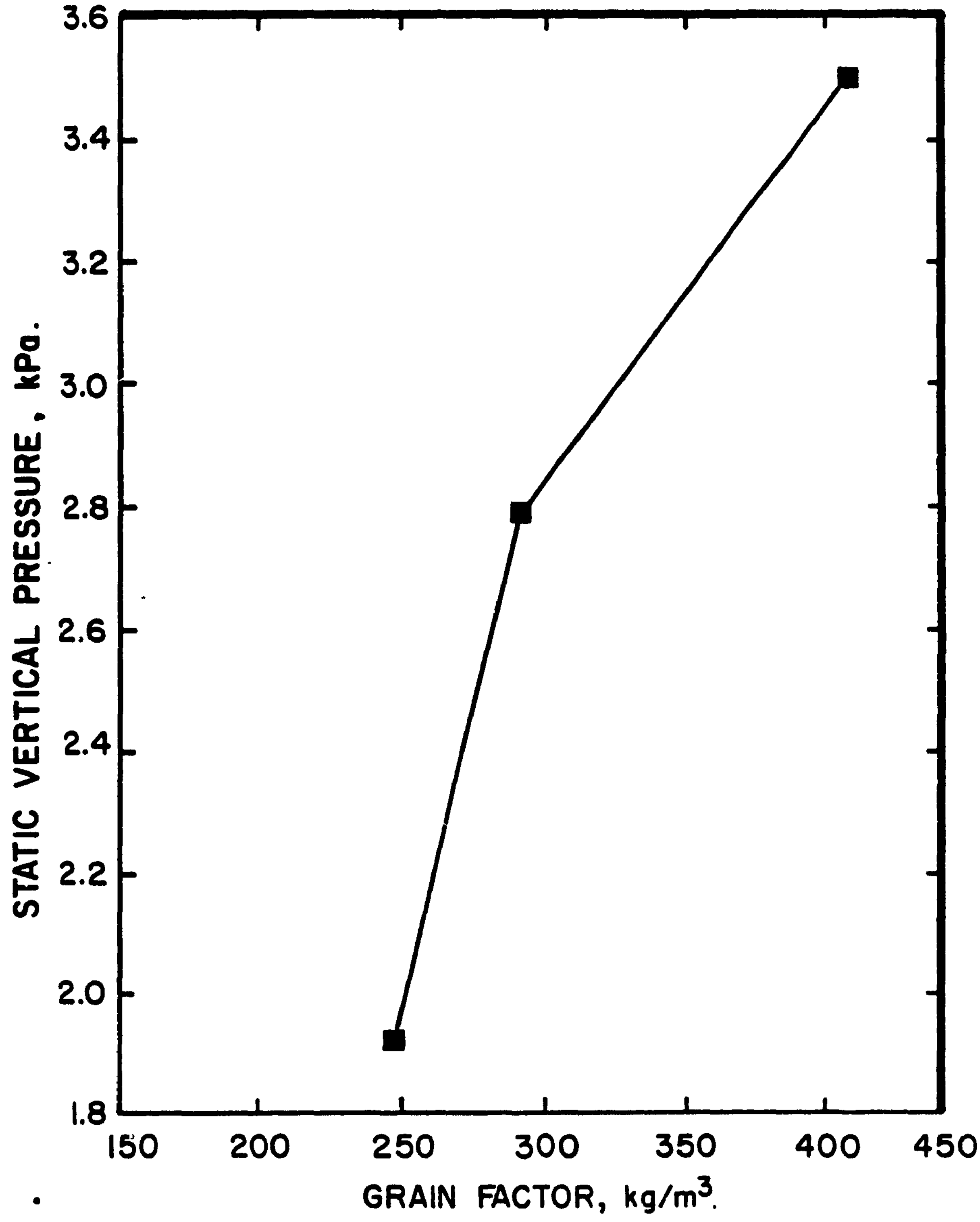

Figure 5.12 Static vertical pressure as the function of grain quantitative factor.

Table 5.2 Comparison of experimental data with estimated values of static vertical pressure of grains on the air entry slots of pilot scale unit.

No	A	θ_s	H_b	Shelled corn Data	Shelled corn Eq	Soybean Data	Soybean Eq	Wheat Data	Wheat Eq
	---	Deg		N/m^2	N/m^2	N/m^2	N/m^2	N/m^2	N/m^2
1	5	0	0.4	1916	1985	2109	2282	1451	1460
2	5	0	0.8	2652	2693	3053	3240	1971	2051
3	5	0	1.2	3248	3124	3677	3787	2251	2399
4	5	0	1.6	3329	3280	3912	3923	1783	2505
5	5	30	0.4	1881	1860	2201	2150	1525	1345
6	5	30	0.8	2726	2477	2855	3022	2212	1849
7	5	30	1.2	3021	2809	3715	3472	2523	2103
8	5	30	1.6	3085	2817	3606	3443	2283	2072
9	5	60	0.4	1834	1810	1979	2122	1260	1293
10	5	60	0.8	2622	2559	3330	3220	1923	1899
11	5	60	1.2	3283	3164	4201	4095	2262	2375
12	5	60	1.6	3274	3543	4415	4629	2538	2652
13	10	0	0.4	2118	2243	2484	2610	1580	1669
14	10	0	0.8	2610	2933	4589	3436	2141	2209
15	10	0	1.2	2384	3068	3042	3394	2187	2248
16	10	0	1.6	3387	2651	2842	2484	3035	1786
17	10	30	0.4	2031	2117	2554	2601	1313	1523
18	10	30	0.8	2730	2691	3818	3436	1496	1928
19	10	30	1.2	1954	2641	3016	3302	1513	1771
20	10	30	1.6	1351	1885	994	2085	1144	982
21	10	60	0.4	2127	2084	2772	2724	1327	1457
22	10	60	0.8	2737	2825	3922	3961	1899	1966
23	10	60	1.2	3349	3059	4594	4394	2047	2012
24	10	60	1.6	2934	2621	3739	3791	1821	1455
25	15	0	0.4	2170	2104	2497	2356	1587	1531
26	15	0	0.8	2769	3029	3439	3340	2445	2215
27	15	0	1.2	3556	3778	3896	3866	2788	2679
28	15	0	1.6	4014	4349	3896	3934	2418	2624
29	15	30	0.4	2262	2098	2693	2727	1296	1440
30	15	30	0.8	3112	2952	3818	3991	1936	1978
31	15	30	1.2	3818	3441	4681	4533	2384	2136
32	15	30	1.6	3824	3441	4589	4180	1878	1809
33	15	60	0.4	1990	2150	3099	3180	1357	1399
34	15	60	0.8	3321	3110	5099	4971	2034	1940
35	15	60	1.2	3426	3632	5518	5939	1960	2041
36	15	60	1.6	3426	3470	5923	5740	1211	1491

wheat generally orient their major axes parallel to the bed bottom so that the vertical pressure at larger slant angles is less. The effects of sphericity and angle of repose may, however, not be linear as was assumed in the development of the equation. Thus, equation 5.1 is seen to lack the proper dependence on some of the independent variables and may have to be modified by linearizing transformations.

5.2 Dynamics of Spouted Bed.

The initial moisture content of grain samples was 13.6 % wet basis (shelled corn), 13.4 % (soybean), and 12.9 % (wheat). Final moisture contents were 9.3 %, 9.2 % and 9 %, respectively. Since variations in initial moisture content were very small, this term was therefore considered to be part of experimental error and was not included in the analysis.

The bulk densities of undried and dried shelled corn were in the range of 687.8 kg/m^3 to 731.8 kg/m^3. A value of 731.8 kg/m^3 was adopted in the analysis for simplicity since it applied to more than 60 % of the samples. The bulk densities of soybean and wheat grains are given in Table A.2. The equation developed by Nelson (1979) can be used to calculate bulk density, and, if it is necessary to take into account the variation of bulk density with moisture content, similar equations may be developed.

The data on grain aerodynamics from the experiments on slant angle, spout width, separation distance, bed length scale-up, similarity scale-up and drying of shelled corn were pooled and then used to generate the PI terms in the models proposed for spouting pressure drop, minimum spouting velocity, solids circulation rate, and average cycle time in Chapter III. The PI terms were then linearized by the natural logarithm (ln) transformation. The data were analyzed using the STEPWISE (Forward or Backward) procedure (STATGRAPHICS, 1989) and the coefficients of dimensionless PI numbers were determined by ordinary least squares. A number of alternate models were created by multiplying or dividing PI terms, while maintaining both the independence of these terms and the total number of terms in each original formulation. The models were evaluated using the following criteria: the R^2_{adj} statistic, standard error, level of significance (α), residual characteristics, and the number of terms in the model. The final selected models describing the dynamic phenomena of slotted 2DSBs with draft plates are presented in the following sub-sections.

5.2.1 Spouting pressure drop.

The effect of separation distance on the spouting pressure drops associated with the three grain varieties are shown in Figures 5.13 to 5.18. The data show that the spouting pressure drop increases with separation distance and varies with grain type. Similar effects were reported for small scale CSB's by Claflin and Fane (1983) and for 2DSB's by Law et al. (1984, 1986). This increase in spouting pressure may be attributed to the higher number of grains entering the spout and at the same time to spouting air pushing the grains towards the downcomer sides to keep the spout open. In these experiments, the highest pressure drop was produced by the beds containing soybean grains, followed by wheat and shelled corn when the separation distance was increased from 10 cm to 20 cm. The recorded data indicated that the magnitude of spouting pressure drop decreased as the

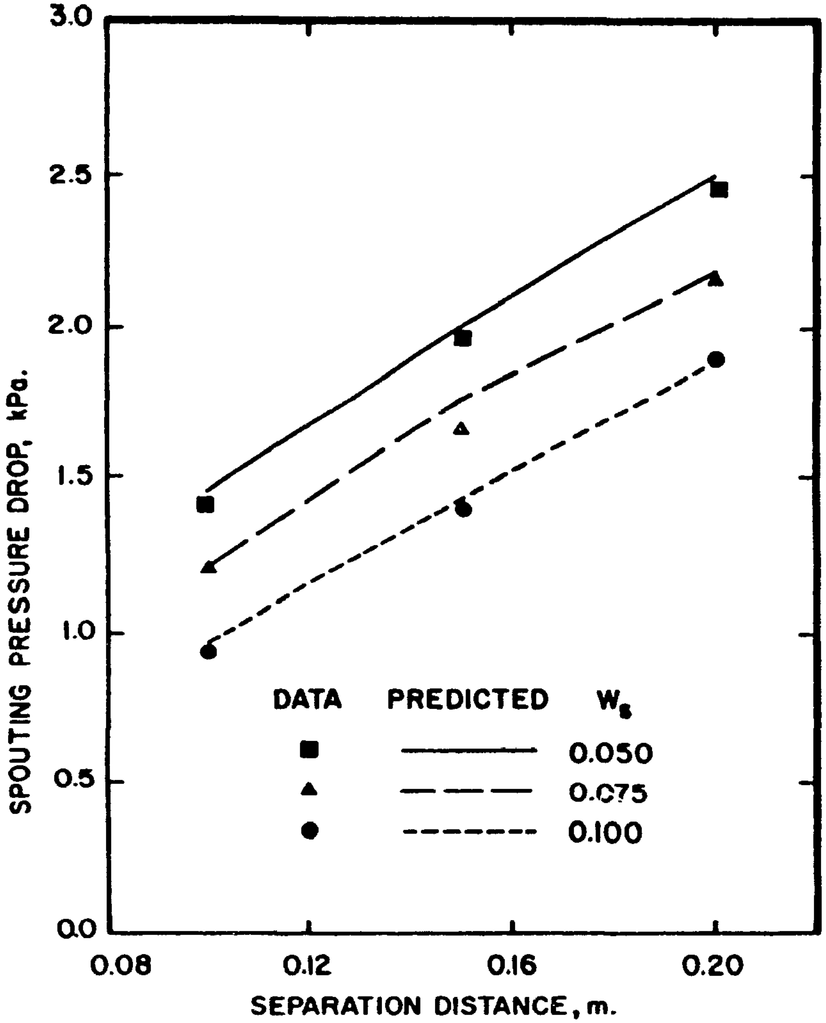

Figure 5.13 Effect of separation distance on spouting pressure drop in pilot scale for shelled corn. $\theta_s = 45°$.

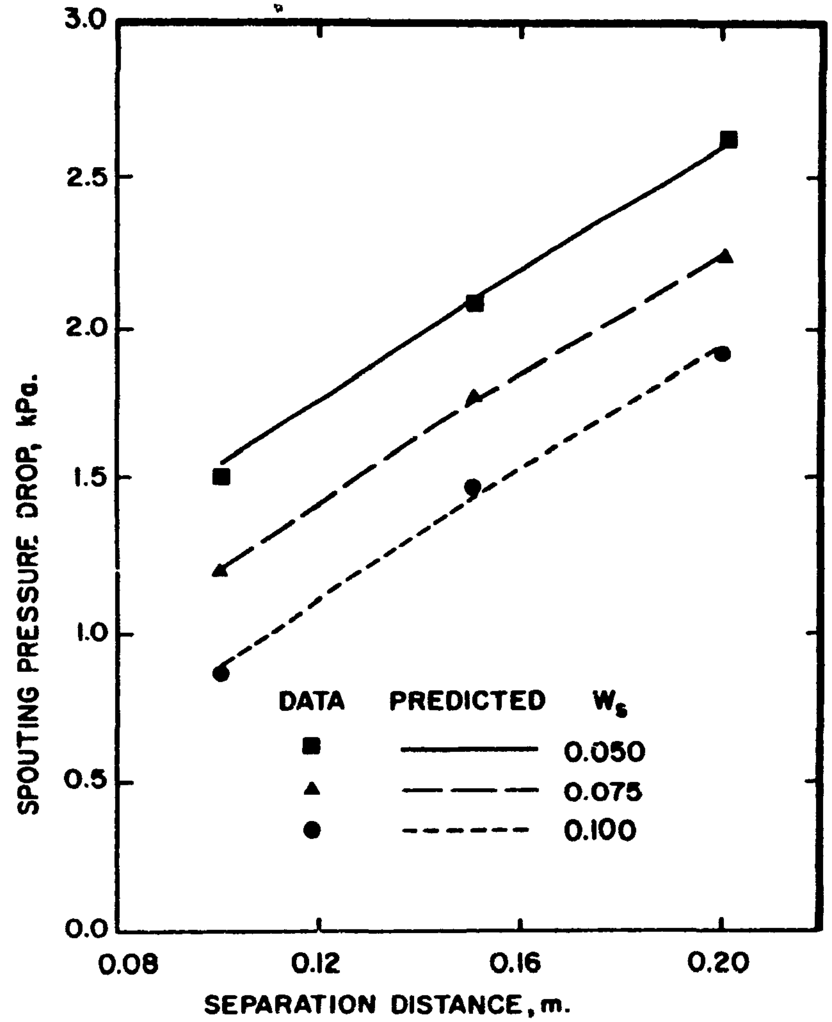

Figure 5.14 Effect of separation distance on spouting pressure drop in pilot scale for shelled corn. $\theta_s = 60°$.

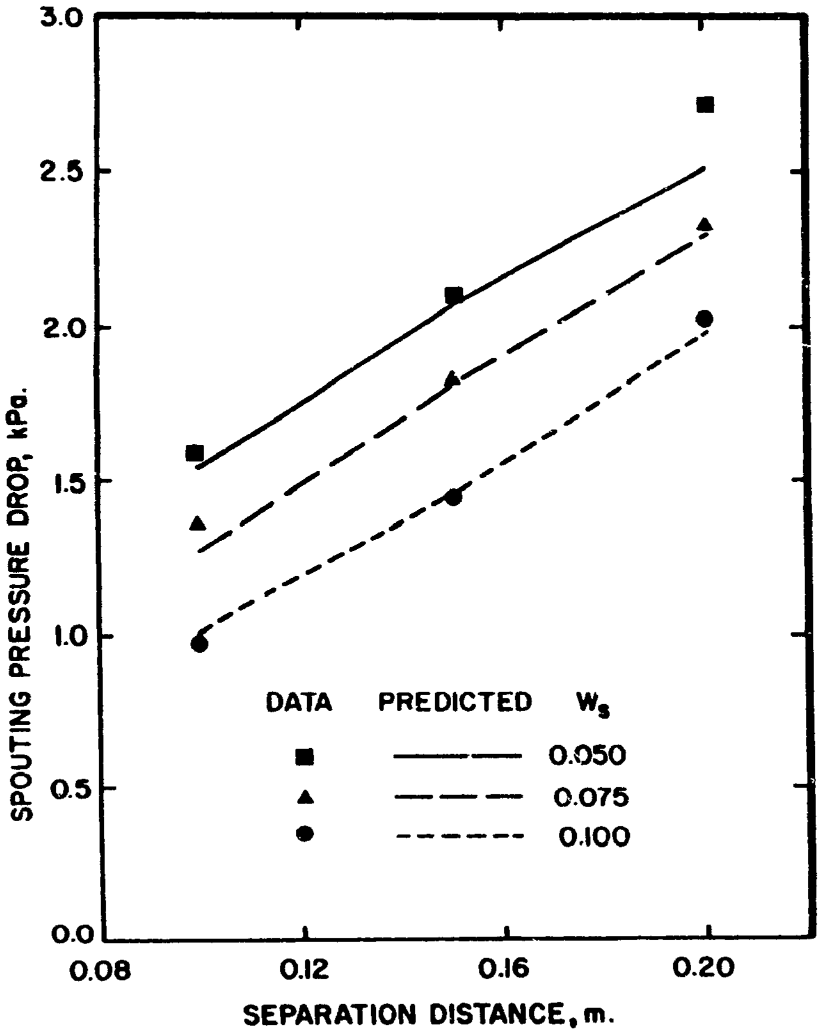

Figure 5.15 Effect of separation distance on spouting pressure drop in pilot scale for soybean. $\theta_s = 45°$.

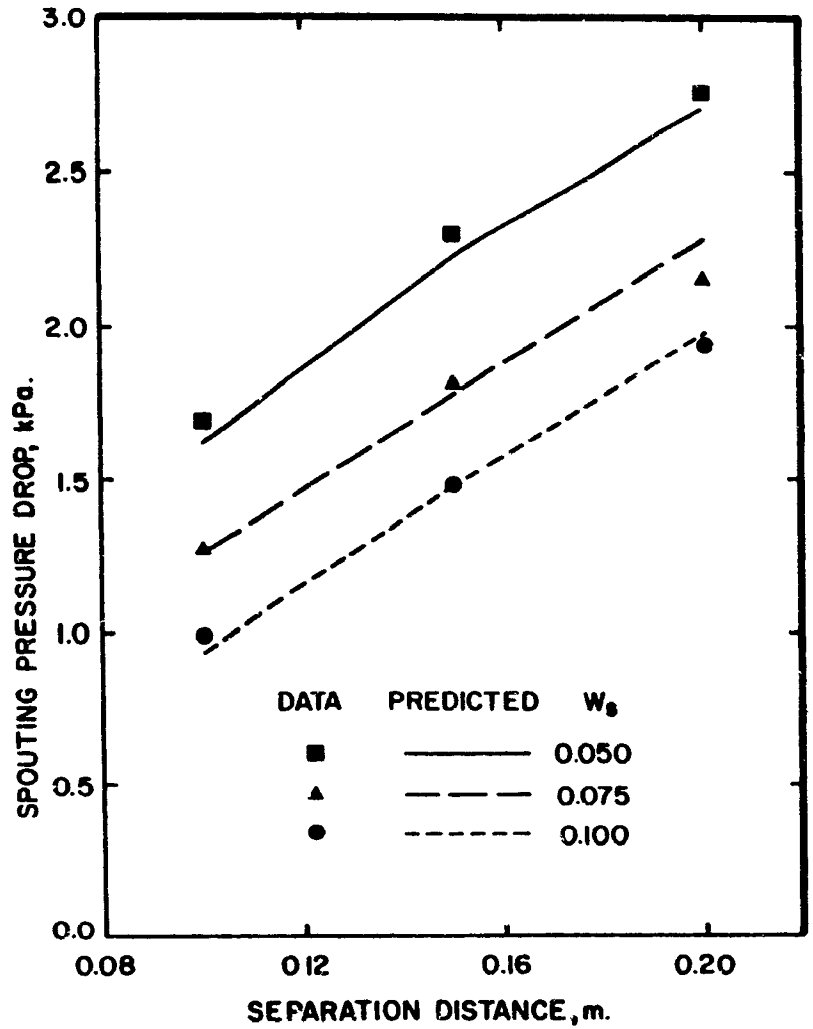

Figure 5.16 Effect of separation distance on spouting pressure drop in pilot scale for soybean. $\theta_s = 60°$.

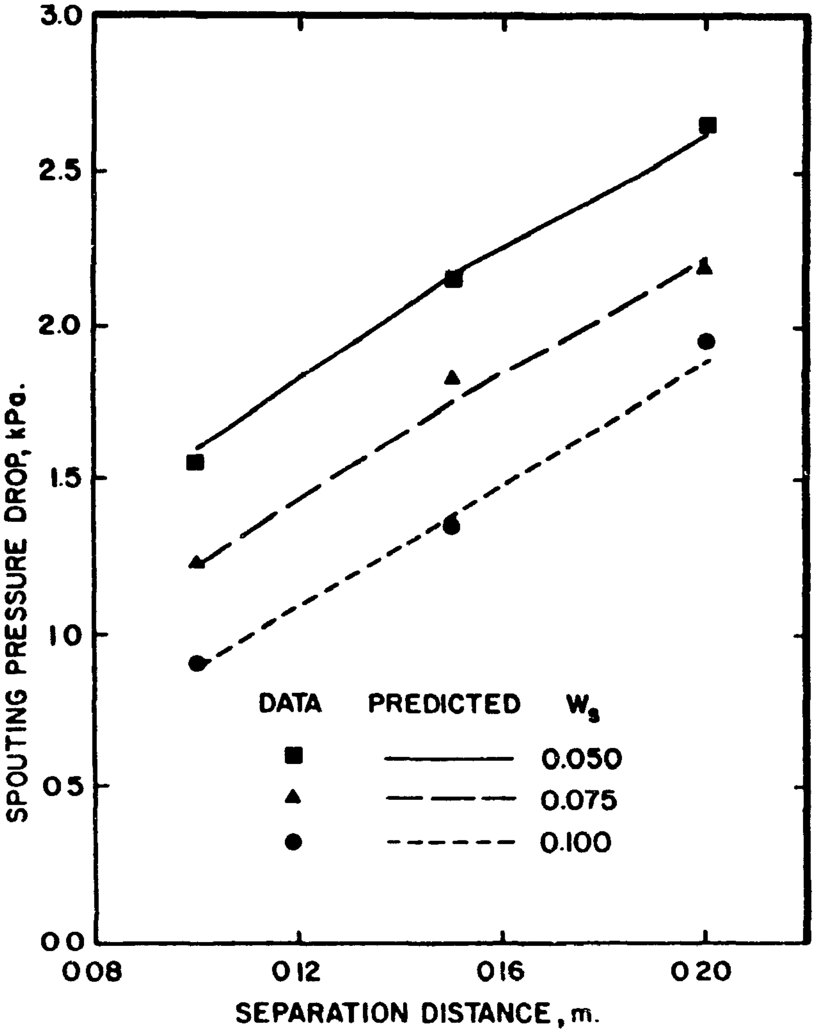

Figure 5.17 Effect of separation distance on spouting pressure drop in pilot scale for wheat. θ_s = 45°.

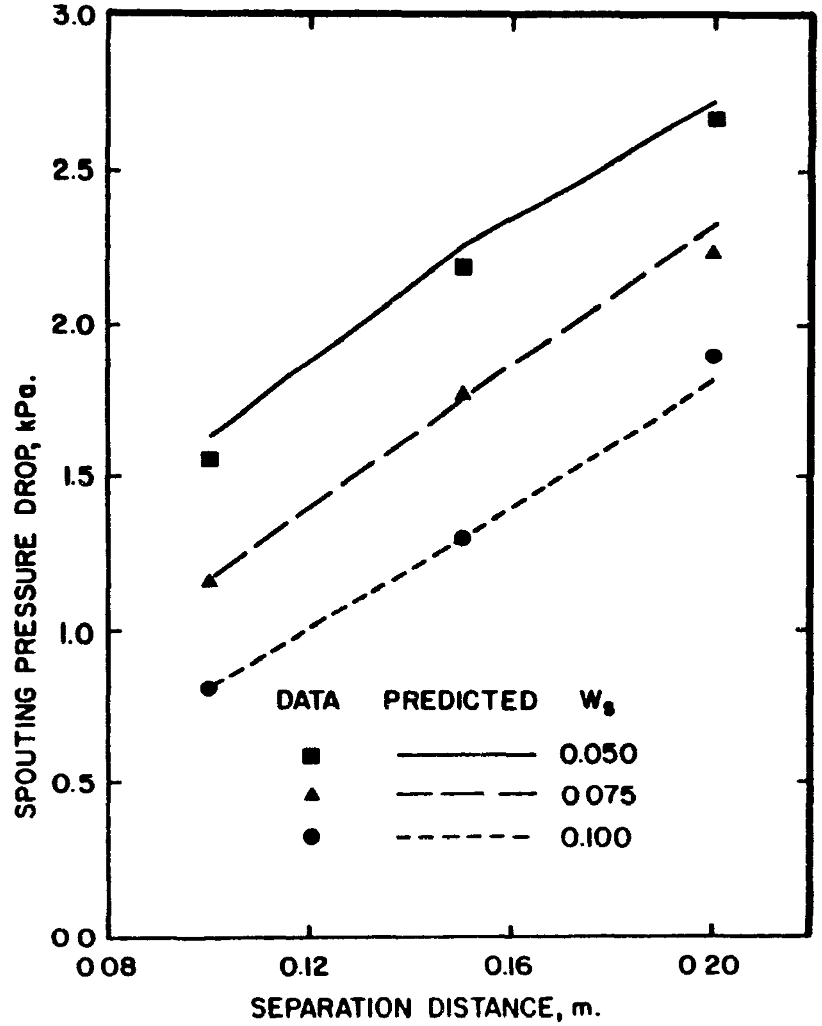

Figure 5.18 Effect of separation distance on spouting pressure drop in pilot scale for wheat. θ_s = 60°.

separation distance increased with an increase in spout width. This effect was larger in the case of wheat. The decrease in the spouting pressure drop is due to reduction in the horizontal pressure of grains and an increased air flow through the spout.

The spouting pressure drop data collected in this study indicated that the spouting pressure drop decreased as the spout width increased from 5 cm to 10 cm (see Figures 5.13 to 5.18). This decrease in spouting pressure drop may be due to a more efficient use of air pressure in pushing grains through the spout and to a lower horizontal pressure of grains from the downcomer on the air jet. The decrease in spouting pressure drop due to the increase in spout width was highest in the case of wheat, followed by soybean and shelled corn. The effects of slant angle were much clearer when the separation distance was 20 cm and the spout widths were 5 cm and 10 cm for the tested grains. It may be concluded that the spouting pressure drop at the minimum spouting conditions is most affected by separation distance, followed by spout width and slant angle.

The model developed for the spouting pressure drop is:

$$\frac{P_s}{g\rho_p H_t} = \left[\frac{Q_p}{Q_f}\right]^{0.46} \left[\frac{W_o}{W_s}\right]^{0.42} \theta_s^{\,0.33} \left[\frac{U_f^2}{gH_t}\right]^{0.21} \left[\frac{H_b W_i}{H_t W_s}\right]^{0.11} \qquad (5.2)$$

The model has R^2_{adj} = 99.92 %, standard error of estimate = 0.0631, α = 0.0001. The residuals exhibited a random distribution when plotted against predicted values of P_s (Figure 5.19). A plot of observed versus predicted values for the selected model of spouting pressure drop is shown in Figure 5.20. Taking

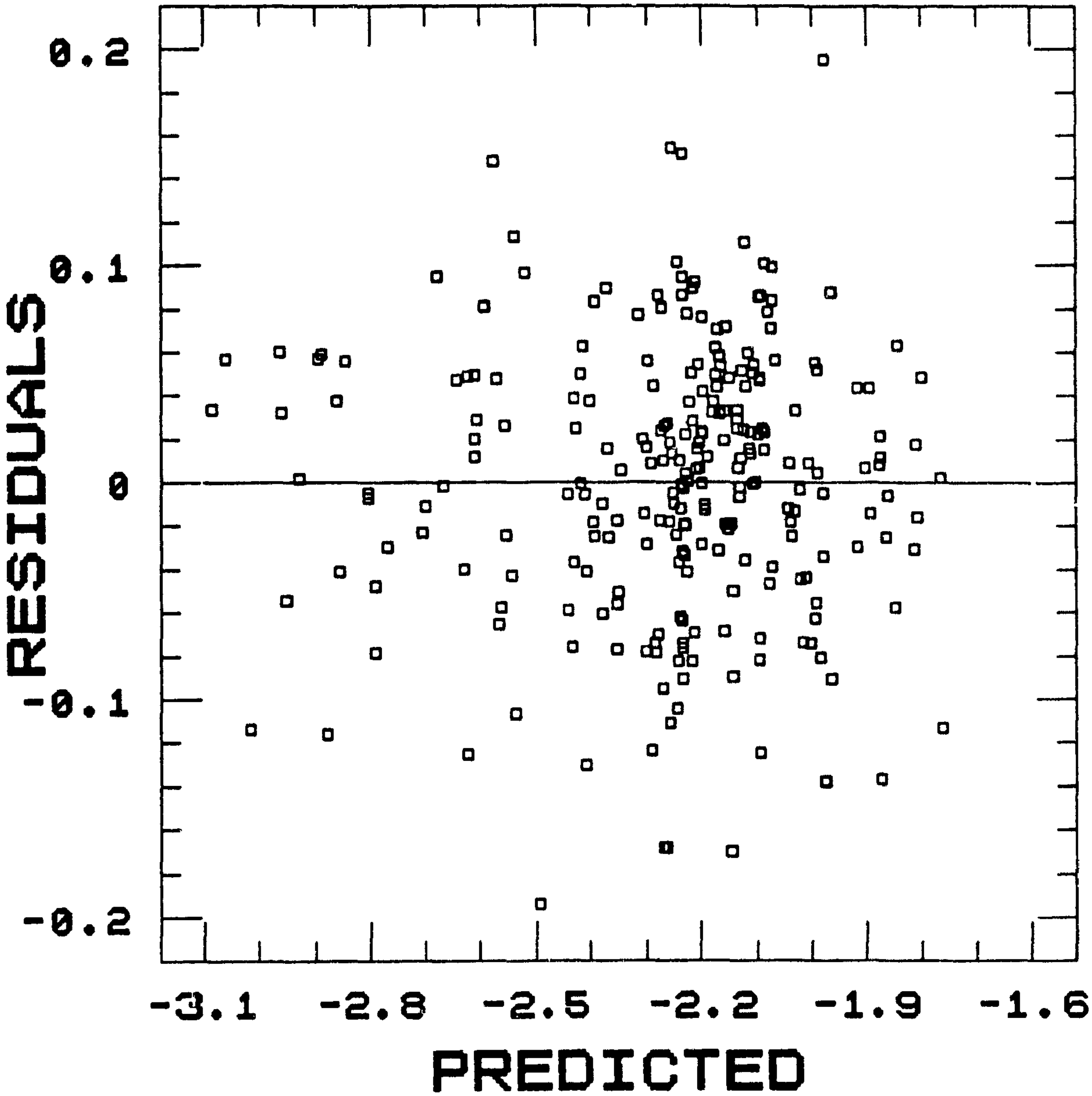

Figure 5.19 Residual plot for spouting pressure drop model, equation (5.2).

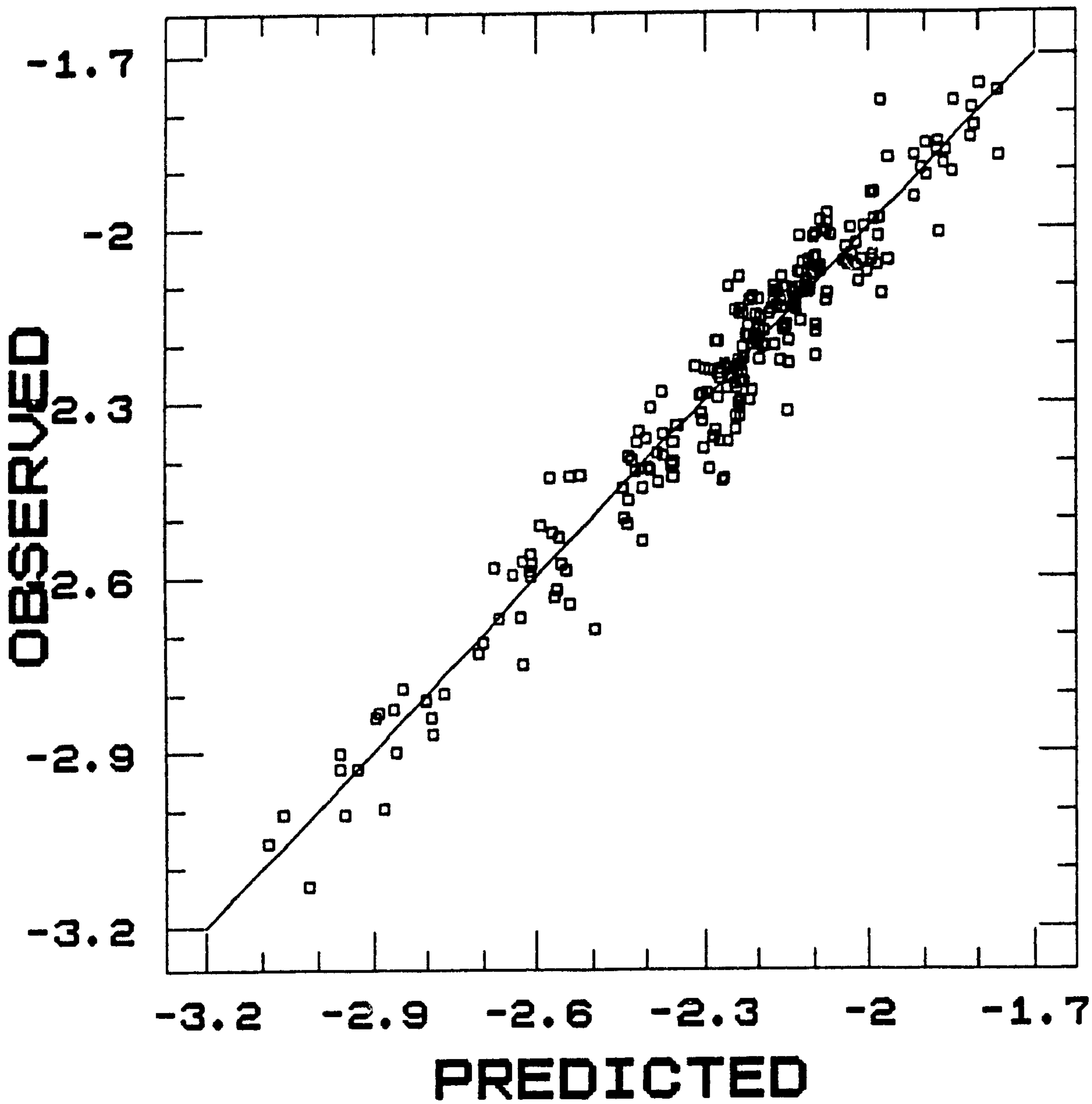

Figure 5.20 Comparison of measured spouting pressure drop with predicted spouting pressure drop by equation (5.2).

equation (5.2), the predicted values of P_s were generated and plotted in Figures 5.13 through 5.18 for comparison with the collected data. The estimates from the model deviated, on average, by ± 4.6 % from the collected data. The 95 % confidence intervals for coefficients are given in Table A.3.

5.2.2 Minimum spouting velocity.

The air flow monitored in the air supply conduit during the dynamics studies was divided by the cross-sectional area of the spouted bed to get the superficial velocity. Some superficial velocity data through pilot scale slotted 2DSBs are presented in Figures 5.21 to 5.26. From these data, it is observed that the superficial air velocity through beds increased as the separation distance increased from 10 cm to 20 cm and varied with grain type. Similar results have been reported by Buchanan and Wilson (1965) and Claflin and Fane (1983) for CSBs and Law et al. (1984, 1986) for small scale 2DSBs. This increase of superficial air velocity may be due to the combined effects of: (1) a larger number of grains entering the spout, (2) more jet air being dispersed into the downcomer at larger separation distances, and (3) physical characteristics of grains leading to higher air flow rates through the spouted beds.

The superficial velocity of air through the beds also increased as the spout width increased from 5 cm to 10 cm for all the grains as shown in Figures 5.21 to 5.26. This increase was due to the higher cross-sectional area of the spout causing higher air flow requirements for transporting an increased number of grains through the spout and to preserve stable dynamic conditions. Similar results were reported for small scale 2DSB's with flat bottoms by Law et al. (1984, 1986), for

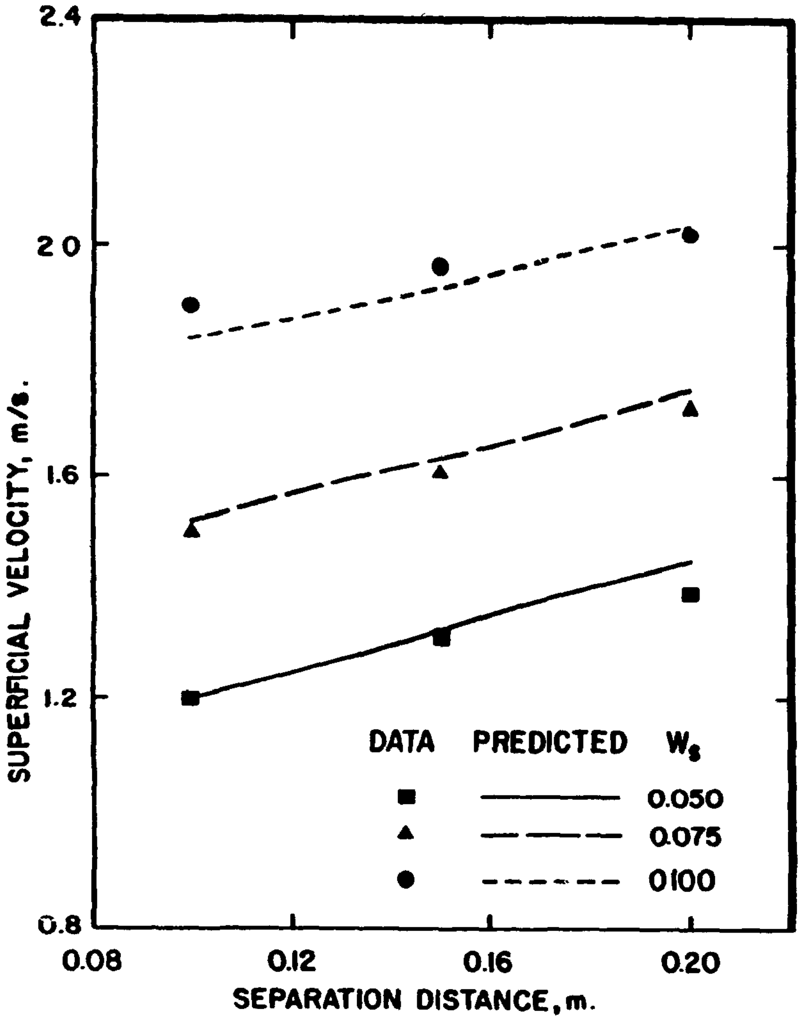

Figure 5.21 Effect of separation distance on minimum spouting velocity in pilot scale for shelled corn. $\theta_s = 45°$.

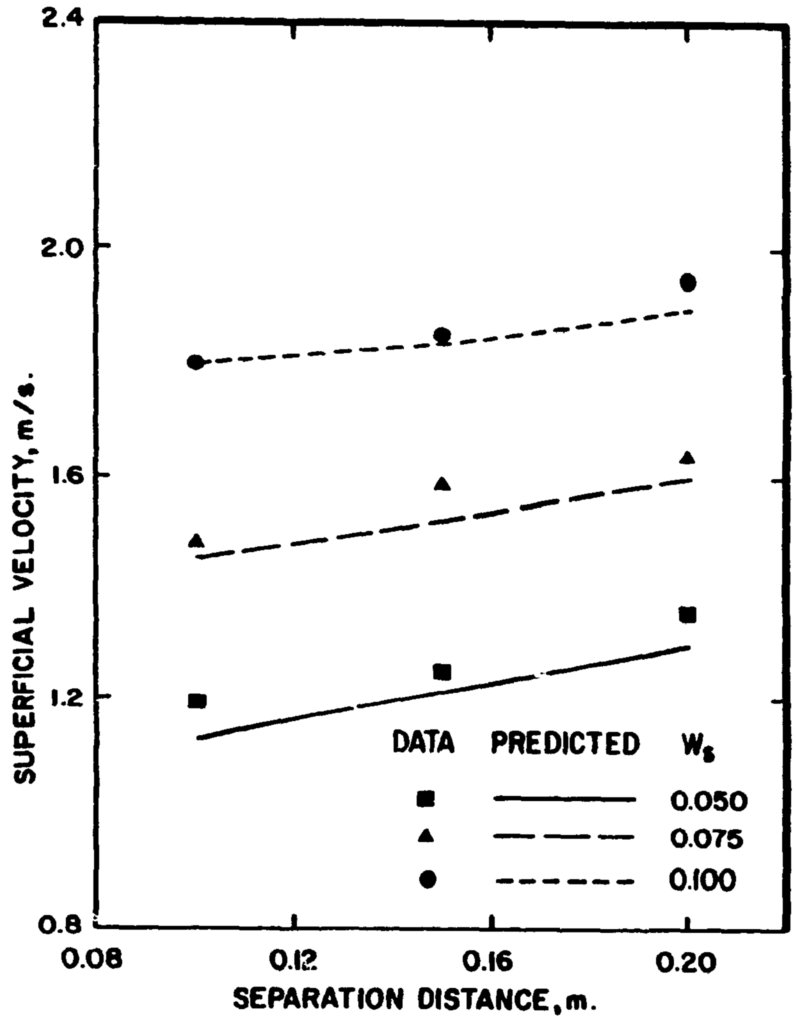

Figure 5.22 Effect of separation distance on minimum spouting velocity in pilot scale for shelled corn. $\theta_s = 60°$.

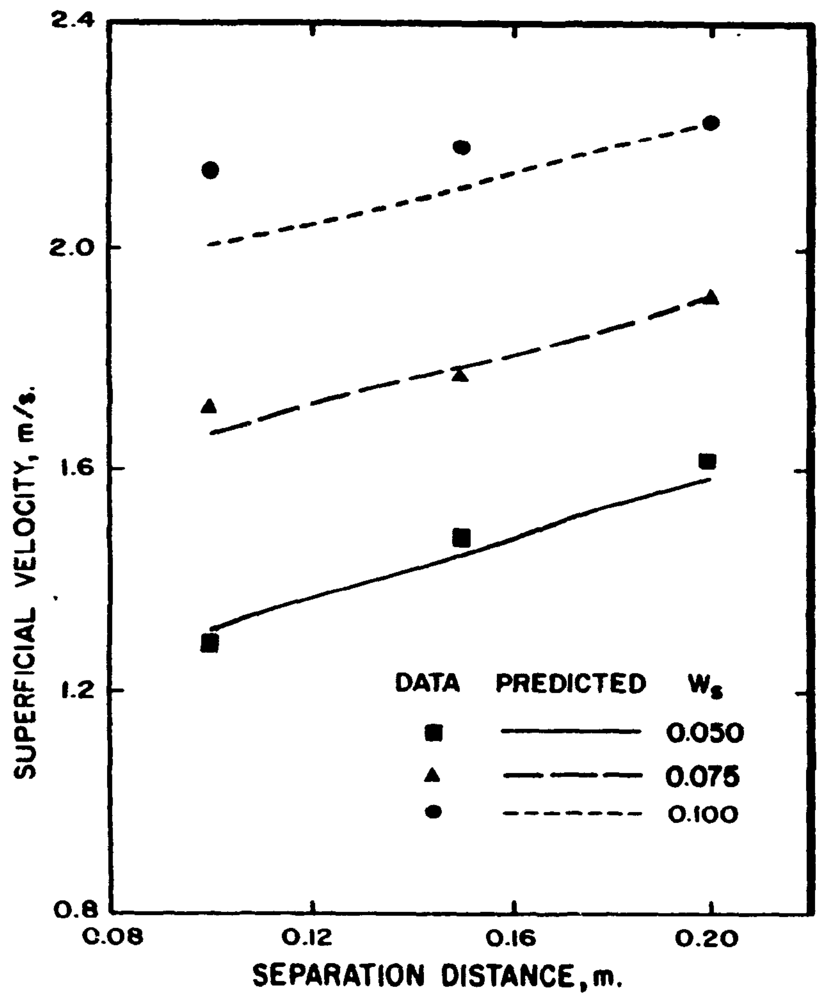

Figure 5.23 Effect of separation distance on minimum spouting velocity in pilot scale for soybean. $\theta_s = 45°$.

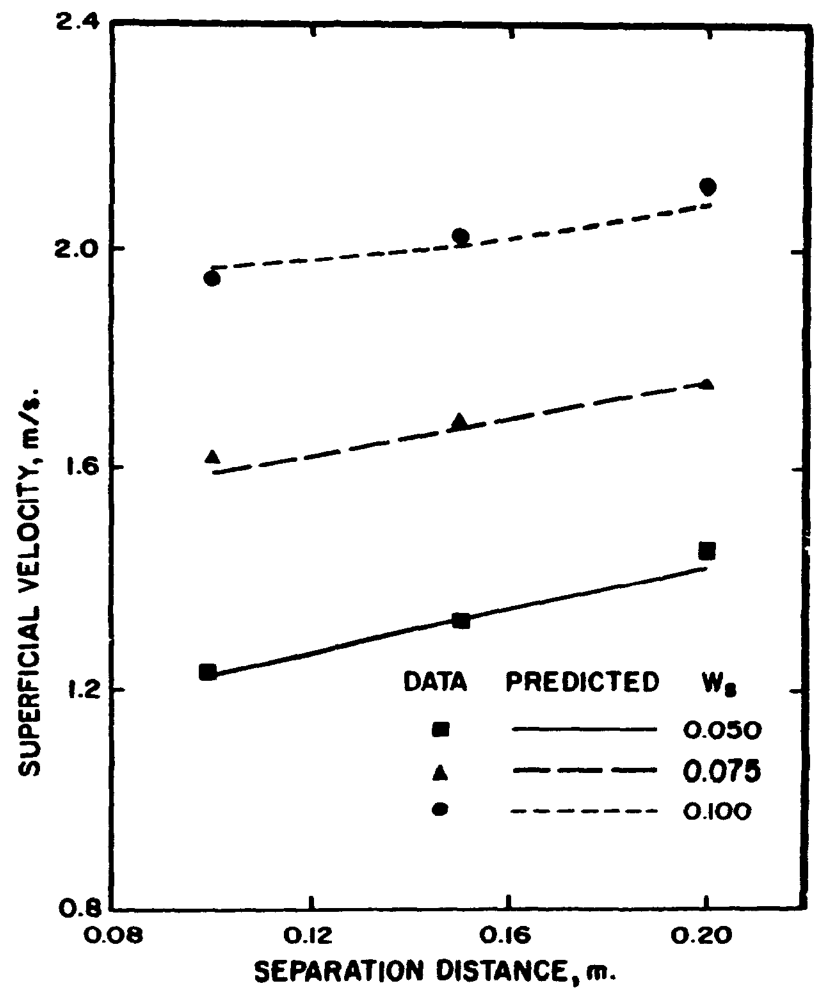

Figure 5.24 Effect of separation distance on minimum spouting velocity in pilot scale for soybean. $\theta_s = 60°$.

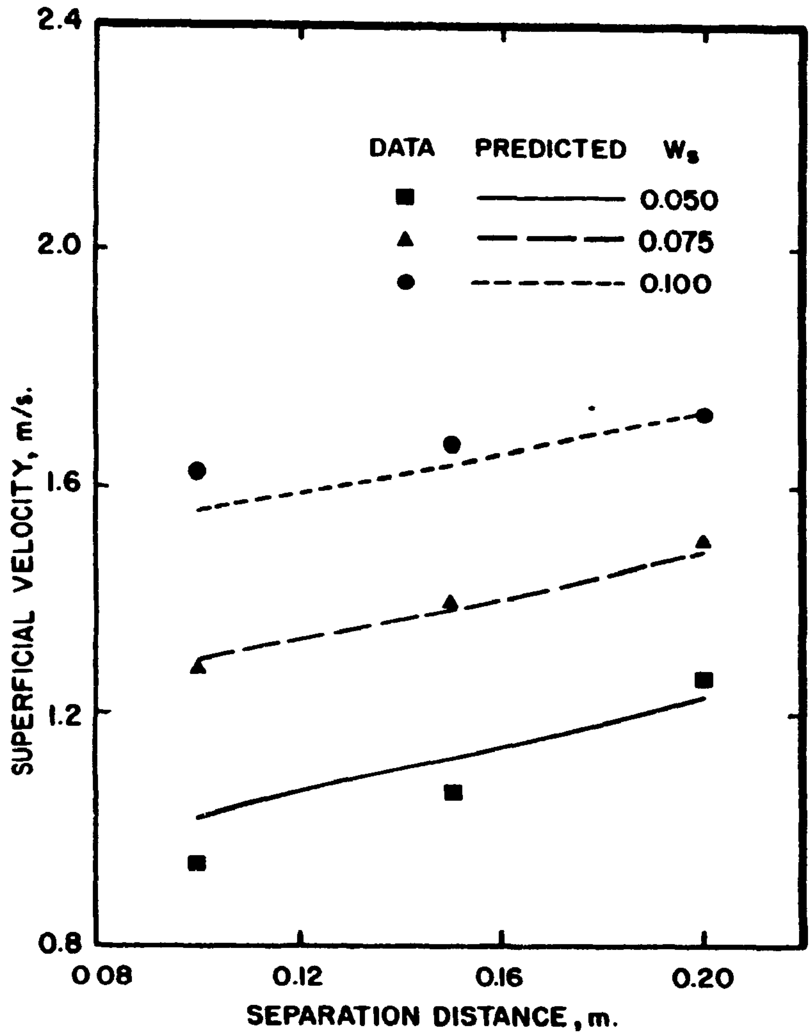

Figure 5.25 Effect of separation distance on minimum spouting velocity in pilot scale for wheat. $\theta_s = 45^\circ$.

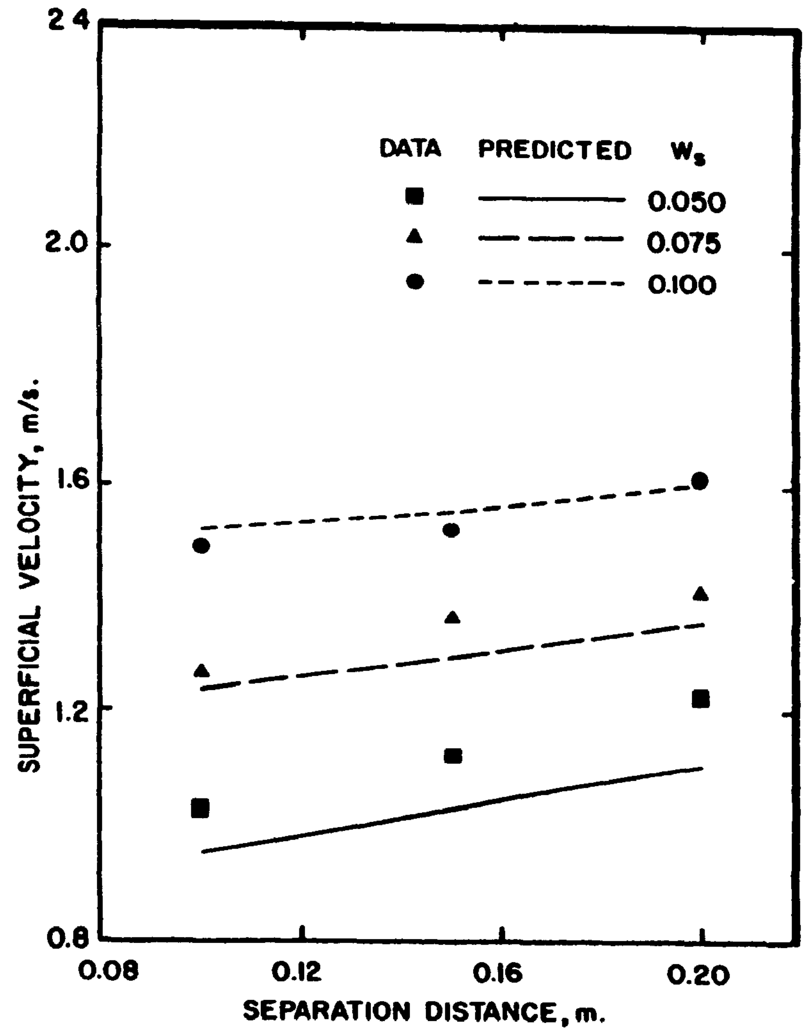

Figure 5.26 Effect of separation distance on minimum spouting velocity in pilot scale for wheat. $\theta_s = 60^\circ$.

rice beds with a slant angle of 45° by Khoe and Brakel (1980), and for wheat beds with a slant angle of 60° in a CSB geometry by Claflin and Fane (1983). Data from this study show that the superficial velocity of air through spouted beds was highest for soybean, followed by shelled corn and wheat.

Figures 5.21 to 5.26 show the differences in superficial velocity due to slant angles, a difference which is particularly noticeable in the case of soybean. The required air flow rates were higher at a slant angle of 45° than at one of 60° at the same separation distance and spout width for soybeans. The shelled corn and wheat beds responded only slightly to slant angles, perhaps due to differences in physical properties of particles. Similar results were reported by Thorley et al. (1959) for CSBs when slant angle was changed from 45° to 60°. It was concluded that the superficial air velocity through large scale 2DSBs increased with separation distance and spout width. However, the superficial air velocity decreased when the slant angle was shifted from 45° to 60° for the three grains used in this study.

The mathematical model obtained for the superficial air velocity through the bed is given below:

$$\frac{U_f}{(gd_p)^{0.5}} = \frac{\left[\left[\left(\frac{W_s}{W_i}\right)\log_{10}\left(\frac{\rho_p-\rho_f}{\rho_f}\right)\right]+\left(\frac{W_o}{L_b}\right)\right]^{0.84}}{\times\left[\frac{W_i}{d_p}\right]^{0.27}\left[\frac{\phi}{\varepsilon_v}\right]^{0.66}\left[\frac{H_t D_s \mu^2}{gH_b W_o d_p^3 \rho_f^2}\right]^{0.06}} \qquad (5.3)$$

The model has R^2_{adj} = 99.77 %, SE = 0.0884, residuals = 1.9151, and α = 0.0001. The plot of residuals against the predicted values of U_f showed randomness of residuals (Figure 5.27). Hence, the developed model accounts for most of the variation found in the collected data. A printout of the observed and predicted values of superficial velocity for spouting of grains is given in Figure 5.28. Using equation (5.3), the predicted values of U_f were generated and compared with the entire observed values of superficial velocity. This comparison indicated that the equation (5.3) predicts with an average error of ± 6.6 % from the observed values. The 95 % confidence intervals for coefficients are given in Table A.4.

The Figures 5.21 to 5.26 also show the predicted data points from the model (equation 5.3) developed for the superficial velocity. The results show that the mathematical model estimates of U_f are in very good agreement with the collected data. The predictions are better for shelled corn and soybean than for wheat grains. This could be due to the fact that the grain-related parameters in the model do not fully account for the effects of differences in shape, orientation, surface roughness and bulk flow of wheat relative to the other grains. The maximum deviations from the data collected while varying the separation distance, spout width, and slant angle were +6.7 to -2.6 % for shelled corn, +3.9 to -4.2 % for soybean, and +10.7 to -8.7 % for wheat.

5.2.3 Solids circulation rate/average particle velocity.

The average particle velocities observed over all the runs were in the range of 1.42 to 4.14 cm/s. The lowest particle velocity was 1.28 cm/s in the case of shelled corn and the highest was 4.33 cm/s in the case of soybean. The solids circulation rates were calculated from the average particle velocity in the downcomers, the effective cross-sectional area of the downcomers, and the average bulk density.

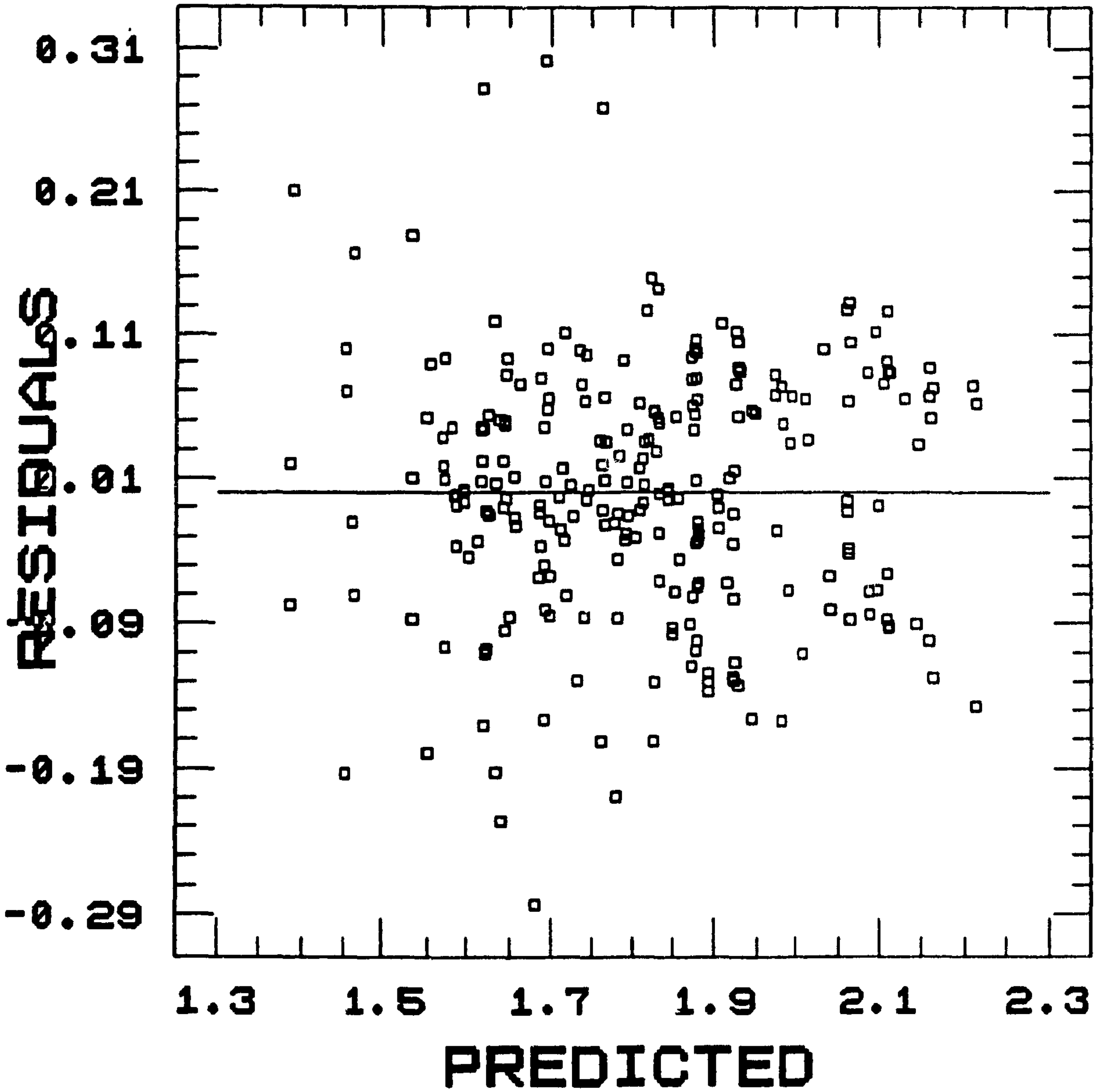

Figure 5.27 Residual plot for minimum spouting velocity model, equation (5.3).

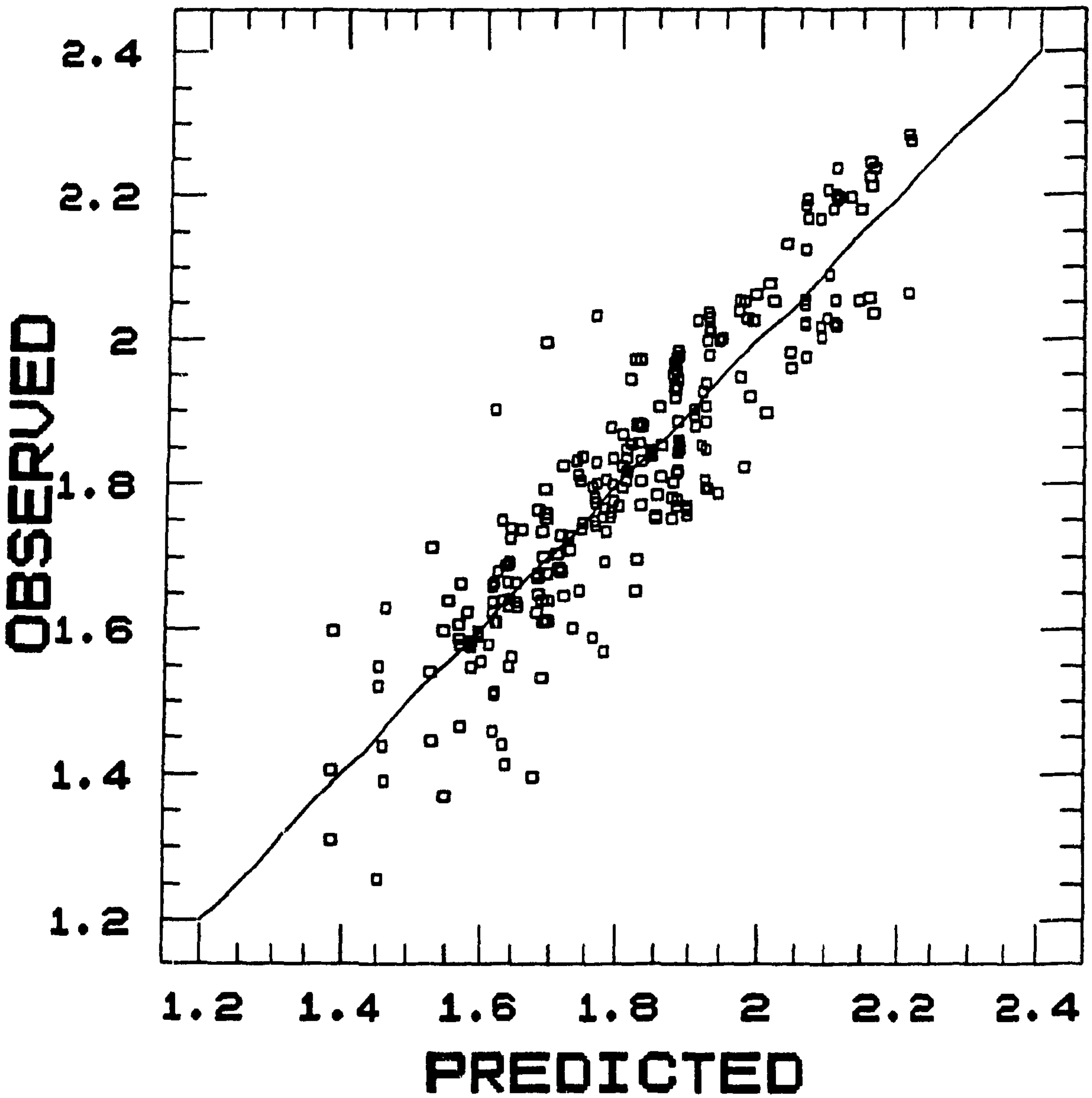

Figure 5.28 Comparison of measured minimum spouting velocity with predicted minimum spouting velocity by equation (5.3).

Plots of solids circulation rate versus separation distance for various spout widths and slant angles are shown in Figures 5.29 to 5.34. It may be observed that the solids circulation rate increased with separation distance and varied with grain type. Similar effects were reported for laboratory scale models by Buchanan and Wilson (1965), Khoe and Brakel (1980), and Claflin and Fane (1983) for CSBs; and Law et al. (1986) for 2DSB. Our solids circulation rates (particle velocities) in the downcomers of 2DSBs are higher than the reported values of Claflin and Fane (1983) for the CSB with slant angle of 60°. The effects of separation distance and air flow on the rate of solids circulation increased with spout width.

The solids circulation rate increased as the spout width increased from 5 cm to 10 cm and its magnitude increased with separation distance regardless of grain type as shown in Figures 5.29 to 5.34. The solids circulation rate was almost the same for shelled corn and soybean when the spout width was increased from 7.5 cm to 10 cm (see Figures 5.29 to 5.32), but the difference became greater as the separation distance increased due to the higher number of grains entering the spout. The effects at spout widths of 7.5 cm and 10 cm were not clear in the case of wheat grains.

The effects of slant angle were detectable when the separation distances were 15 cm and 20 cm and spout widths were 7.5 cm and 10 cm for shelled corn and soybean as can be judged from Figures 5.29 through 5.34. Furthermore, the solids circulation rate remained approximately constant when the separation distance was 10 cm and spout widths were 7.5 cm and 10 cm for all grain types used. This occurs because the solids circulation rate is limited by the dimensions of the orifice formed at the point of normal distance from the slanting base to the bottom of the draft

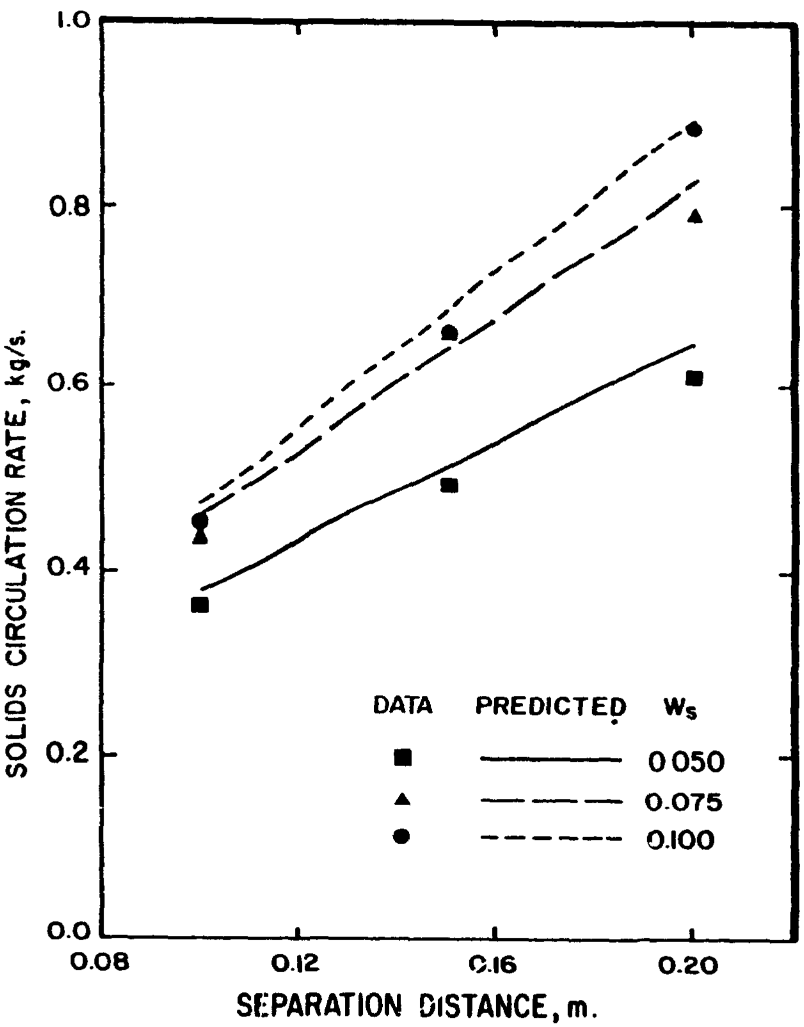

Figure 5.29 Effect of separation distance on solids circulation rate in pilot scale for shelled corn. $\theta_s = 45°$.

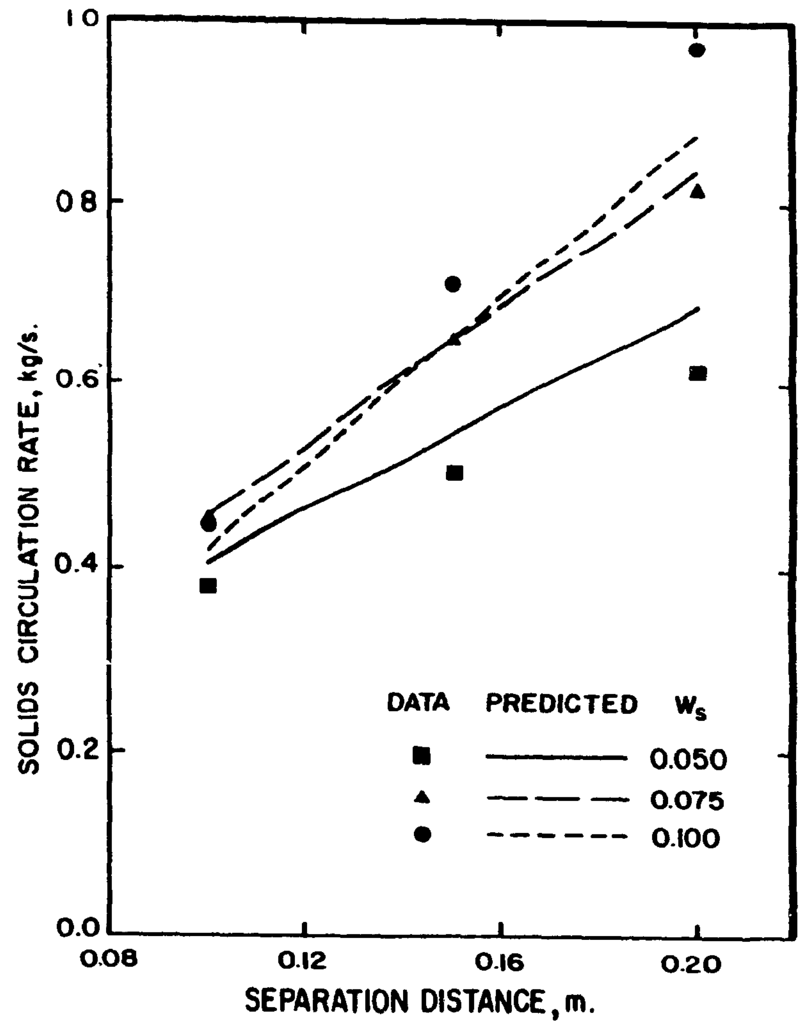

Figure 5.30 Effect of separation distance on solids circulation rate in pilot scale for shelled corn. $\theta_s = 60°$.

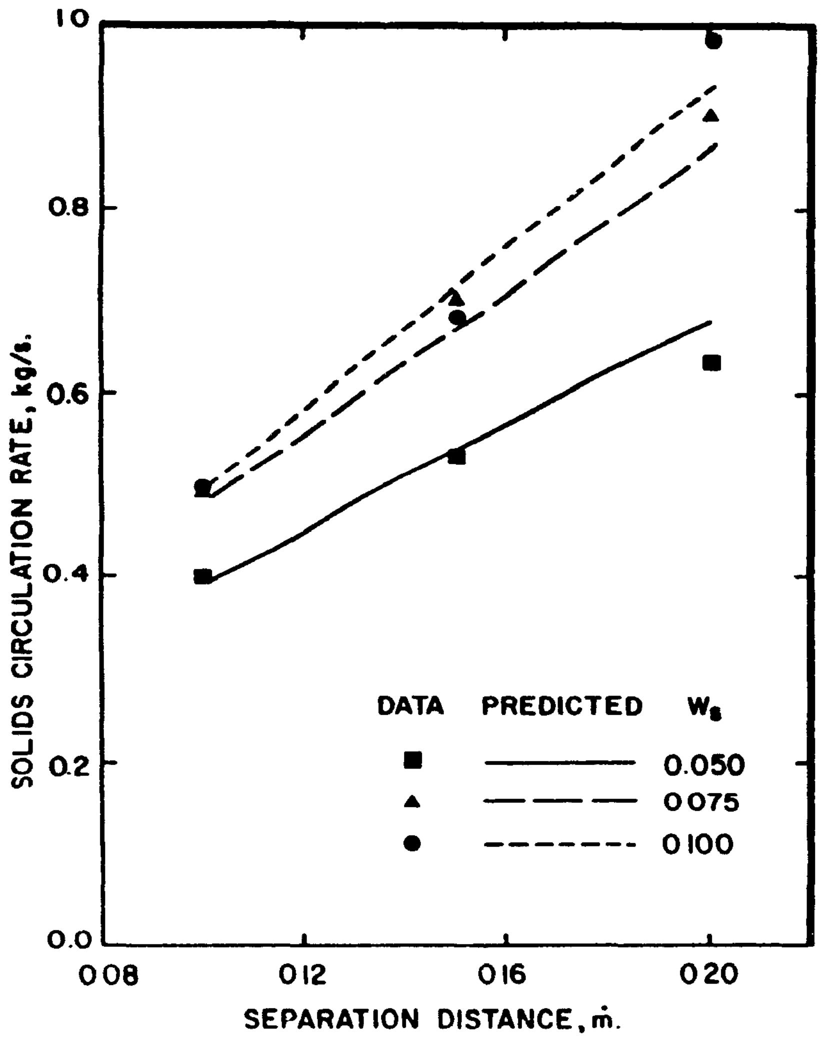

Figure 5.31 Effect of separation distance on solids circulation rate in pilot scale for soybean. $\theta_s = 45^o$.

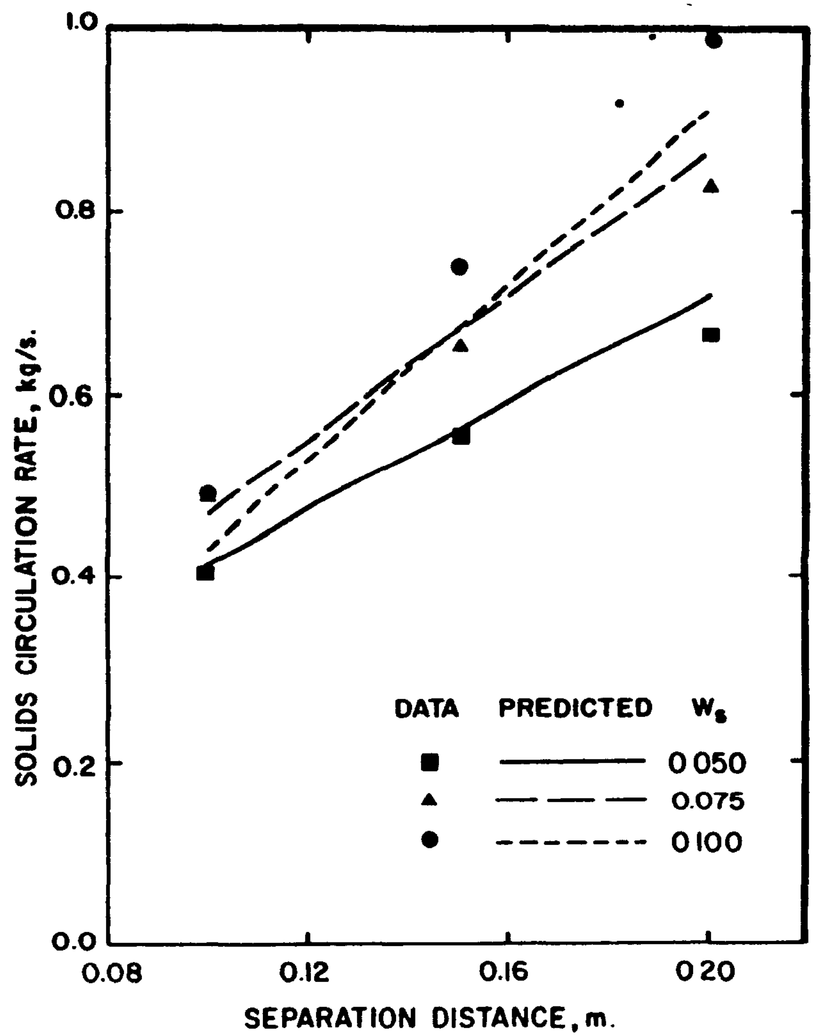

Figure 5.32 Effect of separation distance on solids circulation rate in pilot scale for soybean. $\theta_s = 60^o$.

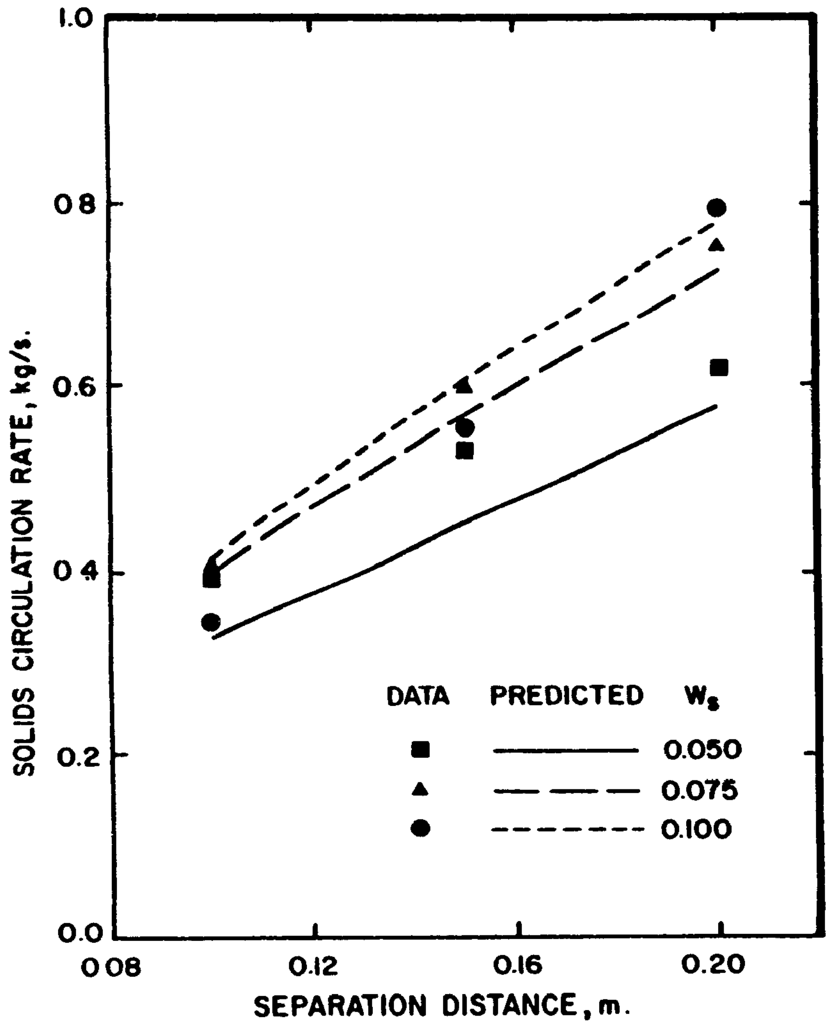

Figure 5.33 Effect of separation distance on solids circulation rate in pilot scale for wheat. $\theta_s = 45°$.

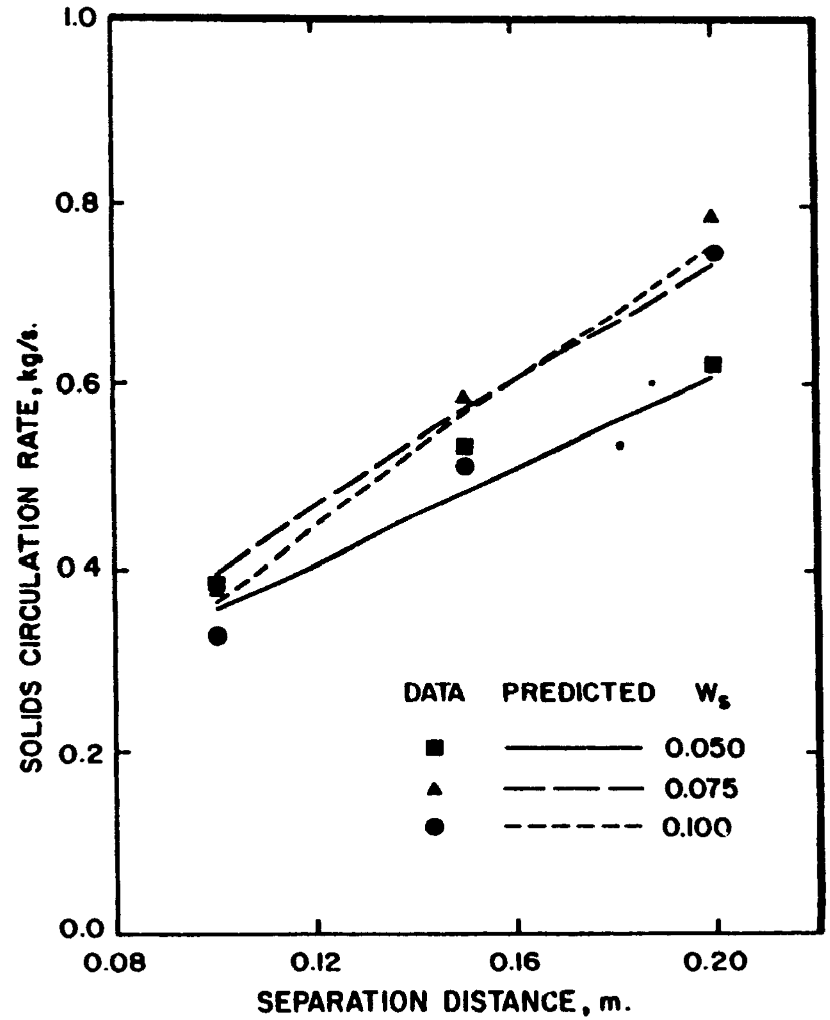

Figure 5.34 Effect of separation distance on solids circulation rate in pilot scale for wheat. $\theta_s = 60°$.

plates. These dimensions decrease as spout width increases at the same separation distance. Hence, higher than minimum air flows through the bed will not enhance the solids circulation rate. Any further increase in spout width decreases the solids circulation rate as well as air percolation into the downcomer which may not be desirable in drying of grains. It should be noted that for a given size of orifice, the flow rate of shelled corn may vary with the variety due to differences in the size of kernel.

The mathematical model obtained for solids circulation rate is:

$$\frac{M_p}{\rho_b A_d (g W_o)^{0.5}} = \left[\frac{D_s}{D_i}\right]^{2.37} \theta_s^{0.6}\, \varepsilon_v^{7.53} \left[\frac{W_o}{W_s}\right]^{0.34} \times \left[\frac{d_p}{D_h}\right]^{0.26} \left[\frac{\rho_p - \rho_f}{\rho_f}\right]^{0.56} \left[\frac{U_f^2 \mu^2}{g^2 H_t d_p^3 \rho_f^2}\right]^{0.07} \tag{5.4}$$

with R^2_{adj} = 99.92 %, standard error of estimate = 0.0924, and α = 0.0001. A print out of residuals against selected model predictions is shown in Figure 5.35. The plot of observed and predicted values for the solids circulation rate model is produced in Fig. 5.36. The developed model predicts the collected data with an average error of $\pm$ 6.8 %. The 95 % confidence intervals for coefficients are given in Table A.5.

The predictions from the solids circulation rate model are presented in Figures 5.29 to 5.34 which show good agreement. The grains used in the aerodynamic experiment were of seed quality, but in other experiments the grain

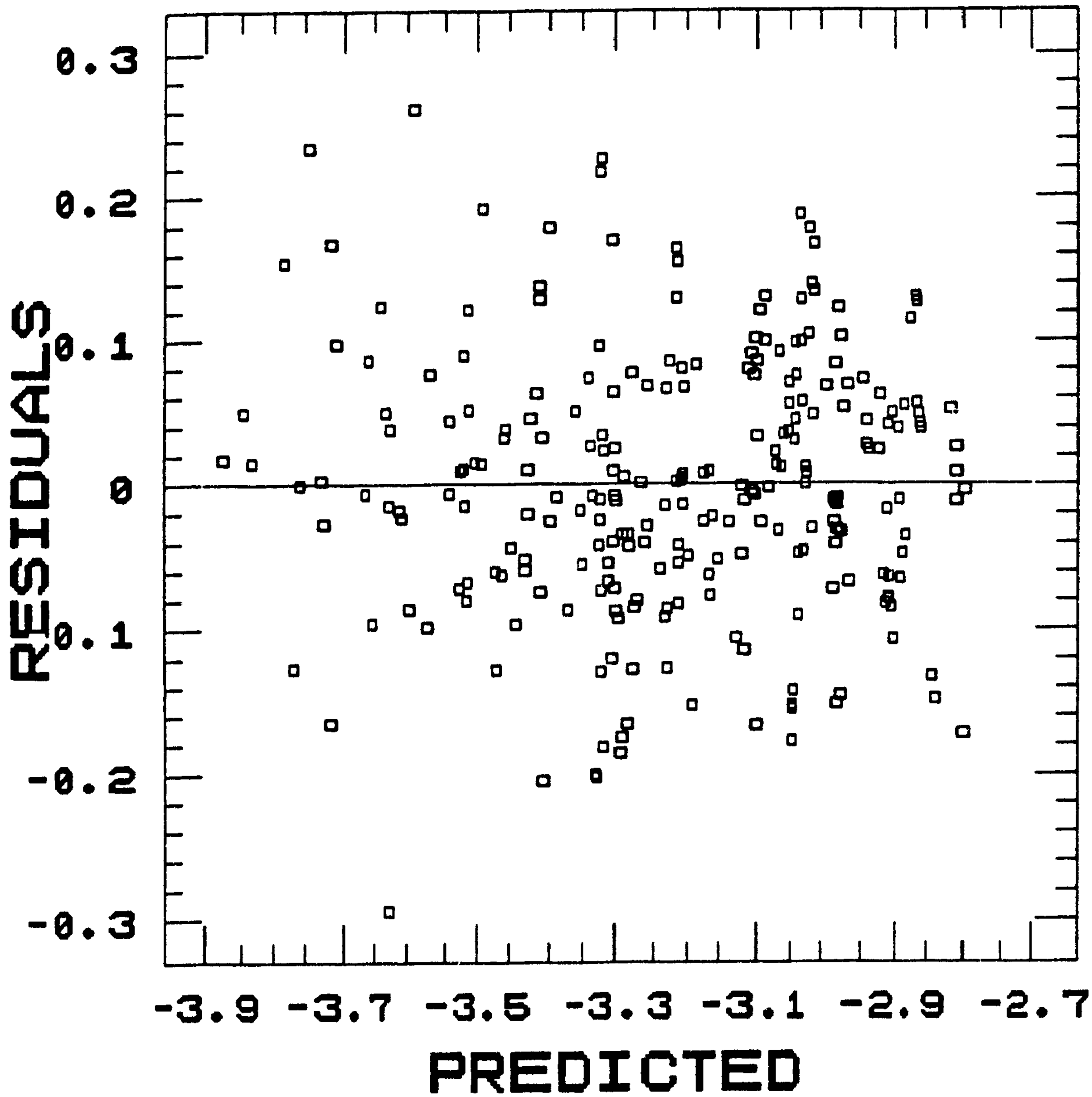

Figure 5.35 Residual plot for solids circulation rate model, equation (5.4).

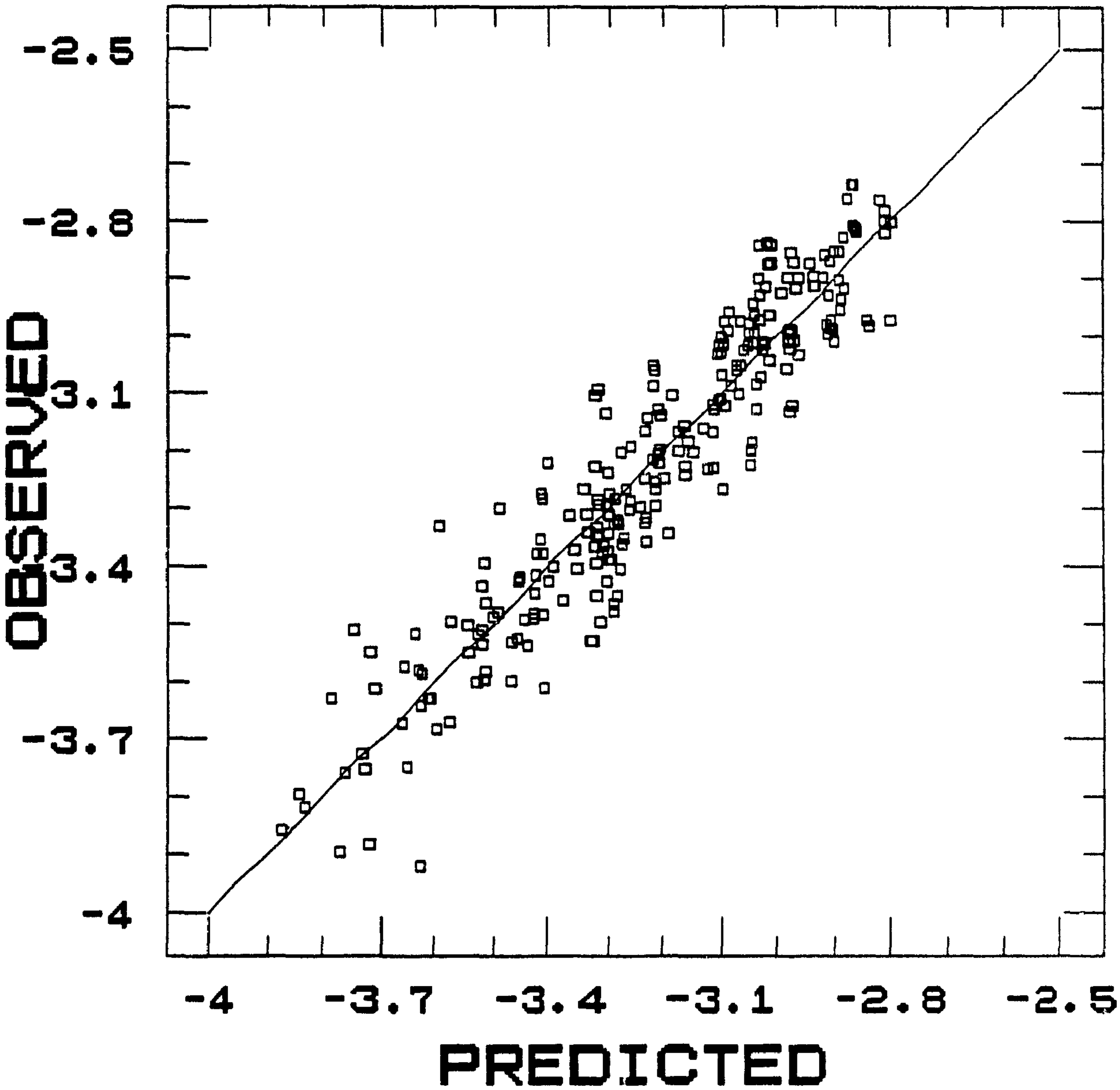

Figure 5.36 Comparison of solids circulation rate measured with solids circulation rate predicted by equation (5.4).

beds included some straw, broken ear heads, weed seeds, pods, corn cob pieces, and broken seeds as would be the case in real applications.

5.2.4 Average cycle time.

The data representing average particle cycle time in the downcomers of the pilot scale unit are plotted against normal distance in Figures 5.37 to 5.39. The cycle times of particles in the case of slant angle of 45° were 5.1 to 9.4 % greater than the slant angle of 60° because of longer particle paths and the mass of grains in the bed. The shortest particle cycle times were observed when the slant angle was 60°, spout width was 10 cm, and separation distance was 20 cm and it was in the range of 28.6 to 31.4 seconds. The longest cycle times were found when slant angle was 45°, spout width was 5 cm, and separation distance was 10 cm and it was in the range of 85.3 to 109.7 seconds. For any given bed geometry, the particle cycle time decreases with the distance of particles in the downcomer from the centre of the spout.

The cycle time data from the third replicates of the aerodynamics experiment, laboratory scale part of the scale-up experiments, and drying runs were regressed against the dimensionless numbers given in Chapter III. In principle, the average cycle time should be equal to the mass of particles in the bed divided by the solids circulation rate. However, as seen in Figures 5.37 to 5.39, this was not so in this study. The problem could be due to unsynchronized recording of particle velocity and cycle time or may be due to the effect of separation distance on the cycle time distribution of individual particles. If the (M_b/M_p) approach is followed, then the average errors may be expected to be in the range of +10.5 % to -12.6 %

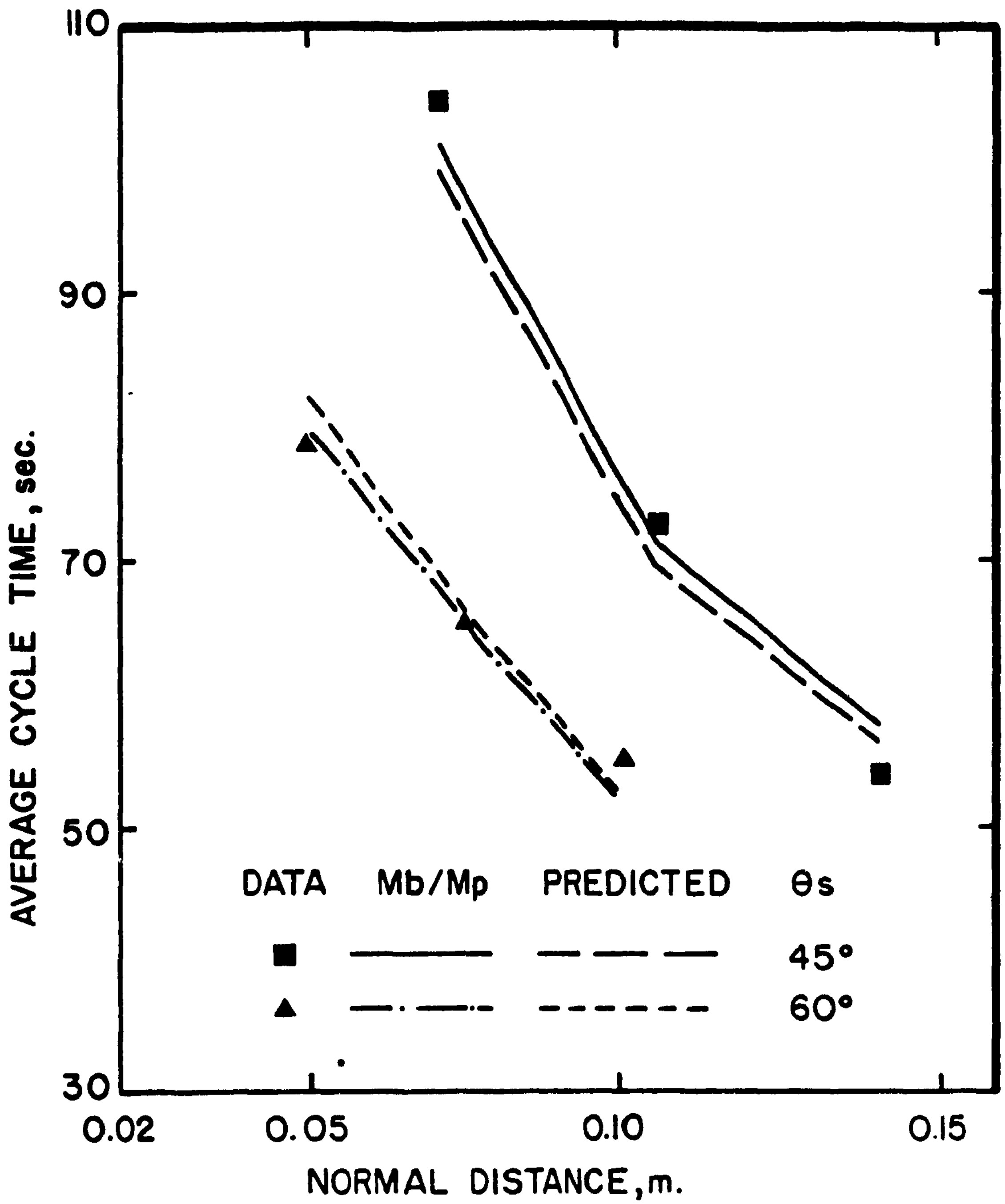

Figure 5.37 Variation of average cycle time with normal distance and slant angle in pilot scale for shelled corn. W_s = 0.05 m.

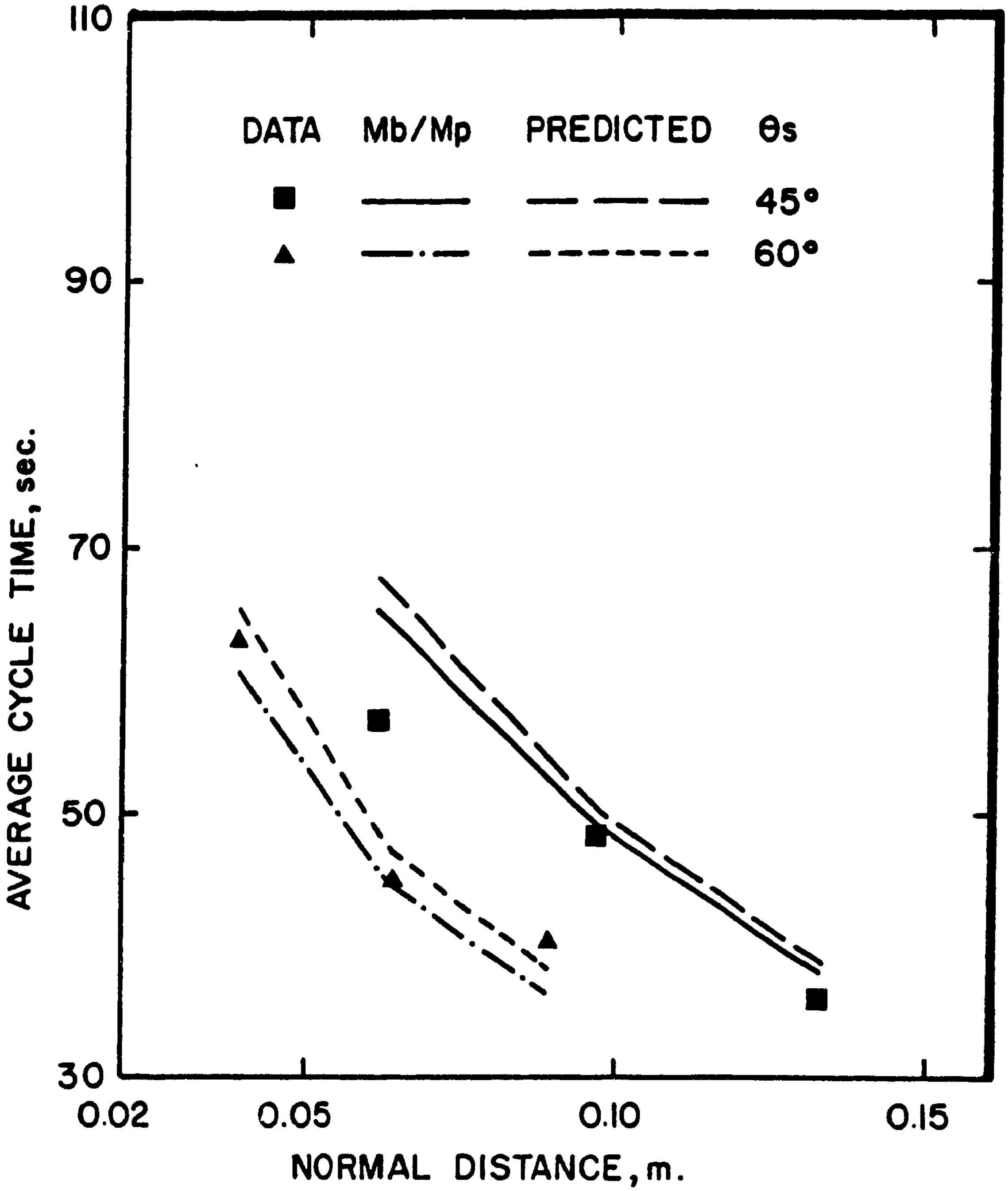

Figure 5.38 Variation of average cycle time with normal distance and slant angle in pilot scale for soybean. W_s=0.075 m.

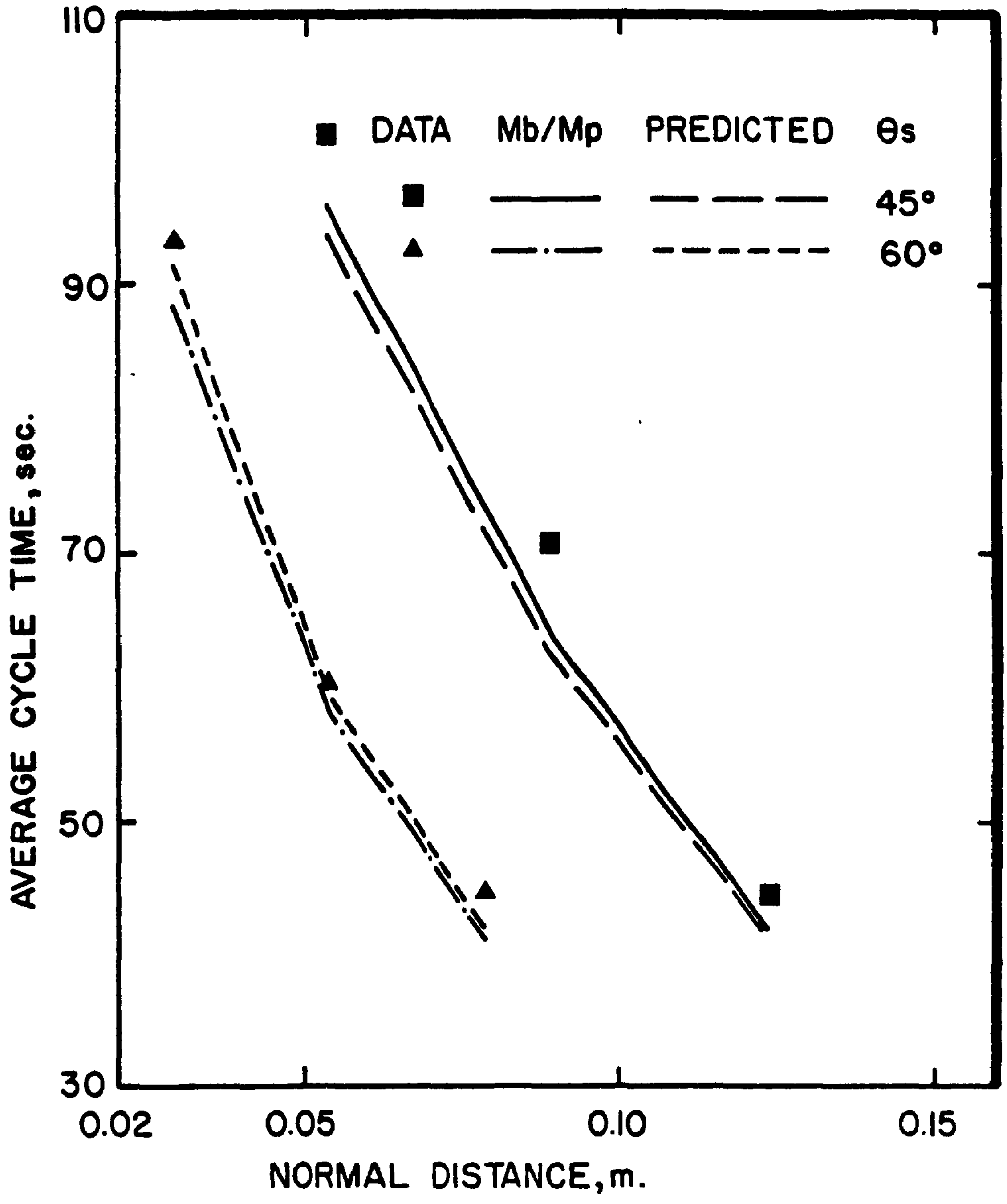

Figure 5.39 Variation of average cycle time with normal distance and slant angle in pilot scale for wheat. W_s =0.10 m.

(Figures 5.37 to 5.39). However, large errors (up to 24 %) were found in case of wheat while spouting in the laboratory scale unit. The reason could be attributed to the presence of foreign material in the bed.

An empirical equation based on the particle velocity could be the best way to determine the average cycle time. In view of this, the cycle time data were reanalysed to get better accuracy. Various models were developed considering all possible combinations, but none was superior to the empirical model:

$$t_c = M_b^{1.02} \, M_p^{-0.89} \left[\frac{H_b d_p}{W_o^2}\right]^{0.05} \tag{5.5}$$

with R^2_{adj} = 99.97 %, standard error of estimate = 0.0649, and significance level = 0.0001. The model predictions vs observed average cycle times are shown in Figure 5.40. It is concluded that the developed model fits the collected data very well. The predicted values were compared with the entire data and average errors were evaluated. This comparison showed that the selected model predicts the data with an average error of +6.5 % to -5.2 %. For purposes of demonstration, the average cycle times vs. separation distance are shown in Figures 5.37 through 5.39 for the pilot scale 2DSBs. The data collected on the cycle time in the laboratory scale 2DSBs are shown in Figure 5.41 against the diameter of grains used in this research. The model predictions fit much better than the M_b/M_p approach. The 95 % confidence intervals for coefficients are given Table A.6.

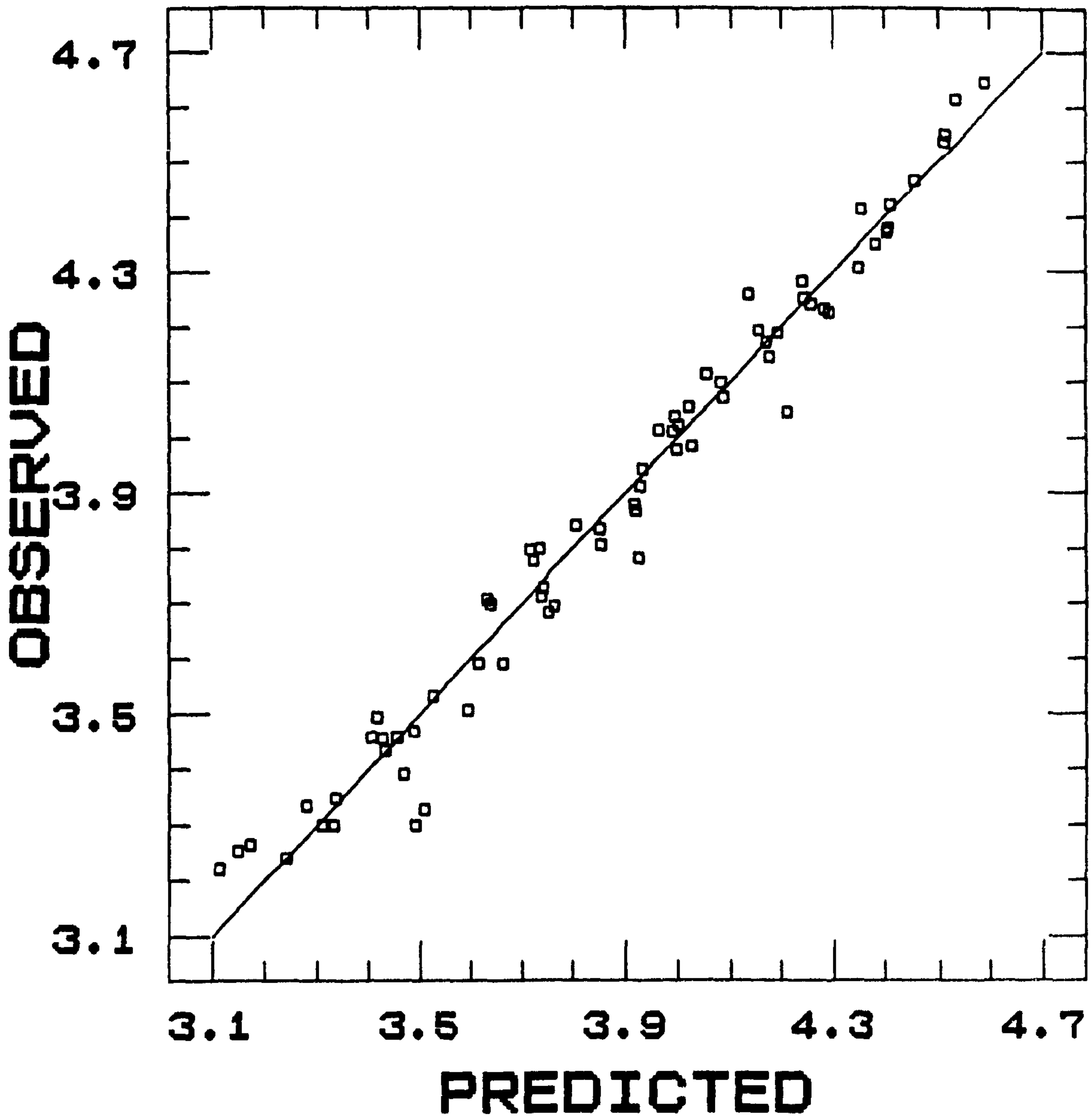

Figure 5.40 Comparison of observed cycle times vs. predicted cycle times by equation (5.5).

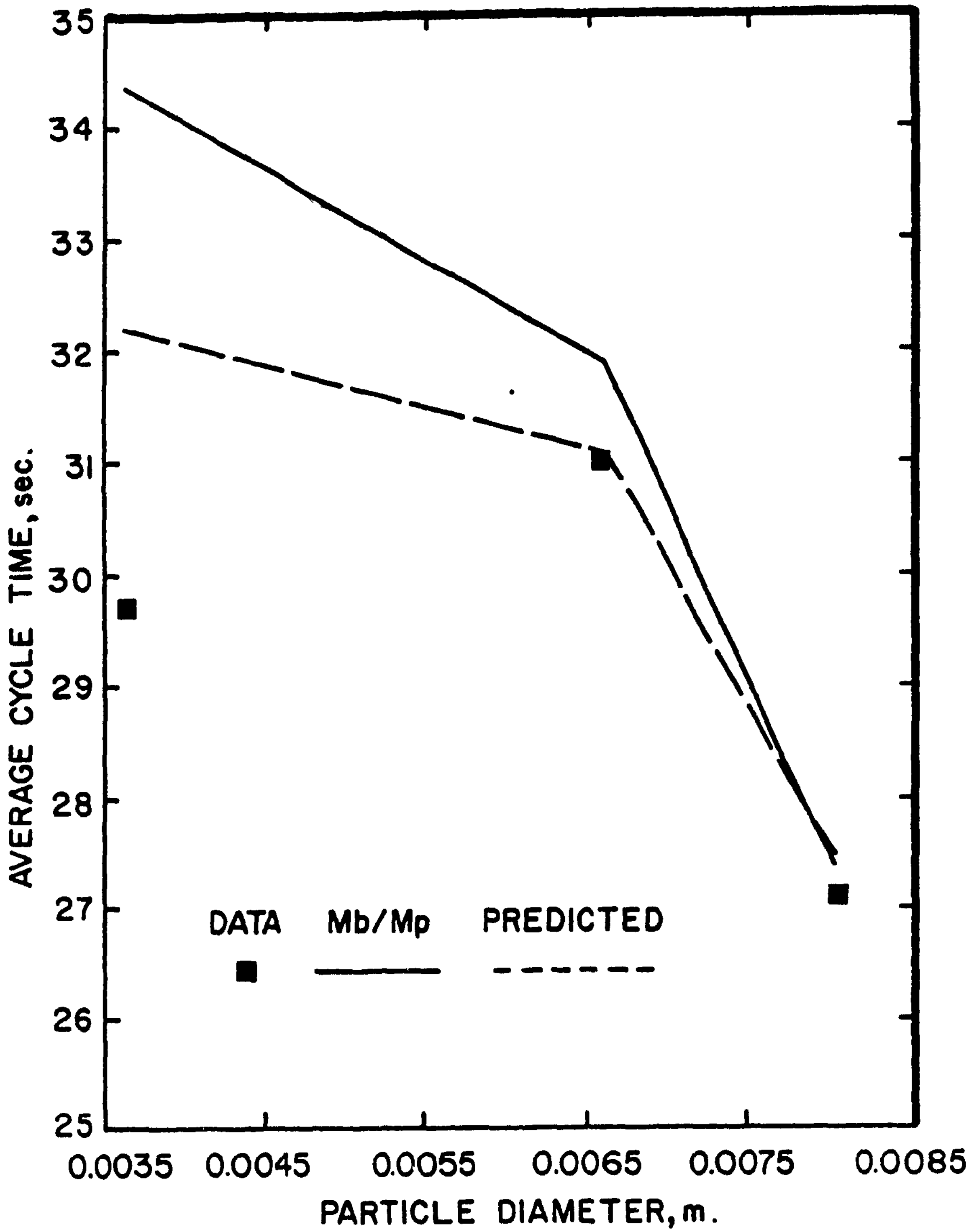

Figure 5.41 Variation of average cycle time with the particle diameter in the laboratory scale for grains.

It should be pointed out that agreement between the proposed models and experimental data for the other experiments, whose graphs have not been shown here for the sake of brevity, are in the same range of accuracy.

5.3 Scale-up.

The scale-up study of two-dimensional spouted beds with draft plates was performed on two bases: 1) by length scale-up, 2) by geometrical similarity. This was greatly facilitated by the design of the pilot scale unit so that it could accommodate various bed lengths and consequently, various cross-sectional aspect ratios (including that of the laboratory scale unit). Thus, manipulation of the various bed geometric factors influencing spouting and solids circulation was greatly simplified and allowed an in-depth study of the scale-up potential of 2DSB's. In this section, the results of both scale-up methods are evaluated.

5.3.1 Spouting pressure drop.

The spouting pressure drop data from the bed length scale-up are shown in Figure 5.42. The spouting pressure drop tended to increase with bed length irrespective of the grains tested. The soybean beds exhibited the lowest pressure drops, followed by wheat and shelled corn. The highest pressure drops associated with shelled corn and soybean occurred at a bed length of 0.15 m whereas the maximum for wheat was at a length of 0.125 m. This can be attributed to the wall effect and the shape of grain represented by sphericity - in the case of spherical grains, more enter the spout, thus artificially increasing the solids concentration between the draft plates. The same is appears true in longer beds where the more

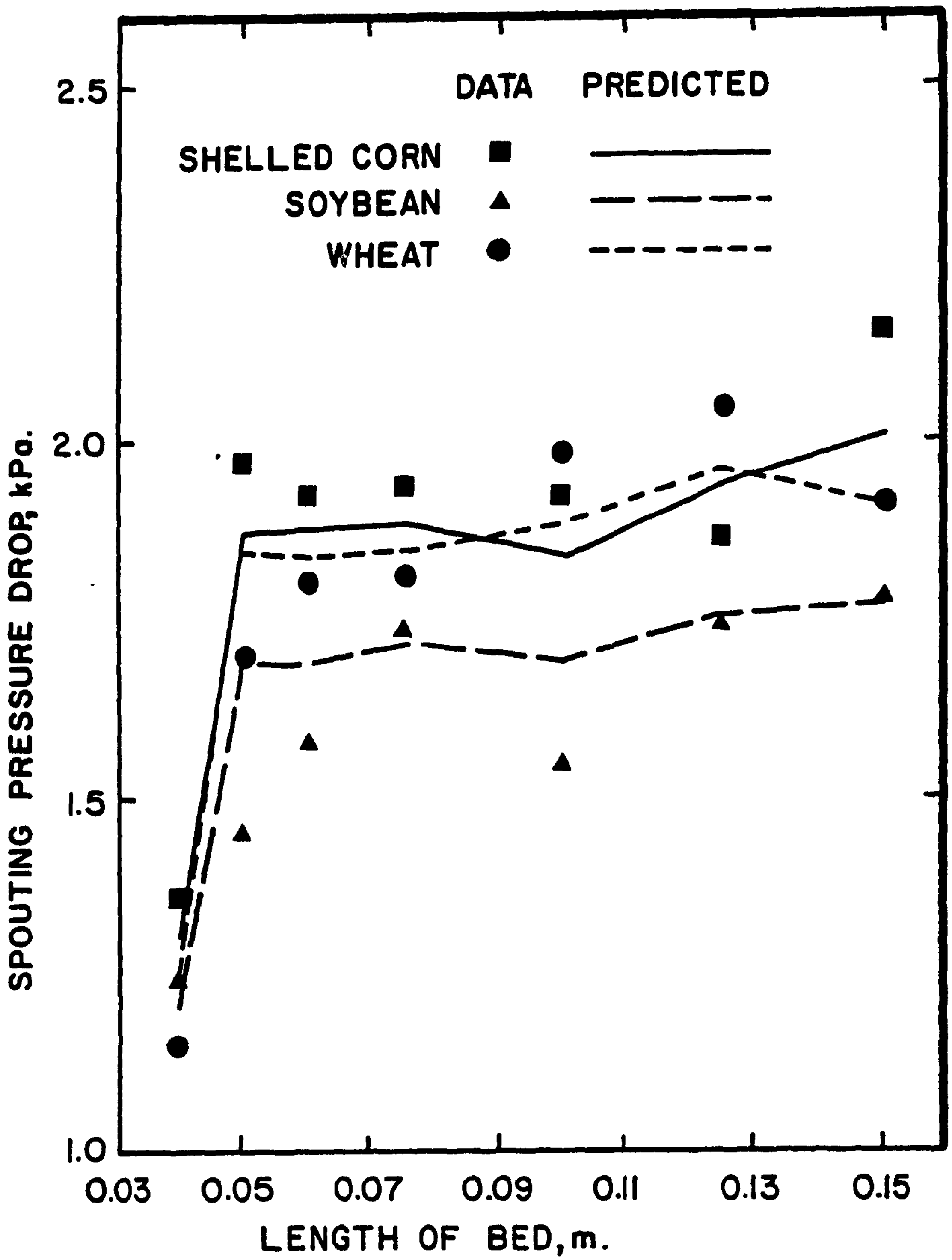

Figure 5.42 Effect of bed length and geometrical similarity (data at $L_b = 0.04$ m and 0.06 m) on the spouting pressure drop for grains.

distanced walls have less of a retarding effect on the entry of grains into the spout. Wheat seems to be an exception to this rule, likely due to its ellipsoid shape.

The data recorded from the two similar beds showed that the pressure drops in the laboratory scale bed were about 70.7 %, 78.7 % and 64.0 % of those in the pilot scale bed, for shelled corn, soybean and wheat, respectively. These results indicate that spouting pressure drop increases directly as the sphericity (see Table A.2) of spouting particles.

Figure 5.42 also shows the predictions from the model of spouting pressure drop. Generally the agreement between the model predictions and the data is fair, especially in the case of wheat beds. The maximum error is ± 8 % and the average error is ± 4 %. Selected data of spouting pressure drop at various bed heights during drying runs of shelled corn are plotted in Figure 5.43. Generally, the overall pressure drop does not decrease while reducing bed height, but unstable spouting occurs when the height of bed is lower than 1/2 of the draft plate height. This condition results in wider pressure drop oscillations. At unstable spouting there could be larger errors in predicted pressure drop because of bubble formation and fluidization in the downcomers. It should be mentioned that there was a limiting screen on top of the laboratory scale spouted bed which should have added to spouting pressure drop. This is why the model predictions are about 8 % below the observed laboratory scale data but agree well with the pilot scale data. The developed model for spouting pressure drop appears to handle the bed length scale-up fairly well. This model can be used for similar situations but should be exercised with care for other bed dimensions.

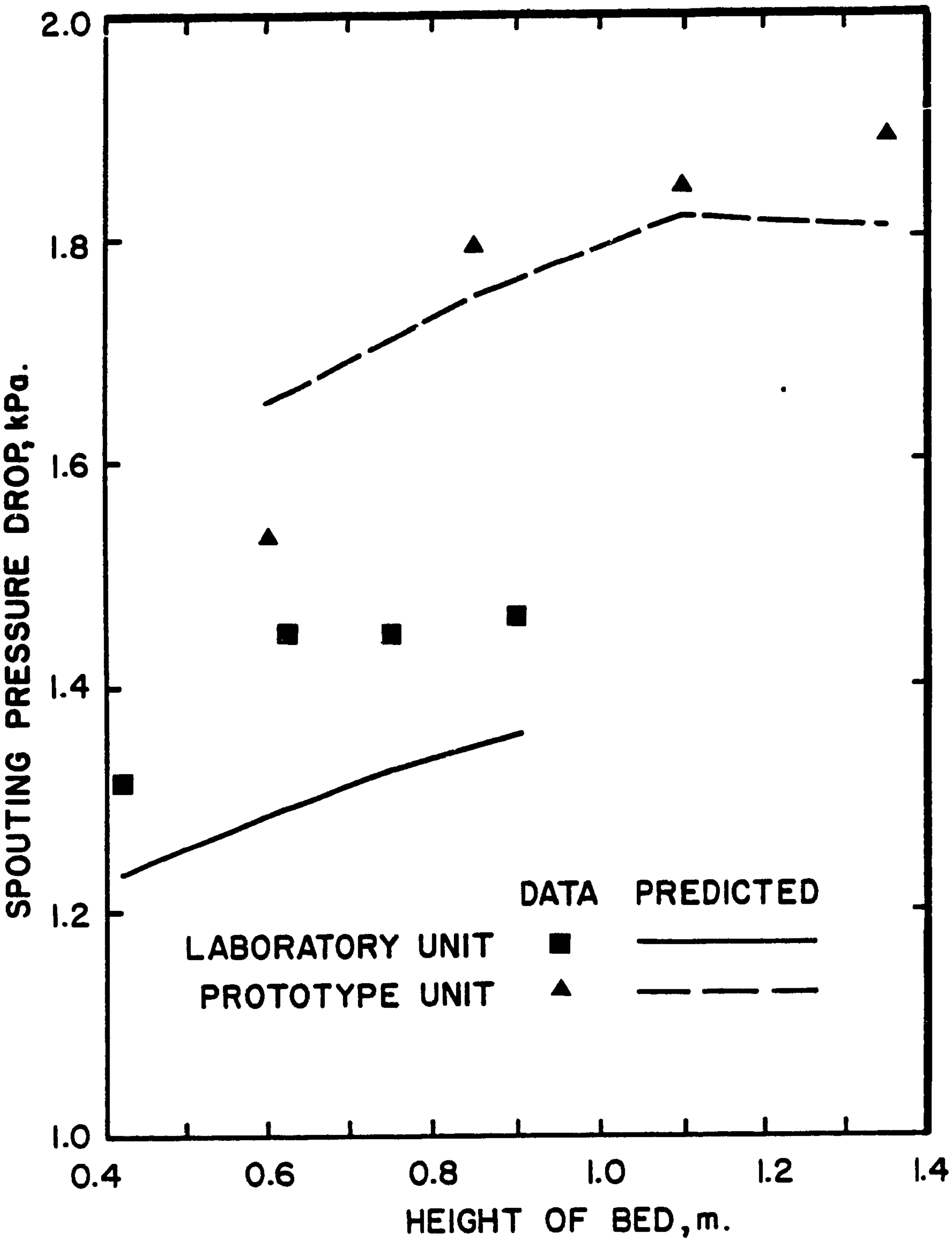

Figure 5.43 Effect of bed height on the spouting pressure drop in two geometrically similar shelled corn beds.

5.3.2 Minimum spouting velocity.

The effect of scale-up on the gas superficial velocity at onset of spouting (minimum spouting velocity) is shown in Figure 5.44 for the three grain varieties tested. The minimum spouting velocity decreased as the bed length increased. In the case of shelled corn and soybean, the maximum reduction is 7.3 % and 11.6 %, respectively, because wall effects are lower than for wheat. Similar quantitative trends have been observed in the two- dimensional fluidized beds for the activated alumina catalyst (Rowe and Everett, 1972), sand (Glicksman and McAndrews, 1985), and silica sand (Kathuria and Saxena, 1987). As the length of the bed increased, more grains entered the spout, resulting in less air flow through the spout. These results indicate that shelled corn and soybean beds remained in the range of two-dimensionality. It was also observed that the minimum spouting velocity is highest at the smallest bed length (0.05 m) for nearly spherical particles e.g. soybean, but this condition occurred at L_b = 0.06 m for shelled corn.

Minimum spouting velocity also exhibited two dimensional behaviour in the wheat spouted beds but with higher magnitudes. The superficial velocity at minimum spouting in wheat beds varied on the average by about -3.5 % at L_b= 0.06 m and +7.7 % at L_b = 0.125 m from that at L_b = 0.05 m. The behaviour observed in the case of wheat beds could be attributed to the ellipsoid shape of the grain. Another reason could be the cross-sectional area of orifice which was about 750 to 2260 times the average particle diameter or orientation of the particle while spouting. It is concluded that the wheat 2DSBs with draft plates can be scaled-up without any difficulty by increasing the bed length unless a uniform air flow can not be established in the spout.

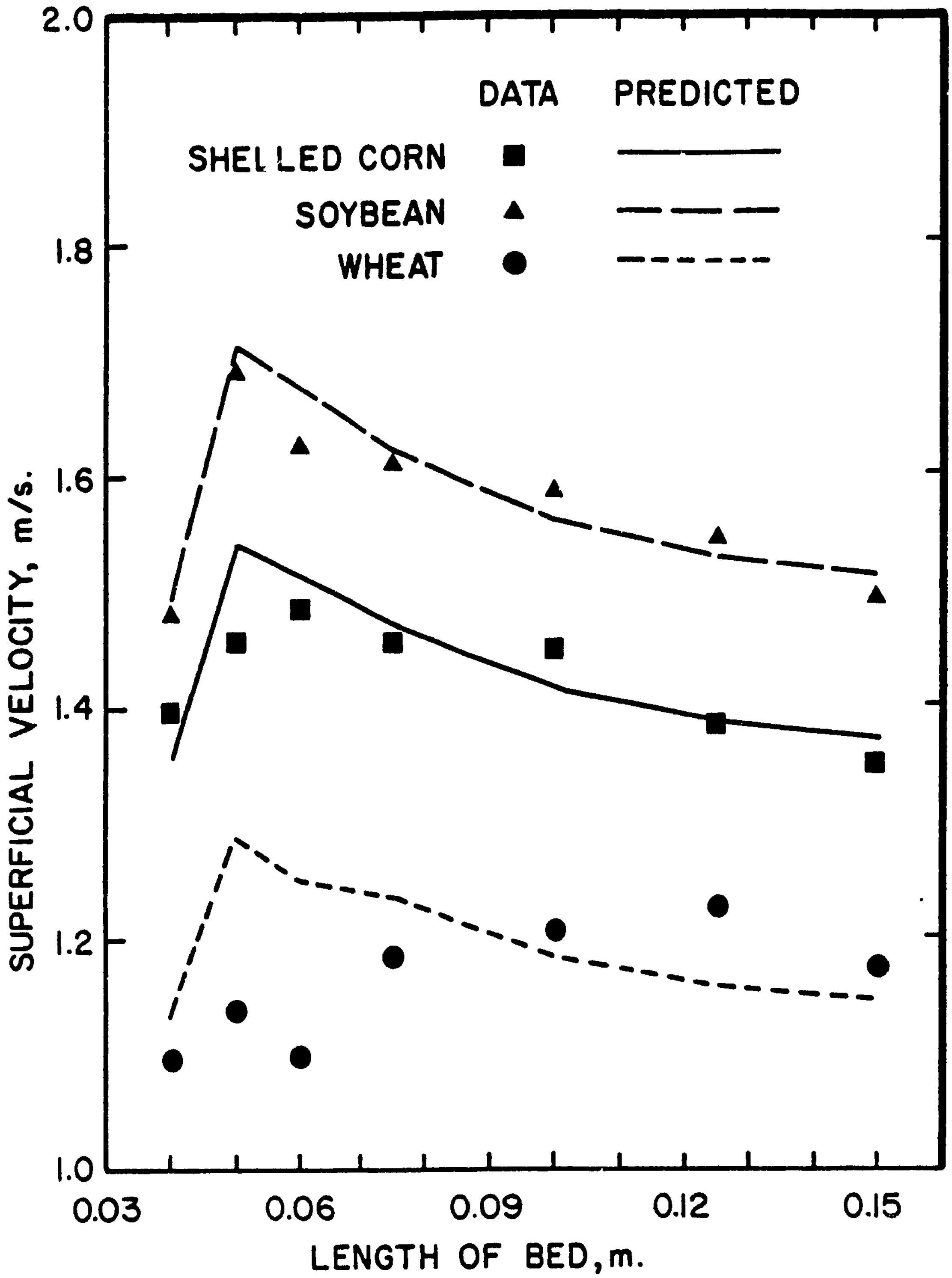

Figure 5.44 Effect of bed length and geometrical similarity (data at L_b = 0.04 m and 0.06 m) on the minimum spouting velocity for grains.

The mathematical model developed for the minimum spouting velocity compares well with the experimental data of shelled corn, soybean, and wheat (Figure 5.44). The developed model predictions were within +5.7 % to -2.3 %, +2.9 % to -1.7 %, and +13.9 % to -5.6 % of observed data for shelled corn, soybean and wheat, respectively. In the case of wheat, the minimum spouting velocity for bed lengths of 5 cm and 6 cm is overestimated due mainly to the numerous impurities in the grain bed.

The minimum spouting velocities through the two geometrically similar beds are plotted in Figure 5.44. The data collected indicate that the superficial velocity decreased as the bed dimensions became smaller. The reason may be that the smaller air inlet requires less air flow to keep the air to mass ratio roughly constant. The superficial velocities at minimum spouting in the laboratory scale bed were 94.06 %, 91.02 %, and 99.84 % of those in the pilot scale bed for shelled corn, soybean and wheat, respectively. The inverse effect of sphericity on minimum spouting velocity is evident (see Table A.2). Hence, the nonisometric or nonspherical particles require higher air flow than nearly spherical particles. Figure 5.44 also indicates the data points from the laboratory scale spouted bed along with the predictions from the model. The model compares well with the minimum spouting velocity data collected from the laboratory scale; the deviations being 3 % for shelled corn, 0.8 % for soybean, and 3.2 % for wheat.

The minimum spouting velocity through the bed also varied due to the heights of beds as shown in Figure 5.45 for the fresh harvested shelled corn. These data indicate that the lower bed heights facilitate the air flow through the bed (downcomers) because of lower resistance to air flow. Figure 5.45 also shows that

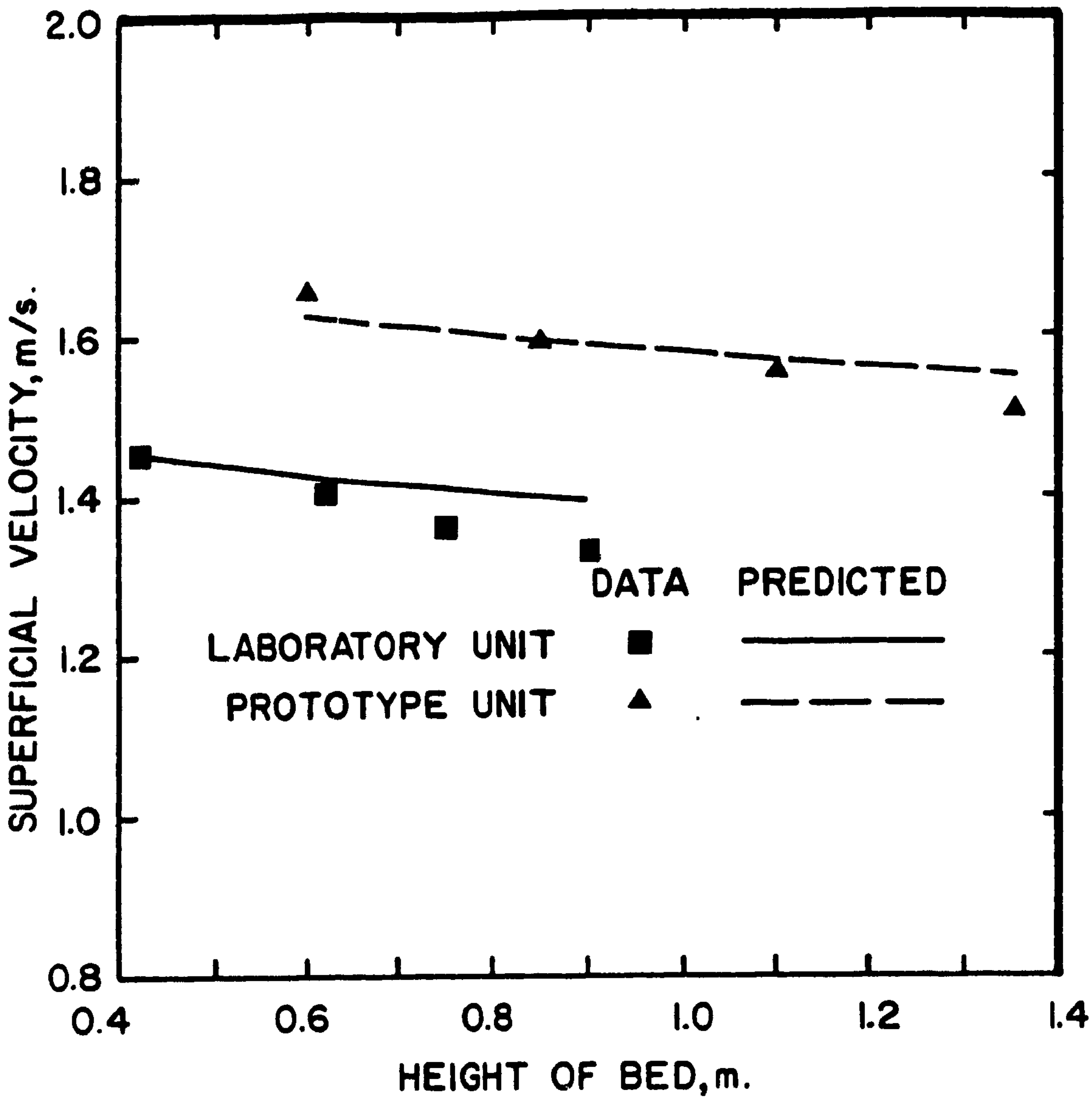

Figure 5.45 Effect of bed height on the minimum spouting velocity in two geometrically similar shelled corn beds.

the model predictions for the pilot scale spouted bed are better than for the small scale unit.

5.3.3 Solids Circulation Rate.

The solids circulation rates of the different grains, as observed in the various scale geometries, are presented in Figure 5.46. The rate of solids circulation increases as the length of bed increases regardless of grain type. The largest increase of solids circulation rate was noted in shelled corn, followed by wheat and soybean. The scale-up achieved by increasing the bed length may have better physical meaning if the solids circulation rate is calculated based on the unit length of bed. This comparison for the pilot scale bed is shown in Table A.7 with the % variation from a bed length of 0.05 m. This table also indicates that the solids circulation rate per unit length increases as the length of orifice increases from 0.05 m to 0.15 m. Similar phenomena have been observed in the bulk flow of solids through the orifices. The solids circulation rate becomes higher with increasing dimensions of the rectangular orifice.

Average particle velocity of grains in the downcomers of the pilot scale unit was higher than in the laboratory scale unit regardless of the grain variety. The data indicate that the solids circulation rates of shelled corn, soybean, and wheat in the laboratory scale unit were 40.0, 42.6, and 37.5 % of those in the similar pilot scale unit. Here again, as particle sphericity increases the solids circulation rate increases (see Table A.2). This analysis indicates that the solids circulation rate drops faster than the scale-down ratio between two geometrically similar spouted beds.

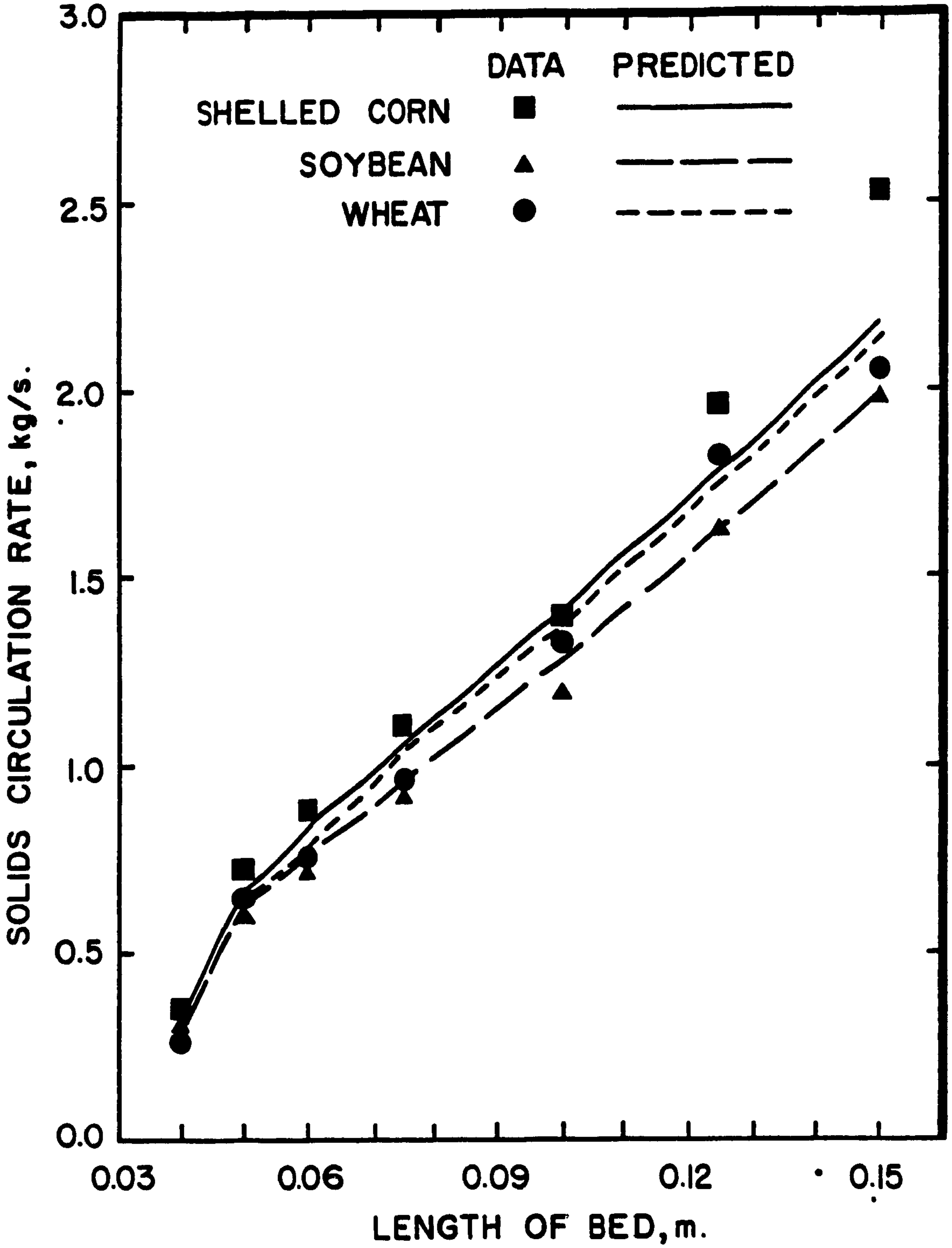

Figure 5.46 Effect of bed length and geometrical similarity (data at L_b = 0.04 m and 0.06 m) on the solids circulation rate of grains.

The model predictions are compared in Figure 5.46. The model predictions are best for soybean, followed by wheat and shelled corn. The deviations from the data are in the range of +1.1 % to -13.6 % for shelled corn, +7.4 % to -0.1 % for soybean, and +7.8 % to - 4.8 % for wheat. The solids circulation rate can also be given per bed cross-sectional area for the beds scaled-up on the basis of geometrical similarity. Some results are presented in Table A.7 for comparison.

The representative variation in solids circulation rate for shelled corn due to effect of the bed height is shown in Figure 5.47. It is clear that the particle flow rate is not influenced by bed heights greater than one half of draft plate height. The model predictions for the other data collected during the drying runs in both beds, are not reported here because they were in close agreement.

The visual observations of spouting in the pilot scale unit bed indicated that bed length can be increased beyond 0.15 m unless uniform spouting can not be maintained. The limiting bed length for shelled corn and wheat is assumed to be in the range of 0.20 to 0.30 m, while for soybean it is between 0.18 and 0.25 m at the standard bed settings. By scaling this way, the major benefit of a two-dimensional spouted bed can be determined and further scale-up by geometrical similarity should make these beds viable in practice.

If the moisture content of grains is above 30 % DB, the percentage of weed seeds, straw, and broken seeds is above 5 %, and the initial temperature of grains is up to 10 °C, then the grain flow in the downcomers of a spouted bed may exhibit stick-slip behaviour.

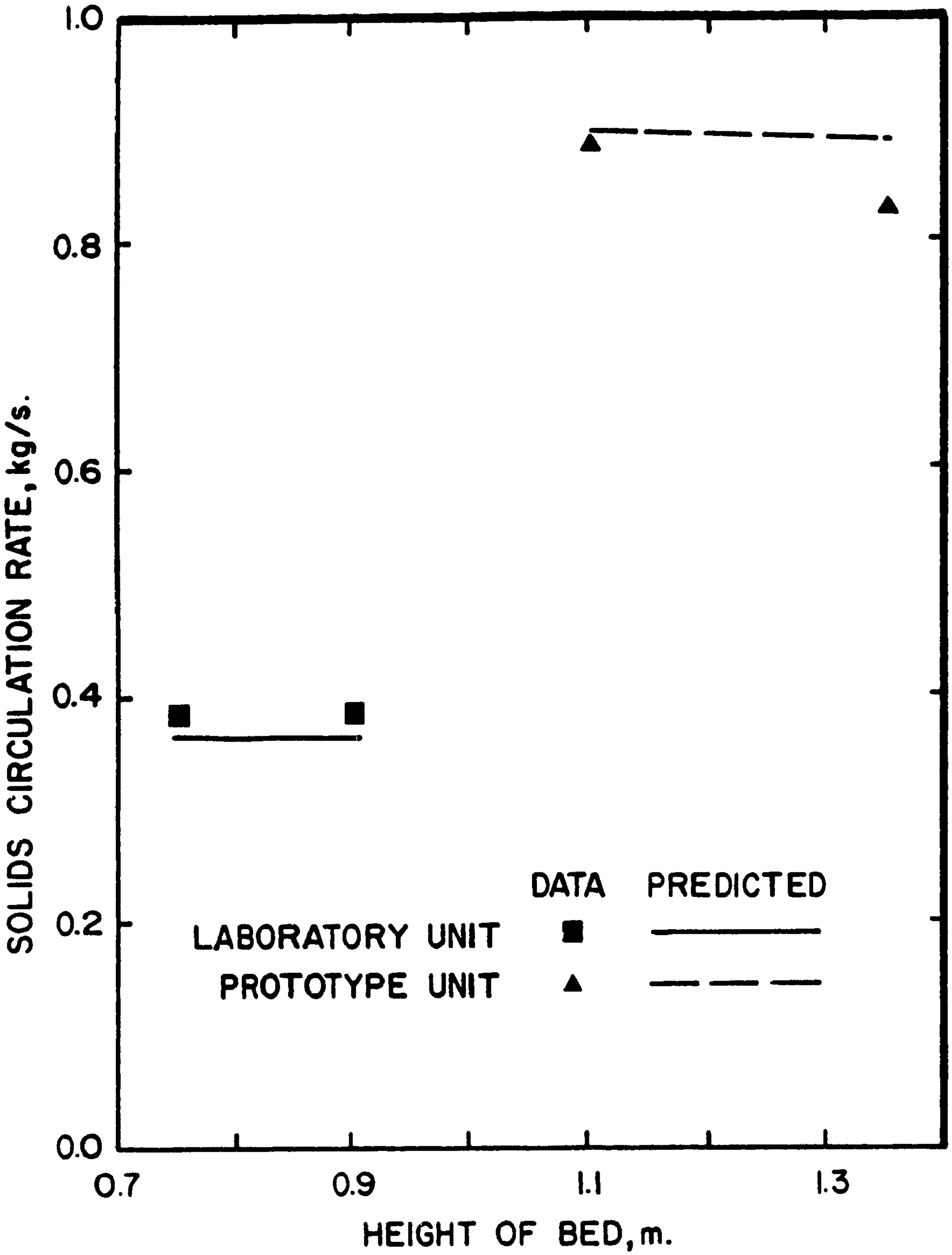

Figure 5.47 Effect of bed height on the solids circulation rate in two geometrically similar shelled corn beds.

5.4 Drying of Shelled Corn

5.4.1 Experimental results.

Drying experiments were performed in the two geometrically similar slotted 2DSBs with draft plates, and these were operated in a batch mode. Temperature data and grain samples were obtained for different inlet air temperatures and bed heights at the predetermined bed standard settings (see CHAPTER IV, sections 4.4) and the minimum spouting conditions. Typical experimental data of bed and outlet air temperatures as functions of time are shown in Figure 5.48 for the laboratory scale dryer and in Figure 5.49 for the pilot scale dryer.

The bed temperature measured at three heights in the downcomers initially differed by several degrees. After 10 to 30 minutes of drying and until termination, differed by 3 to 6 °C. This occurs because the freshly heated grains arriving at the top of the downcomer have intraparticle temperature gradients which shift as the grains travel through the downcomers. The data show that the temperature depression in the downcomers depends on the bed height, total drying time, inlet air temperature, and initial grain temperature. Typical plots are shown in Figures 5.48 and 5.49. The temperature in the downcomers of both units continued to rise as time passed. This occurs because sensible heat accumulates in the drying particles as they pass through the draft tube and spout regions.

The temperature profile of the pilot scale spouted bed, as can be deduced from Figure 5.49, indicates a lower temperature at the top of the downcomer than in the middle when in fact, one would expect the top reading to be the highest. The reason is that the top thermocouple is no longer in contact with grains due to a decrease in bed height resulting from shrinkage of the drying particles and the

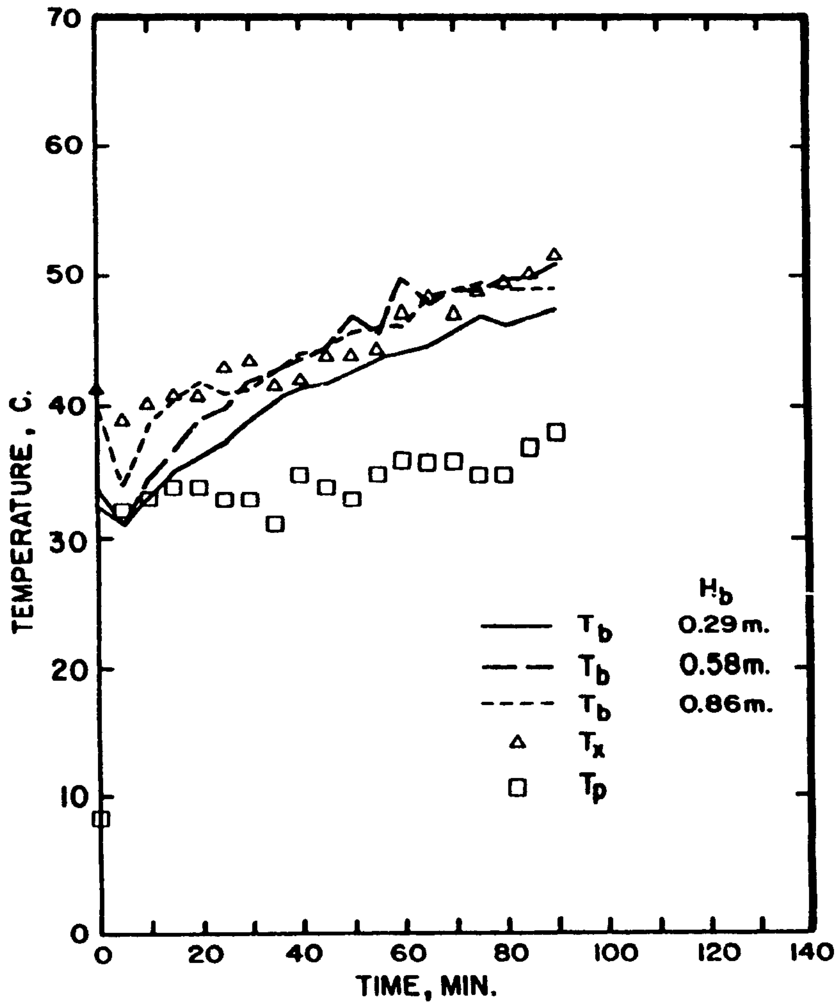

Figure 5.48 Vertical profile of bed (downcomer), material, and exit air temperatures vs. time at T_i = 70 °C in laboratory scale.

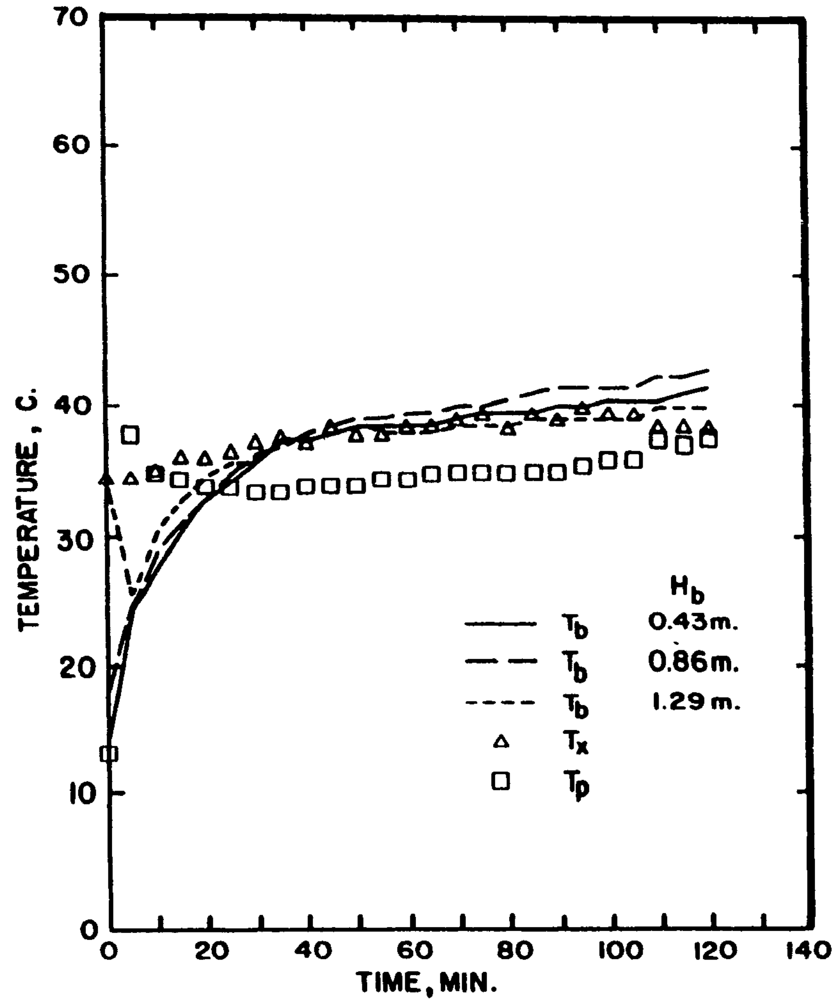

Figure 5.49 Vertical profile of bed (downcomer), material, and exit air temperatures vs. time at T_i = 50 °C in pilot scale.

departure of some of the straw, weed seeds, and broken kernels. Thus, the reading from the top thermocouple is in fact air temperature, not bed temperature. Due to the presence of screens at the top of the laboratory scale unit, impurities could not escape and the bed height reduction was smaller than in the other unit.

The temperature of material was noted at two levels in the downcomers while collecting the sample of grains for moisture determination purposes. The sample plots of material temperature for both spouted beds shown in the Figures 5.48 and 5.49 indicate that material temperature is generally lower than the temperature of bed in the downcomers. This difference increases towards the drying termination but widens as the magnitude of inlet air temperature increases. These results of material temperature may be somewhat erroneous because of their greater differences from the average downcomer (bed) temperatures. The reasons could be the heat losses from material samplers and the material dust on the bare thermocouples. If we accept the thermal equilibrium to the drying particles within a few cm of bed height in the downcomers; above this distance, the upward bed and material temperature should be approximately the same.

The recorded data (e.g. Figures 5.48 and 5.49) also show that the temperature of particles at the top of downcomer was the same as that of exit air except during the first 15 minutes of drying. As the drying proceeded, the grain layers at the top of the downcomer became a bit warmer than the exit air temperature. This difference is more evident in the case of the pilot scale spouted bed than in the laboratory scale spouted bed due to longer residence time of particles in the spout region of the pilot scale unit. It is clear that the dilute phase in the draft tube and fountain attains thermal equilibrium at given operating conditions, in particular at the minimum spouting velocity. This may not be achieved if the gas velocity is higher than the minimum spouting velocity or if the draft plate height is lower than that used in the experiments.

A typical plot of particle moisture content, particle temperature, exit air temperature, and bed temperature in the downcomer as functions of time for the pilot scale unit is shown in Figure 5.50 at 70 °C. As expected, there is no distinct constant drying rate period since the initial moisture content was lower than 31 % (D.B.). Generally speaking, most of the drying data did not exhibit a straight section in the drying curves except at the beginning of one run which lasted about 15 minutes.

Two drying curves from the pilot scale spouted bed (H_b = 105 cm and 130 cm, see Figure 5.57) at an inlet air temperature 50 °C, exhibited a slowly decaying rate during the initial 10 to 15 minutes. This could be due to the slow heating-up of the entire batch of grains and to possible condensation of moisture on the surface of grains from the air passing through the downcomers when the grain is still fairly cool. However, in practice, spouted beds are operated at higher inlet temperatures than 50 °C, so this effect should be insignificant and the whole drying of a batch should be in the falling rate period. The drying of grains in spouted beds is therefore similar to thin layer drying. This conclusion allows us to assume that the drying takes place mainly in the dilute phase with tempering effects in the dense phase.

As a batch of grains is placed in the bed, the particles start to heat rapidly to the wet bulb temperature and then slowly integrates as the layers of moisture dry from the surface to the centre of the particles. The temperature of particles in

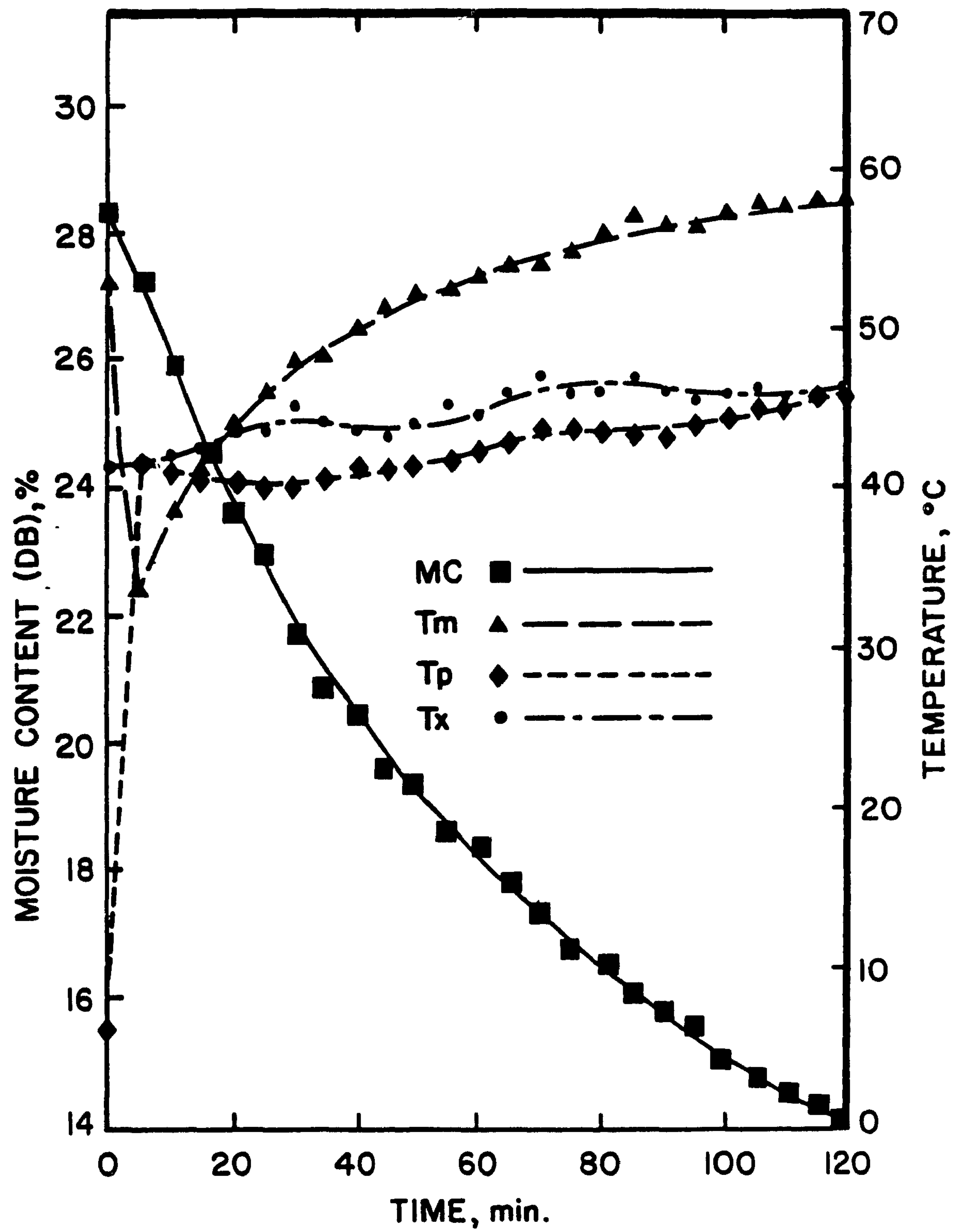

Figure 5.50 Moisture content of particles and average downcomer, material, and exit air temperatures as the function of drying time in pilot scale. H_b = 1.05 m, T_i = 70 °C.

the laboratory scale spouted bed were always lower (by 2 to 25 °C) than the exit air temperature (Figure 5.48). However, in the pilot scale unit, the temperature difference between the drying particles and exit air was within ±5 °C (Figure 5.49). This means that thermal equilibrium between the spouting air and the particles was not attained in the laboratory scale spouted bed because of a short contact time resulting from a small draft plate height. In contrast, the average bed temperature in the downcomers, except during the initial 10 to 15 minutes of drying, was higher than the exit air temperature in both units. This difference increased with the drying time (see Figure 5.50).

The drying rate increased with inlet air temperature which is typically shown in Figure 5.51 for the three runs in the laboratory scale spouted bed at the same bed height. This may be due to the absorption of more sensible heat by the drying particles which would promote the moisture diffusivity and accelerate drying.

The effect of bed height in both spouted beds was quite clear and dramatic. This is shown in Figure 5.52 for an inlet air temperature 90 °C (laboratory scale unit). Since the total number of grains is smaller, each is more frequently drawn through the spout and air flow rates through the downcomers are higher, altogether resulting in faster drying than in a full bed. Similar effects were also observed in the pilot scale unit; however, they were not as sharp. This could be due to the three times greater wet load in the pilot scale unit at about 9 % higher air flow rates than the laboratory scale unit resulting in slow heating of grains at lower energy inputs than in the laboratory scale bed. This indicates that the energy inputs in the pilot scale bed were less per unit mass of load per time. Even though

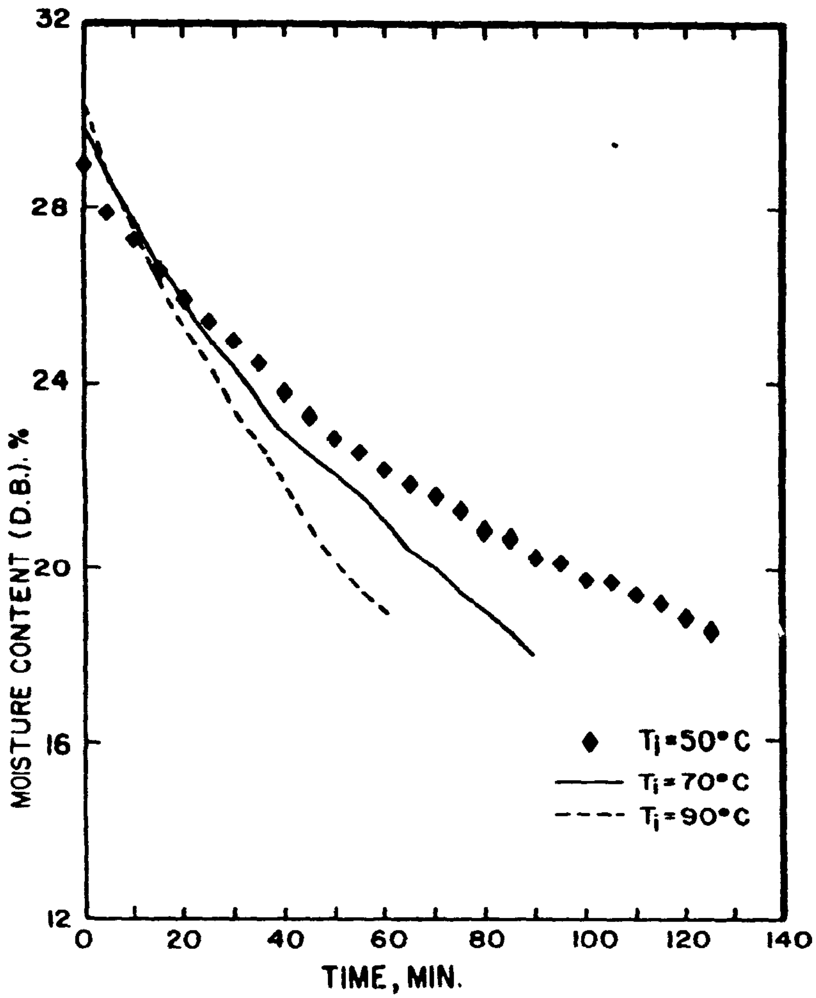

Figure 5.51 Effect of inlet air temperature on the drying rate in laboratory scale spouted bed with H_b = 0.89 m.

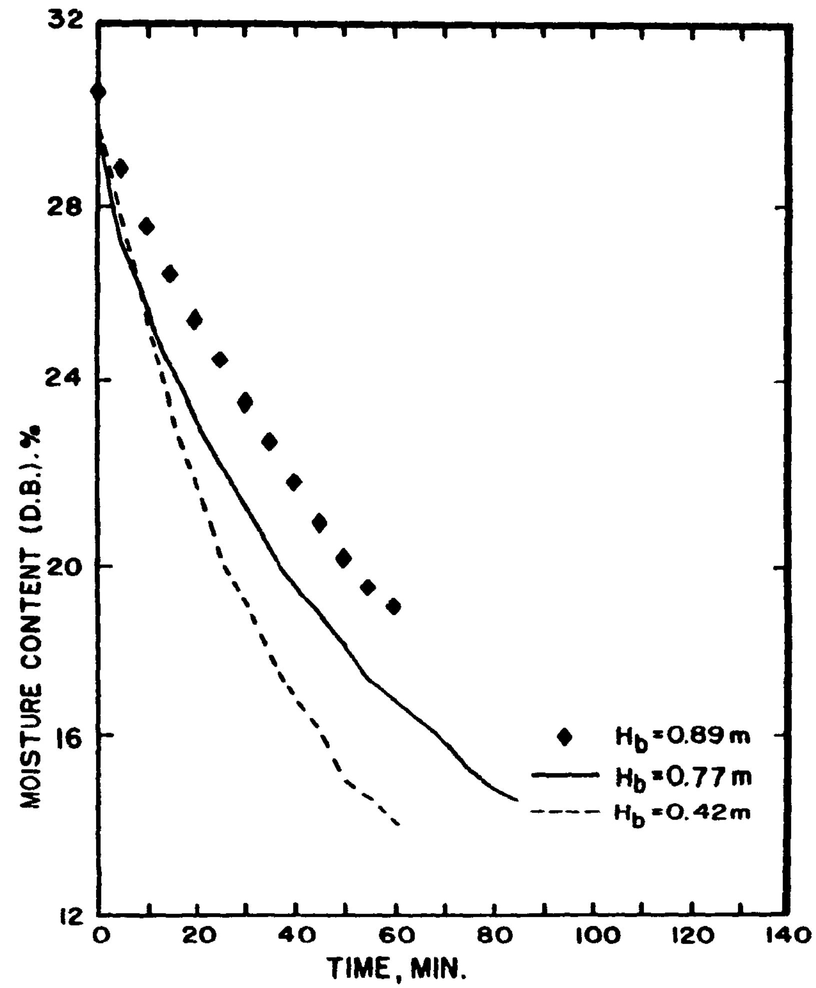

Figure 5.52 Effect of bed height on the rate of drying in laboratory scale spouted bed at T_i = 90 °C.

energy inputs were lower in the pilot scale spouted bed, less time was required to dry a unit mass of load. The concept of a slotted 2DSB with draft plates therefore works very well for the drying of grains where batch drying takes the form of a thin layer drying. It is also concluded that for drying of grains, industrial scale spouted beds are required for better energy utilization with about twice the draft plate height than the bed width. The effect of bed height can also be represented by mass of grains in the spouted bed or average cycle time of particles and the same conclusion may be drawn.

The effects of initial moisture content, relative humidity, and initial temperature of grains were not the subject of a specific investigation; however, the drying curves in this section indicate that at higher initial moisture content, higher relative humidity, and lower initial temperature of grains, drying rates are lower.

5.4.2 Thin layer drying model.

Three empirical models: (1) a lump parameter equation (2.25), (2) a diffusion type equation (2.23), and Page's equation (2.26) were applied to the 10 drying runs from the laboratory scale and 8 runs from the pilot scale spouted beds. A nonlinear method from STATGRAPHICS (1989) was used to estimate the numerical values of the model parameters The fitted models were then evaluated based on R^2, residual mean square (RMS or EMS), standard error, and the best fit to the actual observations (see Table 5.3). The predictions from the fitted models for an experimental run of the laboratory scale spouted bed at inlet air temperature 70° C with bed height 0.62 m, are shown for comparison in Figure 5.53. The lump parameter and diffusion type models were found to be unsuitable for mathematical description of the drying data from either unit. The observed scatter may have resulted from the relaxation effects occurring in the downcomers. In contrast, Page's model, which accounts for the effect of grain tempering, fitted the shelled corn drying data very well.

Table 5.3 R-square, standard error, and error mean square of fitted models.

No	Run	Lump model			Diffusion type model			Page model		
		R^2 %	SD	EMS	R^2 %	SD	EMS	R^2 %	SD	EMS
1	LF89	96.16	0.02152	5.19E-4	98.41	0.01464	2.23E-4	99.80	5.16E-3	2.80E-5
2	LS88	98.87	0.01230	1.68E-4	99.47	0.00894	8.50E-5	99.93	3.26E-3	1.10E-5
3	LS72	97.93	0.01928	4.09E-4	99.01	0.01398	2.07E-4	99.88	4.82E-3	2.50E-5
4	LS62	94.81	0.02940	9.67E-4	98.01	0.01925	3.92E-4	99.90	4.22E-3	1.90E-5
5	LS42	95.99	0.02881	8.99E-4	97.88	0.02178	5.06E-4	99.61	9.36E-3	9.40E-5
6	LN89	99.21	0.01016	1.18E-4	99.67	0.00696	5.30E-5	99.94	2.97E-3	1.00E-5
7	LN78	99.68	0.00730	5.80E-5	99.80	0.00603	4.00E-5	99.93	3.55E-3	1.40E-5
8	LN77	95.15	0.03190	1.12E-3	98.11	0.02090	4.66E-4	99.97	2.70E-3	8.00E-6
9	LN61	96.57	0.02591	7.47E-4	98.50	0.01789	3.49E-4	99.93	3.79E-3	1.60E-5
10	LN42	98.46	0.02111	4.66E-4	98.93	0.01796	3.52E-4	99.71	9.39E-3	9.70E-5
11	PF128	99.25	0.01410	1.24E-4	99.72	6.79E-3	4.80E-5	99.68	7.17E-3	5.50E-5
12	PF105	99.61	0.00763	6.20E-5	99.73	6.55E-3	4.50E-5	99.64	7.51E-3	6.10E-5
13	PF78	99.13	0.01322	1.79E-4	99.26	0.01229	1.58E-4	99.61	8.87E-3	8.40E-5
14	PF56	98.74	0.01784	3.27E-4	99.00	0.01608	2.70E-4	99.54	0.01080	1.24E-4
15	PS130	99.24	0.01183	1.49E-4	99.52	9.71E-3	9.80E-5	99.83	5.74E-3	3.50E-5
16	PS105	96.11	0.03071	1.00E-3	97.83	0.02363	5.83E-4	99.57	0.01047	1.16E-4
17	PS76	98.55	0.02026	4.35E-4	99.20	0.01549	2.51E-4	99.85	6.74E-3	4.80E-5
18	PS54	97.09	0.02779	8.06E-4	98.01	0.02347	5.84E-4	99.33	0.01350	1.95E-4

where L = Laboratory scale, P = Pilot scale, F = 50°C, S = 70°C, N = 90°C. and 42 to 130 = the average bed height under operating conditions, cm.

SD = Standard deviation and EMS = Error mean square.

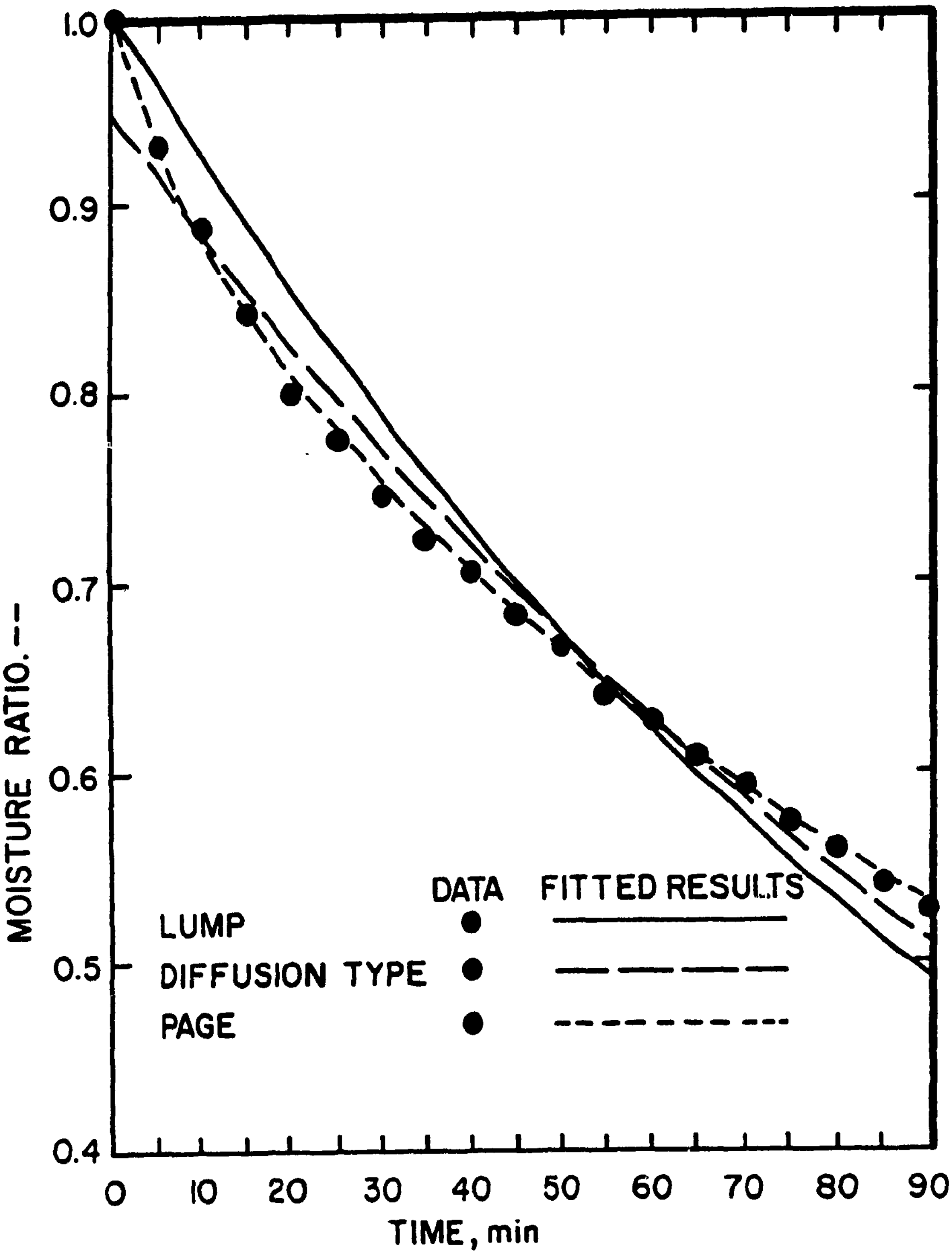

Figure 5.53 Comparison of fitted thin layer models to a typical drying curve of the laboratory scale spouted bed. H_b=0.62 m, T_i=70°C.

In order to find a mathematical relationship between experimental constants of Page's model and the independent variables, the k' and n were assumed to be functions of bed, air, and particle characteristics, i.e. H_t, W_b, W_i, H_b, Q, W_s, W_o, M_b, M_p, t_c, T_i, t_i, M_o, and RH. Linear, non-linear, and dimensionless terms were generated from these variables and processed with a stepwise (Forward Selection or Backward Elimination) linear regression program (STATGRAPHICS 1989). In this way, empirical models were generated for k' and n. but only one was selected for each based on a compromise between goodness of fit as indicated by the coefficient of determination, EMS, SE, and the number of terms in the model. It should be noted that several models correlated better than the selected ones but these had too many terms for the degree of precision gained.

The selected regression equation for the constant k' of Page's model is:

$$k' = \left(\begin{array}{c} +\,39.74\left[\dfrac{W_i W_o}{W_s H_t}\right] - 1.56\left[\dfrac{W_b}{H_b}\right] + 0.82\left[\dfrac{W_b}{H_b}\right]^{1.5} \\ -\,0.95\left[\dfrac{H_b}{H_t}\right]^2 + 0.56\left[\dfrac{H_b}{H_t}\right]^3 + 0.47\left[\dfrac{t_i}{T_i}\right]^3 \\ -0.78t_c^{\,2} + 0.77t_c^{\,3} - 0.0076RH + 0.000234RH^2 \\ -0.00125M_b + 0.0313M_b^{\,0.5} - 0.577M_o \end{array} \right) \qquad (5.6)$$

with R^2_{adj} = 99.96 %, SE = 3.7239E-4, MAE = 1.58E-4, EMS = 1.38675E-7, significance level $\geq$ 0.001, and average errors = 0.96 % to -1.44 % from the fitted values of k'. Predicted vs observed values for k' are shown in Figure 5.54. Similarly, the empirical model for the experimental constant n in Page's equation is:

$$n = \left(\begin{array}{l} +1.86M_o\left[\frac{W_iW_o}{W_sH_t}\right]+0.363\left[\frac{W_b}{H_b}\right]-5.85\left[\frac{t_i}{T_i}\right] \\ +34.23\left[\frac{t_i}{T_i}\right]^2-62.12\left[\frac{t_i}{T_i}\right]^3+3.618t_c-2.836t_c^{\,3} \\ +0.056RH-7.0E\text{-}5RH^3+0.717M_b^{0.5}-2.103M_b^{\frac{1}{3}} \end{array} \right) \tag{5.7}$$

with R^2_{adj} = 99.93 %, SE = 0.0236289, MAE = 0.011665, EMS = 5.58323E-4, significant level ≥ 0.01, and average errors = 1.52 % to -1.26 % from the fitted values of n. Observed vs predicted plot is shown in Figure 5.55.

It should be emphasized that the thin layer performance model in the form of Page's equation was generated from the data obtained over a limited range of drying conditions. The inlet temperature was varied from 50° C to 90° C while relative humidity ranged from 2 % to 20 %, initial bed heights from 0.45 m to 1.35 m, and initial mass of the bed from 2.75 kg to 33.1 kg. Initial moisture content of grains was in the range of 28 % to 31 % dry basis with initial temperature of particles between 6 and 22 °C.

The linear functions developed for k' (equation 5.6) and n (equation 5.7) were then substituted into the original Page model (equation 3.26) to complete the thin layer performance model for the slotted 2DSBs with draft plates. The predictions from this performance model were generated for all the drying runs using the data variables. They were then compared with the collected data of each run in terms

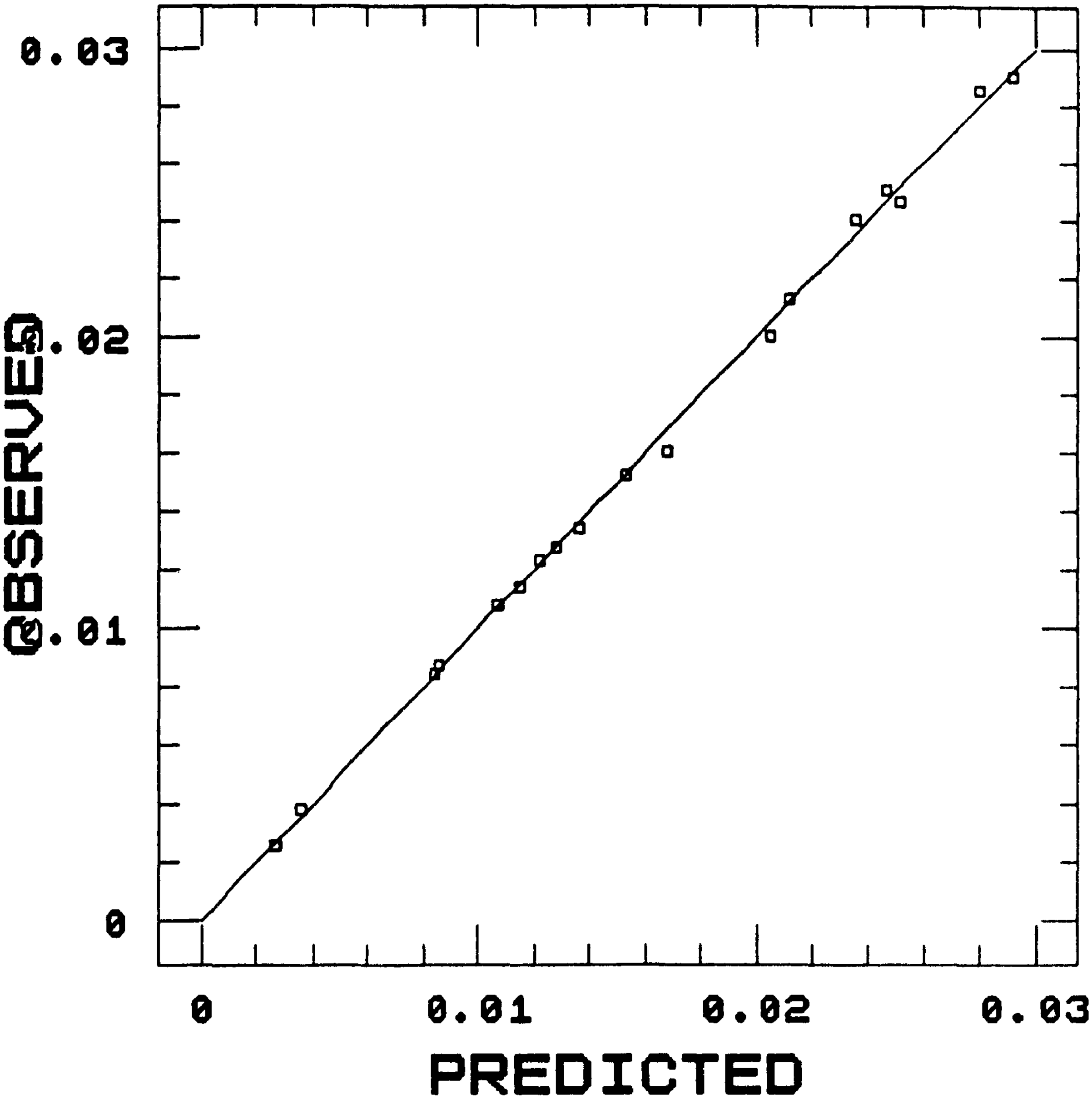

Figure 5.54 Plot of fitted vs. predicted values for k' parameter of Page's model.

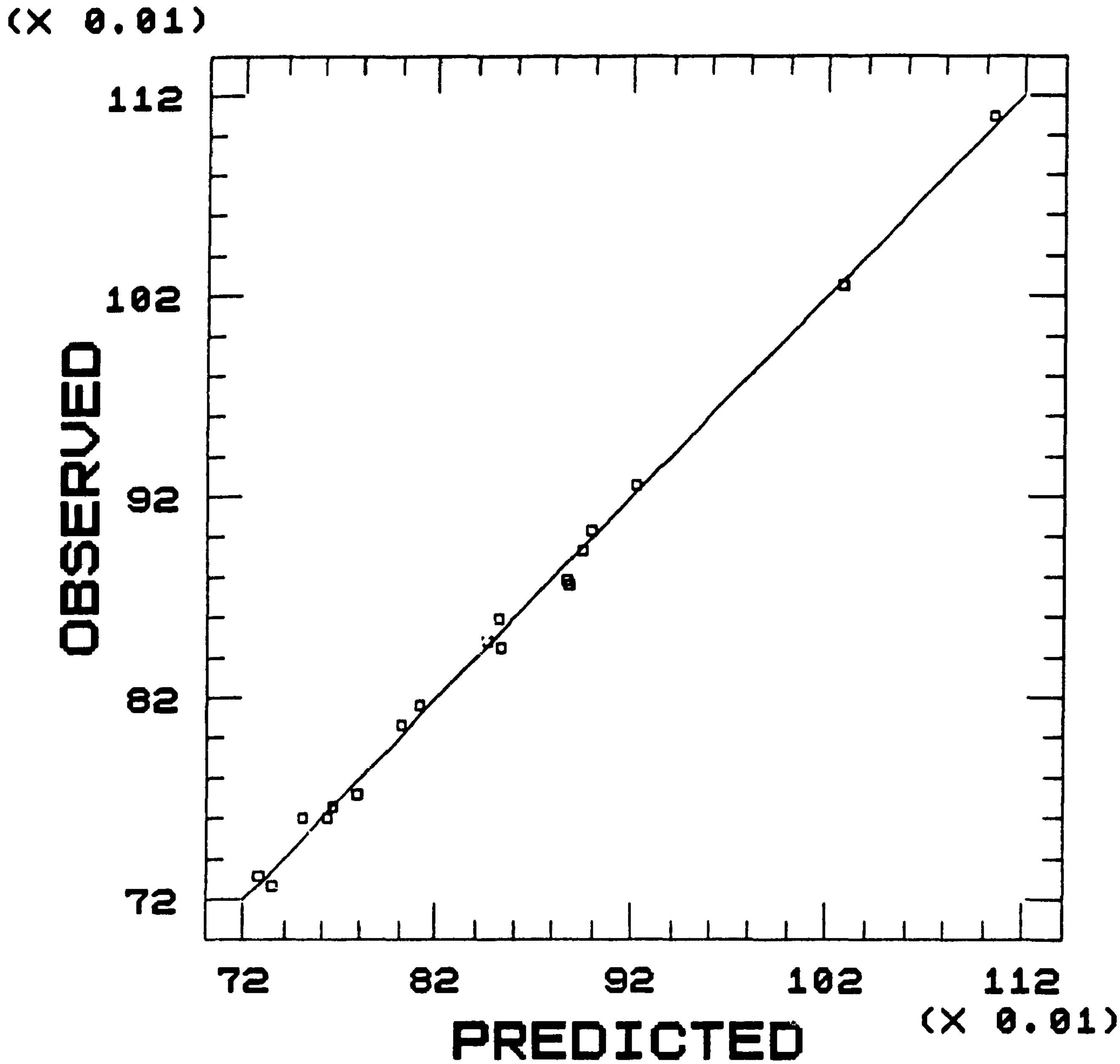

Figure 5.55 Plot of fitted vs. predicted values for n parameter of Page's model.

of variation with time. Some typical graphs of this comparison are shown in Figures 5.56 and 5.57. These plots and others not shown here due to space limitations, indicated that the thin layer performance model developed in this study well describes the drying kinetics in a 2DSB. However, predictions deviated from the data by about ±4 % at the end of some drying runs. Otherwise, the predicted values are almost the same as the data values.

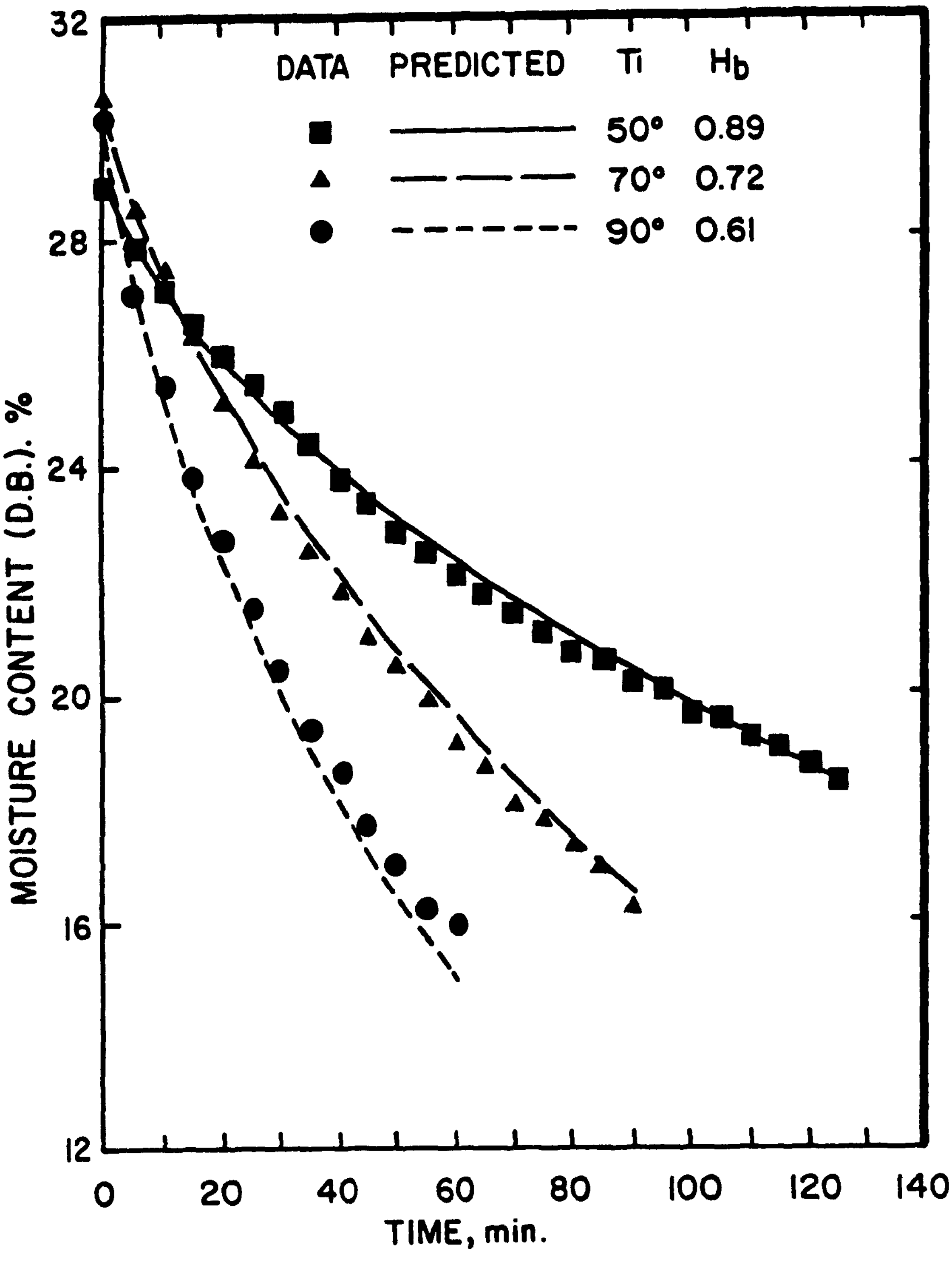

Figure 5.56 Comparison of model predictions with the collected data from laboratory scale spouted bed for various bed heights and inlet air temperatures.

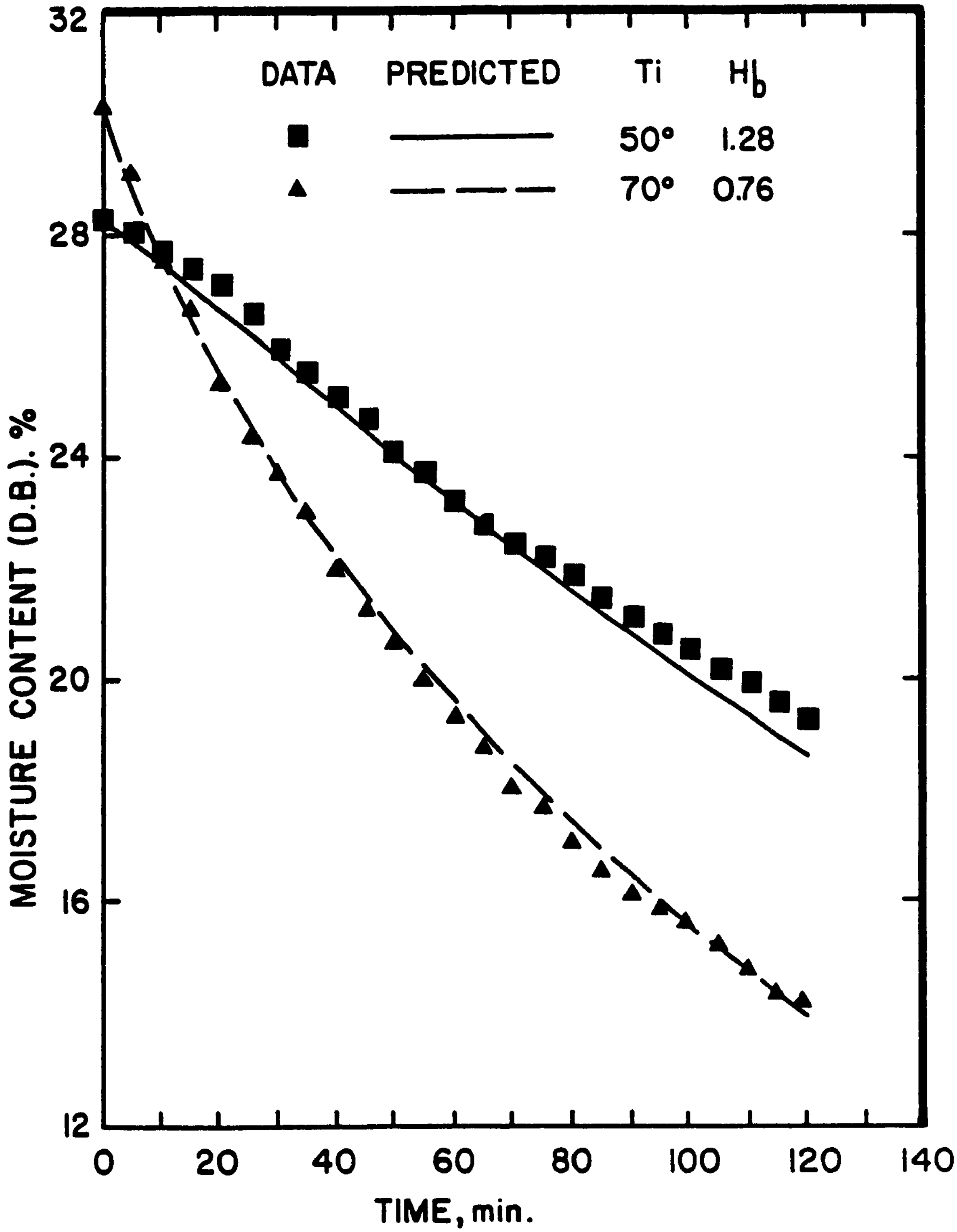

Figure 5.57 Comparison of model predictions with the collected data from pilot scale spouted bed for various bed heights and inlet air temperatures.

VI CONCLUSIONS

6.1 Static Vertical Pressure of Grains.

The static vertical pressure of grains on the air entry slot of the pilot scale spouted bed unit without injecting air through the bed, was measured while varying the bed to slot width aspect ratio, slant angle, and bed height. The following conclusions were drawn:

1. The static vertical pressure was significantly affected by the bed to slot width aspect ratios, side slant angles, type of grain, height of bed, and by the interactions of these factors.
2. The comparison of observed static vertical pressure and estimated values from the Janssen and the Reimbert and Reimbert models showed that neither approach is applicable to nonaerated spouted beds because they cannot account for differences in bed to slot width aspect ratio, side slant angles, and sphericity of grains. The deviations between the observed and estimated values increased as the bed to slot width aspect ratio and sphericity of grains increased.
3. Based on the critical analysis of our data, a new concept for incorporating grain characteristics, termed the "quantitative factor," was proposed. This factor accounts for the combined effects of bulk density, emptying angle of repose, and sphericity and may reflect the action of the granular bed on the bottom of the tank or silo.

4. A statistical model for static vertical pressure was developed; based on the effects of the bed to slot width aspect ratios, slant angle, the grain quantitative factor, and bed heights. The linear model compares fairly with the collected data.

6.2 Dynamics of Spouted Bed.

Spouting pressure drop, minimum spouting velocity, solids circulation rate, and average cycle time of cereal grains were studied in the pilot scale slotted 2DSB with two draft plates at the minimum spouting conditions with respect to side slanting, draft tube width, and the entrainment zone height. The following conclusion were drawn:-

1. Spouting pressure drop increases as the entrainment zone height and slant angle increase, decreases as the spout width increases; and vary with variety of grains, the spouting velocity and the solids circulation rate. The highest pressure drop was produced by the beds of soybean, followed by wheat, and shelled corn.
2. Minimum spouting velocity increases as the entrainment zone height and the draft tube width increase and as the slant angle decreases; and vary with properties of materials. The spouted beds of soybean grains required the highest air flow through the bed, followed by shelled corn and wheat.
3. Solids circulation rate (average particle velocity in the downcomers) were also affected by entrainment zone height, draft tube width, slant angle, and vary with spouting velocity. The lowest solids circulation rate was observed in beds of wheat grains, followed by beds of shelled corn and soybean.

4. Average cycle times of particles near the draft plates are shorter than particles at the length side wall of the downcomer regardless of slant angle, draft tube width, entrainment zone height, or type of grain. The average cycle times were higher in the case of slant angle of 45° than the slant angle of 60° because of a larger mass of grains at a lower flow rate than at the latter angle.
5. Spouting pressure drop and solids circulation rate are not influenced by the bed height if the height is $\geq$ the half the height of draft plates, H_t. Otherwise, unstable spouting, bubbling in the downcomers, and weak fluidization occur. However, the total air flow through the spouted bed increases as the bed height becomes smaller than the draft plate height.
6. The insertion of draft plates to form a tube in the 2DSBs proved very effective in controlling pressure drop, air flow through the bed, and solids circulation rate and to operate in plug flow manner. Hence, the 2DSB with draft plates can satisfy drying requirements in practice.
7. Mathematical models were developed for spouting pressure drop, minimum spouting velocity, solids circulation rate, and average cycle time at the minimum spouting conditions using the dimensional analysis approach. The comparison of the developed models with the experimental data indicated quite close agreement. Further, average cycle time in the 2DSBs can be calculated from the total mass in the spouted bed divided by the solids circulation rate with fair accuracy.

6.3 Scale-up.

1. Spouting pressure drop increases with the length of the same bed and as the dimensions of geometrically similar spouted beds, irrespective of grains tested. Spouting pressure drop varies directly with the sphericity of a spouting particle in the geometrically similar spouted beds Spouting pressure drop model predictions indicated agreement with the data.
2. Minimum spouting velocity decreased in the cases of shelled corn and soybean, but increased in the case of wheat as the length of the same spouted bed increased. The spouting velocity required for stable spouting in the laboratory scale unit was lower than in the pilot scale unit regardless of grain type. This reduction is mainly influenced by the sphericity of particles. The minimum spouting velocity model estimates scale-up data quite good.
3. Solids circulation rate through the downcomers of spouted beds increased as the bed length of the same spouted bed increased. Solids flow in the two similar beds was influenced by the particle sphericity. Solids circulation rate model predictions are also in agreement with the collected data.
4. The scale-up data indicated that scale-up was still possible for the grains used in this study. However, some caution should be exercised for particles nearly spherical in shape e.g. soybean, where there may be some irregular flow of grains through the rectangular orifices at bed lengths over 0.15 m.

6.4 Drying of Shelled Corn.

Drying of shelled corn was performed in the two geometrical similar two-dimensional spouted beds with draft plates at bed settings based on the aerodynamic results. Both beds were operated in batch mode under different drying conditions at minimum spouting only and the following conclusions were drawn:

1. Uniform air temperature in the downcomers of the spouted beds with draft plates is approached shortly after the beginning of drying and it rises as the drying of grains continues.
2. Thermal equilibrium between the spouting air and the drying particles was also achieved in the dilute phase which was evident from the downcomer and exhaust air temperatures.
3. Drying rate was effected by the levels of inlet air temperature, initial grain temperature, mass of grains in the bed, initial moisture content of grains, average cycle time of particles, equilibrium relative humidity, and spouted bed geometry.
4. Batch drying of grains took place in the falling rate period. The drying of a unit mass of grains per unit air flow through the spouted beds was much faster in the pilot scale spouted bed than in the laboratory scale spouted bed. This means that the energy utilization in the large scale spouted bed with draft plates is better than in the small one. This may be due to the longer residence time of spouting particles in the dilute phase. Hence, a two-dimensional spouted bed with draft plates can be used for drying of grains.

5. For spouted bed design purposes, the lump parameters, diffusion type, and Page equations were fitted to the batch drying data. Comparison of these fits to the collected data showed that Page's equation fits the data best because of its ability to account for tempering effects in the downcomer on the drying time.

6. Page's equation parameters were related to the system geometry, operating parameters, and grain characteristics. The empirical models which adequately described the drying kinetics of grains are presented for the prediction of drying rates over the ranges of parameters studied.

VII SUGGESTIONS FOR FUTURE WORK

A spouting pressure drop occurs during the operation of a 2DSB. This pressure drop should be partially influenced by the static horizontal pressure of grains. Theoretically, the static horizontal pressure can be estimated by the bulk storage theories. However, much more work is necessary to confirm their application to spouted beds; in particular, the static horizontal pressure of grains on the spout wall must be investigated. Full studies of the maximum pressure drop and the spouting pressure drop in the pilot scale spouted bed are also needed for comparison with bulk storage theories. Once these data are on hand, further mathematical relationships can be established.

The mathematical models of spouting pressure drop, minimum spouting velocity, solids circulation rate, and average cycle time developed in this work are based on data collected from two geometrically similar 2DSBs with draft plates using three test materials. Additional work is required to generate data for other cereal grains and solids in order to generalize our understanding of the influence of grain characteristics in design. Geometrical similarity should be studied with 2DSB's of dimensions other than those used in this study in order to evaluate and refine the empirical models developed here and to optimize the geometrical parameters studied. The same applies to air flow through the draft tube and downcomers which directly apply to drying applications.

Future research on the drying of grains in 2DSBs with draft plates may take two directions: (1) Empirical and (2) Theoretical modelling. Since the empirical approach is simple and reliable, the application of Page's equation to drying curves of other cereals is highly recommended as an approach to bringing 2DSBs to the front lines of grain drying technology. At the same time, theoretical heat and mass transfer models are to be developed using the diffusion concept. In this regard, more data is needed on the drying of grains noting the temperature profiles of air and grains with time in the dilute and dense phases, air and particle velocities in the draft tube, relative humidity in the draft tube and the downcomers, and energy inputs. The analysis of these data should provide a better understanding of the grain drying process in 2DSBs and optimum energy inputs per unit mass of grains using the large scale spouted beds. Applications of conductive heat and other types of energy show potential for more efficient energy utilization. Work would also be required to assess the quality of the dried grains with respect to various kinds of food processing.

VII REFERENCES

Agrawal, Y.C. and Singh, R.P. 1977. Thin-layer drying studies for short grain rice. ASAE paper N . 77-3531.

Airy, W. 1897. The pressure of grains. Minutes of proceeding, Institution of Civil Engineers, London. 131:347-358.

Allen, J.R. 1960. Application of grain drying theory to the drying of maize and rice. J. Agric.Eng. Research. 5(4):363-369.

Anderson, K., Raghavan, G.S.V. and Mujumdar, A.S. 1984. Characteristics of asymmetric two-dimensional slot spouted beds for grains. In: DRYING'84. p. 205-209.

Angladette, A. 1963. Rice drying principles and techniques. FAO of the U.N. Informal Working Bulletin No. 23.

Anonymous, 1977. Loads imposed by stored products. In: Structures and Environment Handbook, Midwest Plan Service, 122 Davidson Hall, Iowa State University, Ames. p. 11-18.

ASAE 1982. Agricultural Engineers Yearbook. ASAE. p. 311 & 345.

Asenjo, J.A., Munoz, R. and Pyle, D.L. 1977. On the transition from a fixed to a spouted bed. Chem. Eng. Sc. 32:109-117.

Bakker-Arkema, F.W. 1986. Heat and Mass Transfer Aspects and Modelling of Dryers - A Critical Evaluation. In: Concentration and drying of foods. D. McCarthy (ed.). Elsevier Applied Science Publishers, London. p.165-203.

Bakker-Arkema, F.W. and Hall, C.W. 1965. Static versus dynamic moisture equilibria in the drying of biological products. J. Agric. Eng. Research. 10(4):308-313.

Barroso, M.A.S. and Massarani, G. 1984. Grain drying in non-conventional spouted bed. XII ENEMP. Maringa, Brazil. (In Portuguese).

Becker, H.A. 1959. A study of diffusion in solids of arbitrary shape, with application to the drying of the wheat kernel. Journal of Applied Polymer Science. 1:212-226.

Becker, H.A. 1961. An investigation of laws governing the spouting of course particles. Chem. Eng. Sc. 13(4):245-262.

Becker, H.A. and Isaacson, R.A. 1970. Wheat drying in well-stirred-batch and continuous-moving-bed dryers. Can. Jour. of Chem. Eng. 48:560-567.

Becker, H.A. and Sallans, H.R. May 1955. A study of internal moisture movement in the drying of the wheat kernel. Cereal Chemistry. 32:212-225.

Becker, H.A. and Sallans, H.R. 1956. A study of the desorption isotherms of wheat at 25° C and 50° C. Cereal Chemistry, 33(2):79- 91.

Becker, H.A. and Sallans, H.R. 1961. Drying wheat in a spouted bed on the continuous, moisture diffusion controlled drying of solid particles in a well-mixed, isothermal bed. Chem. Eng. Sc. 13(3):97-112.

Beverloo, W.A., Leningen, H.A. and Van de Velde, J. 1961. The flow of granular solids through orifices. Chem. Eng. Sc. 15:260- 269.

Bird, R.B., Stewart, W.E. and Lightfoot, E.N. 1960. Transport Phenomena. John Wiley and Sons, Inc. N.Y. USA. p.1-25.

Boyce, D.S. 1965. Grain moisture and temperature changes with position and time during through drying. J.Agric. Eng. Res. 10(4):333-341.

Bridgewater, J. 1985. Spouted beds. In: Fluidization (2nd Edition). Edited by J.F. Davidson, R. Clift, and D. Harrison. Academic press, New York, USA. p. 201-224.

Britton, M.G. 1977. State of the art-predicting static pressure in grain bins. ASAE Paper # 77-4501, p. 1-8.

Brooker, D. B., Bakker-Arkema, F. W. and Hall, C. W. 1974. Drying Cereal Grains. The AVI Publishing Comp. Inc. Westport, Connecticut. USA.

Bruce, D.M. 1985. Exposed-layer barley drying: Three models fitted to new data up to 150 °C. J. Agric. Eng. Research. 32(4):337- 347.

Brunello, G., Della Nina, G., Nunes, F.C.S. and Nascimento, C.A.O. 1974a. Minimum air requirement for spouting mixed particles. Can. Jour. of Chem. Eng. 52:170-173.

Brunello, G., Peck, R.E. and Della Nina, G. 1974b. The drying of barley malt in the spouted bed dryer. Can. Jour. of Chem. Eng. 52:201-205.

Buchanan, R.H. and Wilson, B. 1965. The fluid-lift solids recirculator. Meth. and Chem. Eng. Trans. (Inst. Eng. Australia). 1:117- 124.

Buckingham, E. 1914. On physical similar systems: Illustrations of the use of dimensional equations. Phys. Rev. IV(4):345-376.

Byler, R.K., Anderson, C.R. and Brook, R.C. 1987. Statistical methods in thin layer parboiled rice drying models. Trans. of the ASAE. 30(2):533-538.

Carslaw, H.S. and Jaeger, J.C. 1959. Conduction of heat in solids. 2nd. ed. Oxford University Press, New York, USA.

Chakraverty, A. and De, D.S. 1981. Post Harvest Technology of Cereals and Pulses. Oxford and IBH Publishing Co. New Delhi, India. p 25-63.

Chang, C.S., Converse, H.H. and Lai, F.S. 1984. Flow rate of corn through orifices as affected by moisture content. Trans. of ASAE. 27:1586-1589.

Charlton, B.G., Morris, J.B. and Williams, G.H. 1965. An Experimental Study of Spouting Beds of Spheres. Rep. No. AERE-R4852. U.K. At. Energy Authority, Harwell.

Chu, S. T. and Hustrulid, A. 1968. Numerical solution of diffusion equations. Trans. of ASAE. 11(5):705-708.

Chung, D. S. and Pfost, H. B. 1966. Adsorption and desorption of water vapour by cereal grains and their products. Part-II. Development of general isotherms equation. ASAE paper No. 66-821.

Claflin, J.K. 1982. The effect of solids flow on fluid distribution in a spouted bed fitted with a draft tube. CHEMECA 82, Australian Conference on Chemical Engineering held in Sydney, New South Wales, Australia. p. 1-9.

Claflin, J.K. and Fane, T. 1983. Spouting with a porous draft-tube. Can. Jour. of Chem. Eng. 61(3):356-363.

Claflin, J.K. and Fane, A.G. 1984a. Fluid mechanics, heat transfer and drying in spouted beds with draft tubes. In:DRYING'84. p. 137-141.

Claflin, J.K. and Fane, A.G. 1984b. Gas distribution and heat transfer in a draft-tube spouted bed. In: Fluidization and Fluid Particle Systems; Recent Advances. Edited by Klinzing, G.E. AIChE Symposium series # 241, Vol. 80, p. 17-23.

Crank, J. 1975. The mathematics of diffusion. Oxford University Press, New York, USA.

Curtis, J.O. and Stanek, B.E. 1979. Lateral loads currently used in silo design. ASAE Paper # 79-4504. p. 1-11.

Epstein, N. and Chandnani, P.P., 1987. Gas spouting characteristics of fine particles. Chem. Eng. Soc. 42(12):2977-2981.

Epstein, N. and Grace, J.R. 1984. Spouting of particulate solids. In:Handbook of Powder Science and Technology. Edited by M.E. Fayed and L. Otten. Van Nostrand Reinhold Company, New York, USA. p. 507-536.

Epstein, N., Lim, C.J. and Mathur, K.B. 1978. Data and models for flow distribution and pressure drop in spouted beds. Can. Jour. of Chem. Eng. 56:436-447.

Epstein, N. and Mathur, K.B.. August, 1971. Heat and mass transfer in spouted beds:- A review. Can. Jour. of Chem. Eng. 49:467- 476.

Ewalt, D.J. and Buelow, F.H. 1963. Flow of shelled corn through orifices in bin walls. Quarterly Bulletin of the Michigan Agricultural Experiment Station. 46(1):92-102. Michigan State University, East Lansing.

Fedler, C.B. and Gregory, J.M. 1989. Material property Effects on granular flow through orifices. Trans. of ASAE. 32(1):263-266.

Flood, C.A., Sabbah, M.A. and Peart, R.M. 1972. Simulation of a natural- air corn drying systems. Trans. of the ASAE. 15:156- 159+162.

Fortes, M. and Okos, M.R. 1980. Drying Theories: Their Bases and Limitations as Applied to Food and Grains. In: Advances in Drying, Vol. I. Hemisphere Publishing Co., N.Y. USA. p.119-154.

Franklin, F.C. and Johansen, L.N. 1955. Flow of granular materials through a circular orifice. Chem. Eng. Sc. 4:119-121.

Gay, E., Nelson, G.L. and Clary, B.L. 1970. Air flow requirements and bed turnover time for a spouted bed peanut drier. Trans. of ASAE. 16(1):104-108.

Gaylord, E.H. and Gaylord, C.N. 1977. Granular material pressures in bins. ASAE Paper # 77-4503. p. 1- 15.

Gaylord, E.H. and Gaylord, C.N. 1984. Design of Steel Bins for Storage of Bulk Solids. Prentice-Hall, Inc. Englewood Cliffs, New Jersey. USA. p. 37-54 & 85-141.

Glicksman, L.R. and McAndrews, G. 1985. The effect of bed width on the hydrodynamics of large particle fluidized beds. Powder Tech. 42:159-167.

Gomez, K. A. and Gomez, A. A. 1984. Statistical Procedures for Agricultural Research. John Wiley and Sons, Inc. New York, USA. p. 357-423.

Golubev, I.F. 1959. Viscosity of Gases and Gas Mixtures. A Handbook. Translated from Russian. Israel Program for Scientific Translations, Jerusalem. 1970. p.1-6 and 133-143.

Gregory, J.M. and Fedler, C.B. 1987. Equation describing granular flow through circular orifices. Trans. of the ASAE. 30(2):529- 532.

Hall, C.W. 1980. Drying and Storage of Agricultural Crops. The AVI Publishing Comp. Inc. Westport, Connecticut. USA. p .

Hall, C.W. and Rodriguez-Arias, J.H. 1958. Equilibrium moisture content of shelled corn. Agricultural Engineering, ASAE, 39(8):466- 470.

Henderson, S.M. 1974. Progress in developing the thin layer drying equation. Trans. of the ASAE. 17(6):1167-1172.

Henderson, J.M. and Henderson, S.M. 1968. A computational procedure for deep-bed drying analysis. J. Agric. Eng. Research. 13(2):87-95.

Henderson, S.M. and Pabis, S. 1961. Grain drying theory, I. Temperature effect on drying coefficient. J. of Agric. Eng. Res. 6:169-174.

Homes, A.G. 1973. Lateral pressures of granular material in silos. Trans. ASME, J.Eng. for Industries.

Hustrulid, A. and Flikke, A.M. 1959. Theoretical drying curve for shelled corn. Trans. of the ASAE. 2(1):112-114.

Hutchinson, D. and Otten, L. 1983. Thin-layer air drying of soybeans and white beans. J. Fd. Technol. 18:507-522.

Isaacson, E. de St Q. and Isaacson, M. de St Q. Dimensional Methods in Engineering and Physics. John Wiley & Sons, Inc. N.Y. USA.

Jamieson, J.A. 1903. Grain pressures in deep bins. Trans. Can. Soc. of Civil Engineers. 17:554-607.

Janssen, H.A. 1895. Versuche uber Getreidedruck in Silozellen Z. Ver. Dtsch. Ing. 39:1045-1049.

Jayas, D.S. and Sokhansanj, S. 1989. Thin-layer drying of barley at low temperatures. Can. Agric. Eng. 31:21-23.

Jenike, A.W., Johnson, J.R. and Carson, J.W. 1973. Bin loads-Part 3: Mass flow bins. Trans. ASME Jour. Eng. for Industries.

Kalwar, M.I., Raghavan, G.S.V., Mujumdar, A.S. and Fanous, M.A. 1988. Aerodynamics of grains in a large scale two-dimensional spouted bed with draft plates. 6th Int. Drying Symp., (IDS'88). Paris, France. 2:P74-P82.

Kathuria, D.G. and Saxena, S.C. 1987. A variable-thickness two-dimensional bed for investigating gas-solid fluidized bed hydrodynamics. Powder Tech. 53:91-96.

Ketchum, M.S. 1907. The Design of Walls, Bins, and Grain Elevators. The Engineering News Publishing Co. London. p. 237-282.

Khoe, G.K. and Brakel, J.V. April 1980. A draft tube spouted bed as small scale grain dryer. Inst. of chem. Eng. Symp. Ser. No. 59, Solids Separation Processes. p. 6:6/1-6:6/13.

Khoe, G.H. and Brakel, J.V. 1983. Drying characteristics of a draft tube spouted bed. Can. Jour. of Chem. Eng. 61(3)411-418.

Kmiec, A. 1980. Hydrodynamics of flows and heat transfer in spouted beds. Chem. Eng. Jour. 19(3):189-200.

Koenen, M. 1896. Berechnung des Seiten-und Bodendrucks in Silozellen. Centralblatt der Bauverwaitung. p. 446-449.

Kudra, T., Mujumdar, A.S. and Raghavan, G.S.V. 1989. Gas-to-particle heat transfer in two-dimensional spouted beds. Int. Comm. Heat Mass Transfer. 16:731-741.

Kugo, M., Watanabe, N., Uemaki, O. and Shibata, T. 1965. Drying of wheat by spouting bed. Bull. Hokkaido Univ. Sapporo, Japan. 39:95-

Law, L.K.C., Ziaie, B., Malhotra, K. and Mujumdar, A.S. 1984. Pressure drop and particle circulation studies in modified slot spouted beds. In:DRYING' 84. p. 386-389.

Law, L.K.C., Malhotra, K. and Mujumdar, A.S. 1986. Some aerodynamic and solids circulation measurements in a slotted spouted bed of grains. Powder Tech. 46:141-148.

Lewis, W.K. 1921. The rate of drying of solid materials Ind. Eng. Chem. 13:427-432.

Li, H. and Morey, R.V. 1984. Thin-layer drying of yellow dent corn. Trans. of the ASAE. 27:581-585.

Li, H., Morey, R.V. and Afinrud, M. 1987. Thin-layer drying rates of oilseed sunflower. Trans. of the ASAE. 30:1172-1175+1180.

Lim, C.J. and Grace, J.R. 1987. Spouted bed hydrodynamics in a 0.91 m diameter vessel. Can. Jour. of Chem. Eng. 65:366-372.

Littman, H. and Morgan III, M.H. 1983. A general correlation for the minimum spouting velocity. Can. Jour. Chem. Eng. 61(3):269-273.

Littman, H. and Morgan III, M.H. 1989. The measurement, prediction and correlation of the minimum spouting velocity, pressure drop, maximum spoutable height and spout diameter in spouted beds of coarse particles. In:Transport in Fluidized Particle Systems. Transport Processes in Engineering, 1. Editors L.K. Doraiswamy and A.S. Mujumdar. Elsevier Science Publishers B.V., Amsterdam, Netherlands. p. 287-315.

Malek, M.A. and Lu, B.C.-Y. 1964. Heat transfer in spouted beds. Can. Jour. of Chem. Eng. 42:14-20.

Manbeck, H.B., Goyal, M.G., Nelson, G.L. and Singh, M.G. 1977. Dynamic overpressures in model bins during emptying. ASAE Paper # 77-4505.

Mathur, K.B. and Epstein, N. 1974a. Dynamics of spouted beds. In:Advances in Chemical Engineering. The Academic Press Inc. New York. p. 111-191.

Mathur. K.B. and Epstein, N. 1974b. Spouted Beds. The Academic Press Inc. New York. P. 0-304.

Mathur, K.B. and Gishler, P.E. 1955a. A technique for contacting gases with coarse solid particles. Jour. of Am. Inst. of Chem. Eng. 1(2):157-164.

Mathur, K.B. and Gishler, P.E. 1955b. A study of the application of the spouted bed technique to wheat drying. Journal of Applied Chemistry, 5:624-636.

Misra, M.K. and Brooker, D.B. 1980. Thin-layer drying and rewetting equations for yellow corn. Trans. of the ASAE. 23:1254- 1260.

Mohsenin, N.N. 1970. Physical Properties of Plant and Animal Materials. Vol. I, Structure, Physical Characteristics and Mechanical Properties. Gordon and Breach Science Publishers, New York, USA. p. 51-74,566-624.

Mujumdar, A.S. 1982. Keynote lecture on spouted bed technology. Proc. Brazilian conf. on Transport Processes in Particulate Systems. Sa˜ Carlos, Brazil.

Mujumdar, A.S. 1984. Spouted bed technology - A brief review. DRYING'84, Hemisphere Publishing Corporation, New York, USA. p. 151- 157.

Mujumdar, A.S. and Raghavan, G.S.V. 1984. Canadian research and development - A survey. In:DRYING'84. p. 1-10.

Nedderman, R.M. 1985. The flow of granular materials through orifices. I.CHEM.E. Sym. ser. No. 91. p. 281-293.

Nellist, M.E. 1976. Exposed layer drying of ryegrass seeds. J. Agric. Eng. Research. 21:49-66.

Nellist, M.E. and O'Callaghan, J.R. 1971. The measurement of drying ratio in thin layers of ryegrass seed. J. Agric. Eng. Res. 16(4):192.

Nelson, G.L. 1960. A new analysis of batch grain-drier performance. Trans. of the ASAE. 4:81-85+88.

Nelson, S.O. 1979. RF and microwave dielectric properties of shelled, yellow-dent field corn. Trans. of the ASAE. 22:1451-1457.

Nemeth, J., Pallai, E. and Aradi, E. 1983. Scale-up examination of spouted bed dryers. Can. J. Chem. Eng. 61(3):419-425.

Newman, A.B. 1931. The drying of porous solids: diffusion calculations. AIChE. 1931:310-333.

Page, G.E. 1949. Factors influencing the maximum rates of air-drying shelled corn in thin layers. M.S. thesis. Purdue Univ. Indiana, USA.

Pallai, E., Nemeth, J. and Arandi, E. 1984. Development of spouted bed dryer. In:DRYING'84. Academic Press, New York, USA. p. 158-165.

Passos, M.L., Mujumdar, A.S. and Raghavan, G.S.V. 1987. Spouted beds for drying: Principles and design considerations. In:Advances in Drying. Edited by A.S. Mujumdar. Hemisphere, N.Y. Vol. 4. p.359-397.

Peterson, W.S. 1962. Spouted bed dryer. Can. Jour. of Chem. Eng. 40:226- 230.

Pieper, K. and Wenzel, F. 1962. Comments on DIN1055 design loads for buildings, loads in silo bins. Beton und stahlbetonbau. p. 6-11.

Qazi, M.A. 1975. Flow properties of granular masses: A review on the angle of repose. The Arabian Jour. for Sc. and Engineering, Saudi Arabia. 1(2):69-78.

Reimbert, M.L. and Reimbert, A.M. 1976. SILOS: Theory and Practice. Trans Tech Publications, Clausthal, West Germany. p. 5-61.

Rowe, P.N. and Everett, D.J. 1972. Fluidised bed bubbles viewed by X-rays. Part II - The transition from two to three dimensions of undisturbed bubbles. Trans. Inst. Chem. Engrs. 50:49-53.

Rowe, R.J. and Gunkel, W.W. 1972. Simulation of temperature and moisture content of alfalfa during thin-layer drying. Trans. of the ASAE. 15(5):805-810.

Safarian, S.S. and Harris, E.C. 1985. Design and Construction of Silos and Bunkers. Van Nostrand Reinhold Comp. Inc. New York. p. 10- 64.

SAS. 1985. SAS software and User's Guide. Statistics, Version 5 Edition, ANOVA, GLM, and STEPWISE. SAS institute Inc. Cary, N.C. USA. p. 113-138, 433-506, & 763-774.

Sharaf-Eldeen, Y.I., Hamdy, M.Y. and Blaisdell, J.L. 1979. Falling rate drying of fully exposed biological materials: a review of mathematical models. ASAE paper No. 79-6522.

Sherwood, T.K. 1931. Application of theoretical diffusion equations to the drying of solids. AIChE 27:190-202.

Simmods, W.H.C., Ward, G.T. and McEwen, E. 1953. The drying of wheat grain. Part I. The mechanism of drying. Trans. Inst. of Chem. Eng. 32:265-278.

Singh, R,, Barre, H.J. and Hamdy, M.Y. 1972. Drying spherical porous bodies. Trans. of the ASAE. 15(2):338-341.

Smith, D.L.O. and Lohnes, R.A. 1980. Grain silo overpressures induced by dilatancy upon unloading. ASAE Paper # 80-3013. p. 1-10.

Smith, J.W. and Reddy, K.V.S. 1964. Spouting of mixed particle-size beds. Can. Jour. of Chem. Eng. 42:206-210.

Spencer, H.B. 1969. A mathematical simulation of grain drying. Journal of Agric. Eng. research. 14(3):226-235.

Stahl, B.M. 1950. Grain bin requirements. USDA Circular 835. Washington.

Staley, L.M. 1981. Agricultural Materials Handling Manual. Part 7 Engineering properties. Section 7.1. Properties of agricultural materials. p. 31.

STATGRAPHICS 1989. Version 3. Statistical Graphics Corporation. 2115 East Jefferson Street, Rockville, Maryland, USA.

Syarief, A.M., Morey, R.V. and Gustafson, R.J. 1984. Thin-layer drying rates of sunflower seed. Trans. of the ASAE. 27:195-200.

Thompson, T. L., Peart, R. M. and Foster, G. H. 1968. Mathematical simulation of corn drying-A new model. Trans. of ASAE. 11(4):852-6.

Thorley, B., Saunby, J.B., Mathur, K.B. and Osberg, G.L. 1959. An analysis of air and solid flow in a spouted wheat bed. Can. Jour. of Chem. Eng. 37:184-192.

van Rest, D. and Isaacs, G.W. 1966. Exposed-layer drying rates of small grains. Trans. of the ASAE. 9:688-691.

Verlaan, T.D. 1984. The performance of a two dimensional spouted bed grain dryer. A report submitted to Agric. Eng. Dept. Macdonal College of McGill University, Ste. Anne de Bellevue, H9X 1C0. p.14-21.

Viswanathan, K. 1986. Model for continuous drying of solids in fluidized/spouted beds. Can. Jour. of Chem. Eng. 64(1):87- 95.

Viswanathan, K., Lyall, M.S. and Raychaudhuri, B.C. 1986. Spouted bed drying of agricultural grains. Can. Jour. of Chem. Eng. 64(2):223-232.

White, G.M., Bridges, T.C., Loewer, O.J. and Ross, I.J. 1981. Thin-layer drying model for soybeans. Trans. of the ASAE. 24:1643- 1646.

Zaremba, A. 1977. Metoda obbliczania srednich konwekcyjnie. (Method of calculation of average temperatures and moisture content in a deep bed of wheat during convective drying.) Ph.D. Thesis (unpubl.), University of Krakow, Poland.

Zuritz, C.A. and Singh, R.P. 1980. Mathematical modelling of rough rice drying in a spouted bed. J. of Food Process Eng. 4(1):19- 52.

IX APPENDIX

9.1 Viscosity of Air.

Extensive experimental and theoretical work has been done on the viscosities of gases at low density (Bird et al., 1960; Golubev, 1959). The experimental results may be found in the form of tables or charts in engineering books which are very handy when one has to estimate only a few viscosity values. However, when many estimates are needed, working with the tables or charts becomes very tedious. For this purpose, Bird et al. (1960) developed a relationship for predicting the viscosity of a pure nonpolar monatomic gas after considering the Lennard-Jones potential:

$$\mu = 2.6693\times10^{-5}\frac{\sqrt{MT}}{\sigma^2\Omega_\mu} \qquad (9.1)$$

Bird et al. (1960) and Golubev (1959) reported that even though equation (9.1) was developed for monatomic gases, its predictions for polyatomic gases are remarkably good. Note that viscosity does not depend on pressure (up to 10 atm) in the low density range.

The values of the Lennard-Jones parameters (ε, $\varepsilon/\mathbf{K}$, and Ω_u) may also be found in handbooks of heat and mass transfer. These parameters have fixed numerical values for a particular gas, but Ω_u varies slowly with the dimensionless temperature (KT/ε). Again, use of these tables may be tedious if many estimates are needed, therefore an empirical equation for the estimation of Ω_u based on the dimensionless temperature was developed. These efforts were directed to air as a sample gas because air is used for drying of cereal grains as well as other solids. A polynomial function was first assumed and various linear and nonlinear forms of dimensionless temperature were used. The Lennard-Jones parameters values for air are ε = 3.617 Å and ε/K = 97.0 K. The tabulated values of Ω_u from 1.081 to 0.8242 and corresponding values of KT/ε from 2.6 to 10 were used as model data in the range of absolute temperature 252 to 970 K (Bird et al., 1960). The empirical model which described the tabulated data of Ω_u very well is given below

$$\Omega_\mu = C_0 + C_1X + C_2X^{1.5} + C_3X^{2.0} + C_4X^{2.5} \tag{9.2}$$

where,

$$X = \ln\left[\frac{T}{(\frac{\varepsilon}{\kappa})}\right] = \ln\left(\frac{\kappa T}{\varepsilon}\right)$$

$$C_0 = 1.7168,\ C_1 = -1.8786,\ C_2 = 1.8646,\ C_3 = -0.7411,\ C_4 = 0.1053$$

The selected equation has R^2 (adj for DF) = 99.9997 %, standard error of estimate = 1.22431E-4, all factors significant at α=0.01, and the maximum deviations from tabulated values were $\pm$ 0.027 %. The observed (i.e. tabulated) and predicted values are shown in Figure 9.1. The viscosity of air estimated by equation (9.1) with combination of equation (9.2) were compared with tabulated values of Bird et al. (1960) and a few textbooks. This comparison indicated that the

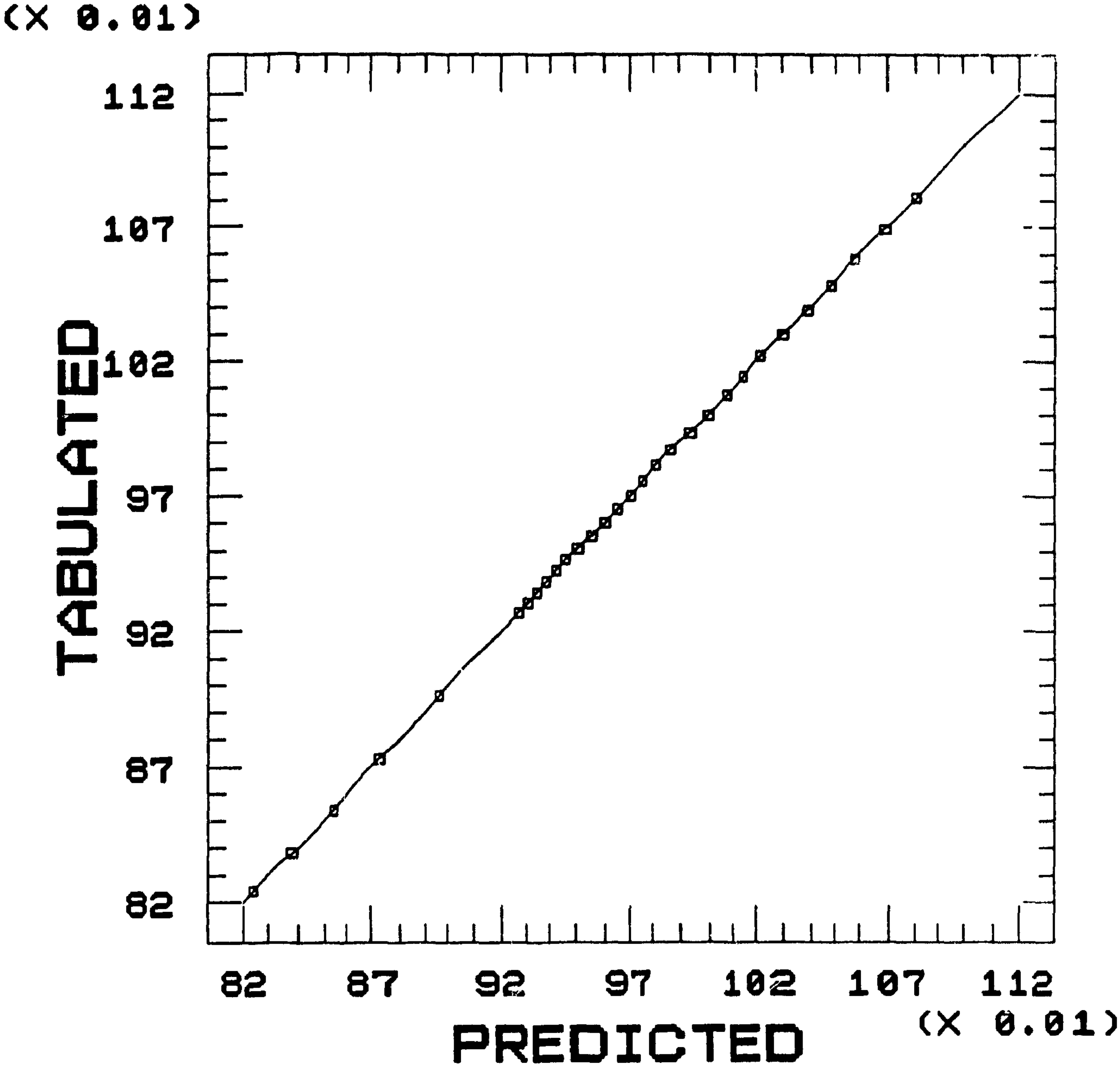

Figure 9.1 Tabulated vs. predicted Ω_μ values by equation (9.1).

predictions of equation (9.1) approximate the tabulated data with errors less than $\pm$ 0.05 %. This model was used to estimate the viscosities for the experimental data which were used in developing mathematical models for slotted 2DSBs with draft plates.

9.2 Normal Distance.

The normal distance (W_o) in a spouted bed with draft tube can be calculated using the entrainment zone height (H_E) and θ_s for the spouted bed when $W_s \geq W_i$. From Figure 9.2 we know that,

(a) $\theta_s = \theta_o$ because, $\theta_E + \theta_s = 90^o$ and $\theta_E + \theta_o = 90^o$ when $W_s = W_i$.

Therefore,

$$\text{Cos } \theta_o = \text{Cos } \theta_s = (DE/AD)$$

or, $DE = AD \text{ Cos } \theta_s$ i.e. $W_o = H_E \text{ Cos } \theta_s$ (9.3)

(b) when $W_s > W_i$, then $\theta_s = \theta_o$ because $\theta_E = \theta_e$ i.e. are opposite angles.

Then $AB = [\{(W_s - W_i)/2\} + t_p]$ and $BC = AB \text{ Tan } \theta_s$

$$CD = BD - BC \quad \text{or} \quad CD = H_E - [\{(W_s - W_i)/2\} + t_p] \text{ Tan } \theta_s$$

$$DE = CD \text{ Cos } \theta_s \quad \text{or} \quad W_o = CD \text{ Cos } \theta_s \tag{9.4}$$

Therefore, for $W_s \geq W_i$ from equations (9.3) and (9.4) we have

$$W_o = (H_E - [\{(W_s - W_i)/2\} + t_p] \text{ Tan } \theta_s) \text{ Cos } \theta_s \tag{9.5}$$

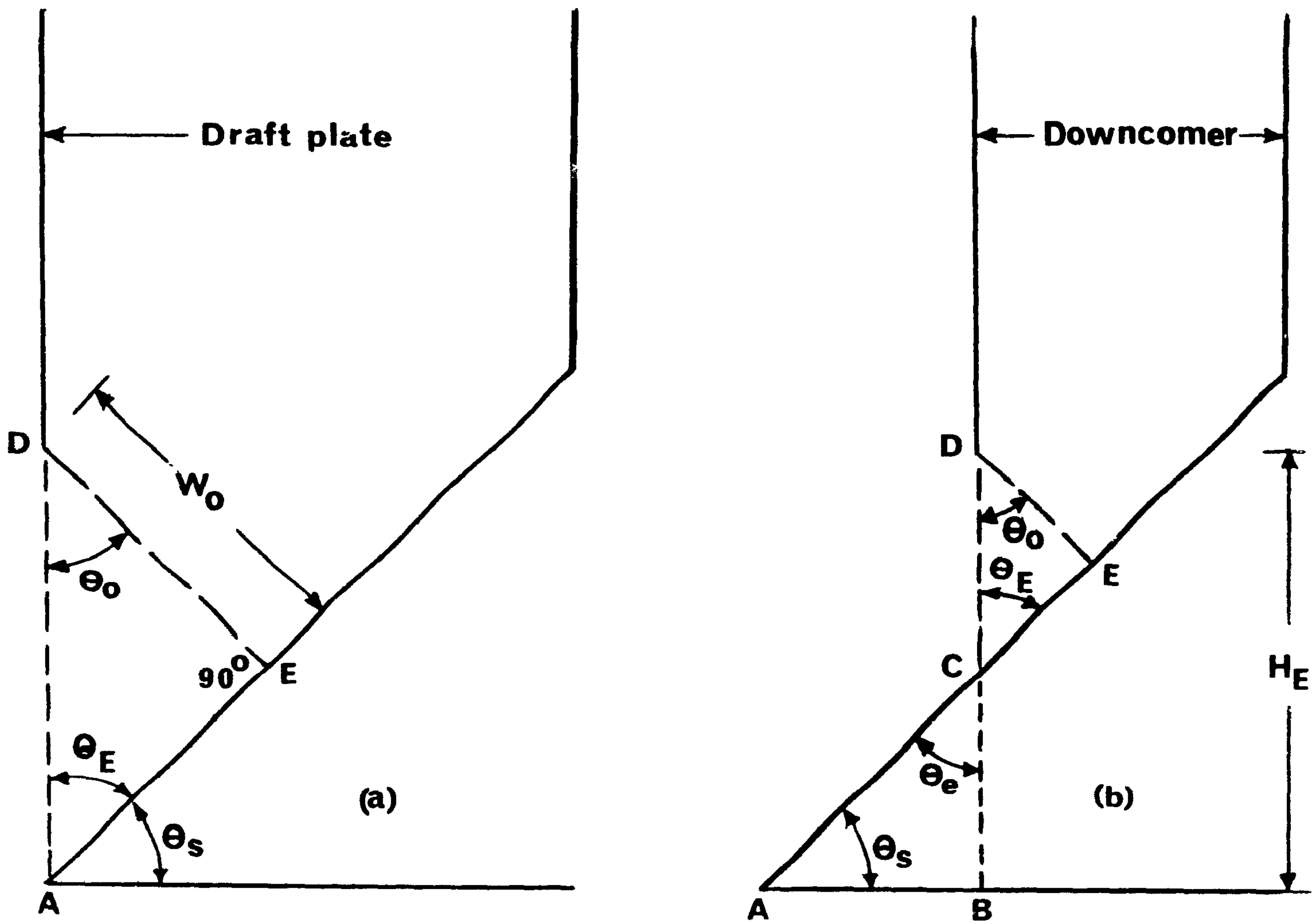

Figure 9.2 Geometrical representation of normal distance. (a) $W_s = W_i$ and (b) $W_s > W_i$.

9.3 Volume of Spouted Bed.

The volume of downcomers of the slotted 2DSB with draft piates can be approximaied by:

$$Vb = L_b\{H_b{*}W_b \text{ - spout area - draft plates cross-sectional area}$$
$$\text{- (angle area - angle area in spout)}\}$$

$$V_b = L_b[H_b(W_b - W_s - 2t_p) - \{(W_b - W_i)/2\}\tan\theta_s\{(W_b - W_i)/2\}$$
$$+ \{(W_s - W_i)/2\}\tan\theta_s\{(W_s - W_i)/2\}] \qquad (9.7)$$

The equation (9.7) can be simplified to:

$$V_b = L_b(W_b - W_s - 2t_p)[H_b - [(\tan\theta_s/4)\{(W_b + W_s) - 2W_i\}]] \qquad (9.8)$$

or,

$$V_b = A_d[H_b - [(\tan\theta_s/4)\{(W_b + W_s) - 2W_i\}]] \qquad (9.9)$$

9.4 Operational Note.

The visual observations of the pilot scale slotted 2DSBs with draft plates showed that the minimum spouting air velocity is higher when the draft tube and the air entry slot are not centrally aligned. Any deviation from the central axis affects the air flow as well as the solids circulation rate on both sides of the downcomer and requires higher spouting pressure drop for stable spouting.

Table A.1 Physical properties of grains used in the static vertical pressure of grains on the air-entry slots.

Grain	a	b	c	d_p	ϕ	ρ_b	ρ_p	ε_v	θ_r
	mm	mm	mm	mm	---	kg/m^3	kg/m^3	---	---
Corn	11.021	8.657	4.993	7.810	0.709	731.8	1200	0.390	29.2
Soya	8.529	7.207	5.757	7.073	0.829	746.4	1204	0.380	33.3
Wheat	6.593	3.086	2.950	3.915	0.594	774.3	1258	0.384	28.2

Table A.2 Physical properties of grains used in the aerodynamics and drying characteristics of grains.

Grain	a	b	c	d_p	ϕ	ρ_b	ρ_p	ε_v
	mm	mm	mm	mm	---	kg/m^3	kg/m^3	---
Corn	10.666	9.087	5.384	8.051	0.755	731.8	1231.2	0.406
Soya	7.728	6.909	5.459	6.631	0.858	756.0	1242.8	0.392
Wheat	5.839	3.050	2.678	3.627	0.621	764.9	1306.3	0.411

Table A.3 95 % confidence intervals for coefficient estimates of spouting pressure drop.

Dimensionless product	Estimate	Standard error	Lower limit	Upper limit
$\ln (Q_p / Q_f)$	0.46371	0.00653	0.45263	0.47480
$\ln (W_o / W_s)$	0.42091	0.01198	0.39730	0.44451
$\ln (\theta_s)$	0.33085	0.01798	0.29543	0.36627
$\ln \left(\frac{U_f^2}{gH_t}\right)$	0.20479	0.01140	0.18232	0.22726
$\ln \left(\frac{H_b W_i}{H_t W_s}\right)$	0.11325	0.02150	0.07090	0.15560

Table A.4 95% confidence intervals for coefficient estimates of superficial velocity.

Dimensionless Product	Estimate	Standard Error	Lower Limit	Upper Limit
$\ln\left[((\frac{W_s}{W_i})\log_{10}(\frac{\rho_p-\rho_f}{\rho_f})) + (\frac{W_o}{L_b})\right]$	0.83670	0.03063	0.77635	0.89704
$\ln\ (W_i\ /\ d_p)$	0.26928	0.01467	0.24037	0.29819
$\ln\ (\phi\ /\ \varepsilon_v)$	0.65934	0.06047	0.54021	0.77847
$\ln\left(\frac{H_t D_s \mu^2}{g H_b W_o d_p^3 \rho_f^2}\right)$	0.05965	0.00587	0.04808	0.07122

Table A.5 95% confidence intervals for coefficient estimates of average particle velocity.

Dimensionless product	Estimate	Standard error	Lower limit	Upper limit
$\ln\ (D_s/D_i)$	2.36531	0.08565	2.19657	2.5340
$\ln\ (\theta_s)$	0.60113	0.02635	0.54921	0.6530
$\ln\ (\varepsilon_v)$	7.52585	0.41617	6.70588	8.3458
$\ln\ (W_o/W_s)$	0.34399	0.02309	0.29850	0.3894
$\ln\ (d_p/D_h)$	0.25818	0.02330	0.21227	0.3041
$\ln\left(\frac{\rho_p-\rho_f}{\rho_f}\right)$	0.56673	0.05212	0.46404	0.6694
$\ln\left(\frac{U_f^2\ \mu^2}{g^2 H_t\ d_p^3\ \rho_f^2}\right)$	0.07029	0.01032	0.04997	0.0906

Table A.6. 95% confidence intervals for coefficient estimates of average cycle time.

Dimensionless product	Estimate	Standard error	Lower limit	Upper limit
$\ln (M_b)$	1.011894	0.00442	1.01011	1.02778
$\ln (M_p)$	-0.88533	0.02249	-0.93023	-0.84042
$\ln \left(\frac{H_b \, d_p}{W_o^2} \right)$	0.05181	0.01037	0.03109	0.07252

Table A.7 Solids circulation rate of grains during scale-up.

Grain	H_t	W_b	W_i	W_s	H_E	L_b	M_p/L_b	M_p/A_d	%
	m	m	m	m	m	m	kg/ms	kg/m^2 s	
Corn	0.90	0.50	0.033	0.050	0.10	0.040	8.80	19.68	
Corn	1.35	0.75	0.050	0.075	0.15	0.050	14.53	21.65	0.0
Corn	1.35	0.75	0.050	0.075	0.15	0.060	14.67	21.87	1.0
Corn	1.35	0.75	0.050	0.075	0.15	0.075	14.77	22.01	1.7
Corn	1.35	0.75	0.050	0.075	0.15	0.100	13.94	20.78	- 4.0
Corn	1.35	0.75	0.050	0.075	0.15	0.125	15.62	23.28	7.5
Corn	1.35	0.75	0.050	0.075	0.15	0.150	16.76	24.98	15.4
Soya	0.90	0.50	0.033	0.050	0.10	0.040	7.65	17.11	
Soya	1.35	0.75	0.050	0.075	0.15	0.050	12.03	17.93	0.0
Soya	1.35	0.75	0.050	0.075	0.15	0.060	11.96	17.83	- 0.6
Soya	1.35	0.75	0.050	0.075	0.15	0.075	12.26	18.28	1.9
Soya	1.35	0.75	0.050	0.075	0.15	0.100	11.92	17.76	- 1.0
Soya	1.35	0.75	0.050	0.075	0.15	0.125	12.98	19.35	7.9
Soya	1.35	0.75	0.050	0.075	0.15	0.150	13.16	19.61	9.3
Wheat	0.90	0.50	0.050	0.050	0.10	0.040	7.02	15.70	
Wheat	1.35	0.75	0.050	0.075	0.15	0.050	12.62	18.81	0.0
Wheat	1.35	0.75	0.050	0.075	0.15	0.060	12.48	18.60	- 1.1
Wheat	1.35	0.75	0.050	0.075	0.15	0.075	12.74	18.98	0.9
Wheat	1.35	0.75	0.050	0.075	0.15	0.100	13.29	19.81	5.4
Wheat	1.35	0.75	0.050	0.075	0.15	0.125	14.54	21.67	15.2
Wheat	1.35	0.75	0.050	0.075	0.75	0.150	13.66	20.35	8.2